Characterization of Novel Proteins involved in Catabolite Degradation of Fructose-1,6-bisphosphatase in *Saccharomyces cerevisiae*

Von der Fakultät Geo- und Biowissenschaften der Universität Stuttgart
zur Erlangung der Würde eines Doktors der
Naturwissenschaften (Dr. rer. nat.) genehmigte Abhandlung

vorgelegt von
Thorsten Pfirrmann
aus Heidelberg

Hauptberichter: Prof. Dr. Dieter H. Wolf
Mitberichter: PD Dr. Wolfgang Heinemeyer
Tag der mündlichen Prüfung:
21.06.2006

Institut für Biochemie
Universität Stuttgart

2006

Hiermit versichere ich, dass ich diese Arbeit selbst verfasst und dabei keine anderen als die angegebenen Quellen und Hilfsmittel verwendet habe.
Stockholm, den 18.04.2006

Thorsten Pfirrmann

CONTENTS

CONTENTS **3**

ABBREVIATIONS **6**

1 ABSTRACT **10**

2 INTRODUCTION **14**

2.1 THE UBIQUITIN SYSTEM 14
2.2 THE PROTEASOME 20
2.3 GLUCONEOGENESIS AND FRUCTOSE-1,6-BISPHOPHATASE 23
2.4 OBJECTIVES 26

3 RESULTS **28**

3.1 EXPRESSION PROFILES OF THE GID PROTEINS 28
3.1.1 Construction of C-terminal HA fusion proteins 28
3.1.2 Expression patterns of the Gid fusion proteins 31
3.1.3 Purification of polyclonal antiserum against Gid4 and Western blot analysis 32
3.2 SUBCELLULAR LOCALIZATION OF THE GID PROTEINS 33
3.2.1 Construction of C-terminal GFP fusion proteins 34
3.2.2 Biochemical localization studies of Gid proteins 37
3.3 GLYCEROL GRADIENT DENSITY CENTRIFUGATION 38
3.4 THE GID PROTEIN COMPLEX 41
3.4.1 Interaction studies of Gid proteins using co-immunoprecipitation 42
3.4.2 Direct interactions of Gid proteins in a two hybrid system 43
3.4.3 Separation of Gid complexes by native gel electrophoresis 45
3.4.4 Interaction studies of Gid proteins with FBPase 47
3.5 POSSIBLE FUNCTIONS OF GID PROTEINS AND THE GID PROTEIN COMPLEX 48
3.5.1 Functional domains of the Gid proteins: A bioinformatic approach 48
3.5.2 General involvement of Gid proteins in the ubiquitin proteasome pathway 51
3.5.3 Involvement of Gid proteins in the polyubiquitination of FBPase 53
3.5.4 Point mutations in the conserved cysteine residues of the Gid2 RING domain 54
3.5.5 F-Box proteins 55
3.5.6 Construction of TAP tagged FBPase 56
3.5.7 Immunoprecipitations of FBPase and detection of interacting partners 57
3.5.7.1 Small scale immunoprecipitation of FBPase-TAP and FBPaseP1/S-TAP 57
3.5.7.2 Large scale immunoprecipitation of FBPase-TAP and FBPaseP1/S-TAP 58
3.6 SUBCELLULAR LOCALIZATION OF FBPASE 59
3.6.1 Involvement of SUMO in the catabolite degradation of FBPase 62
3.6.2 Involvement of classical nuclear import mechanisms in the catabolite degradation of FBPase 63
3.6.3 Involvement of Snl1 in the catabolite degradation of FBPase 65

3.7 PHOSPHORYLATION OF FBPASE AND POSSIBLE FUNCTIONS 66
3.7.1 Caffeine sensitivity of GID deletion strains and the catabolite degradation of FBPase 67
3.7.2 Involvement of PKA dependent phosphorylation processes in the catabolite degradation of FBPase 69
3.7.3 Snf1 dependent catabolite degradation of FBPase 70
3.7.4 Possible new phosphorylation sites of FBPase 71

4 DISCUSSION 74

5 MATERIAL & METHODS 83

5.1 MATERIALS 83
5.1.1 Chemicals, materials and their suppliers 83
5.1.2 Antibodies 84
5.1.3 Laboratory equipment 84
5.1.4 Enzymes 86
5.1.5 E.coli strains 86
5.1.6 S. cerevisiae strains 86
5.1.7 Plasmids 90
5.1.8 Oligonucleotides 92
5.1.9 Media for yeast and E.coli cultivation 94
5.2 METHODS 97
5.2.1 Crossing haploid yeast strains 97
5.2.2 Sporulation of yeast and the dissection of tetrades 97
5.2.3 Determination of the mating type 97
5.2.4 General growth conditions for yeast 98
5.2.5 Induction of gluconeogenesis and the catabolite degradation of FBPase 98
5.2.6 General growth conditions for E.coli 99
5.3 DNA WORK 99
5.3.1 Isolation of plasmid DNA from E.coli cultures 99
5.3.2 Isolation of chromosomal DNA from S.cerevisiae 100
5.3.3 Isolation of plasmid DNA from yeast (plasmid rescue) 101
5.3.4 Transformation Methods 101
5.3.4.1 Preparation of competent *E. coli* cells for electrotransformation 101
5.3.4.2 Standard Transformation Method for E. coli 102
5.3.4.3 Standard transformation method for *S. cerevisae* 102
5.3.5 Southern blot analysis 103
5.3.5.1 DNA digestion and transfer onto a nylon membrane 103
5.3.5.2 Generation of a sequence specific DNA sonde 104
5.3.5.3 Hybridisation and detection of the DNA sonde 105
5.3.6 Site directed mutagenesis 105
5.3.7 The Polymerase Chain Reaction (PCR) 106
5.3.8 Agarose Gel Electrophoresis 108

5.3.9 DNA Digestion with Restriction Endonucleases ... 108
5.3.10 5' Dephosphorylation of linearised plasmid DNA ... 109
5.3.11 Nucleic acid ligations ... 109
5.3.12 Sequencing of plasmid DNA ... 109
5.4 PROTEIN WORK ... 110
5.4.1 SDS-PAGE (SDS Gel Electrophoresis) ... 110
5.4.2 Native gel electrophoresis ... 111
5.4.2.1 Sample preparation ... 111
5.4.2.2 Separation of the Gid complex by native gel electrophoresis ... 112
5.4.3 Coomassie staining of SDS-gels ... 112
5.4.4 Silver staining of SDS gels ... 113
5.4.5 Western Blot ... 114
5.4.6 Pulse chase analysis ... 115
5.4.6.1 Growth conditions and radioactive labelling of the samples ... 115
5.4.6.2 Cell lysis and immunoprecipitation ... 116
5.4.7 Expression and purification of GST fusion proteins in E.coli ... 117
5.4.8 Purification of crude antiserum with purified GST-antigene ... 117
5.4.9 The Two Hybrid Screen ... 118
5.4.9.1 Preparation of Two Hybrid Constructs ... 118
5.4.9.2 Screening for two hybrid interactions ... 119
5.4.10 The tandem affinity purification (TAP) ... 120
5.4.10.1 Construction of TAP fusion proteins ... 120
5.4.10.2 Purification of TAP fusion proteins ... 121
5.4.11 Co-Immunoprecipitation ... 122
5.4.12 Glycerol density gradient fractionation ... 122
5.4.13 Polyubiquitination of FBPase ... 123
5.4.14 Determination of protein concentrations ... 123
6 LITERATURE ... 125

ABBREVIATIONS

°C	Degree Celsius
µ	Micro
µl	Microliter
A	Adenine bzw. Ampere
AB	Antibody
Ala, A	Alanine
Amp	Ampicillin
APS	Ammoniumpersulfat
Asp, D	Aspartate
ATP	Adenosine 5´-triphosphate
ATPase	Adenosintriphosphatase
Bp	Base pair
BSA	Bovine serum albumine
C	Cytosine
CHX	Cycloheximide
CM	Synthetic media
cm	Centimetre
Cys	Cysteine
Da	Dalton
DUB	Deubiquitinating enzyme
ddH_2O	Double deionised water
DMSO	Dimethylsulfoxide
DNA	Deoxyribonucleic acid
DNase	Deoxyribonuclease
dNTPs	Deoxyribonucleic acids
DTT	D,L Dithiothreitol
E. coli	*Escherichia coli*
E1	Ubiquitin activating enzyme
E2	Ubiquitin conjugating Enzyme
E3	Ubiquitin –Protein- Ligase
ECL	Enhanced chemiluminescence
EDTA	Ethylenediamin tetra-acetic acid

Fig	Figure
G	Guanine
G	Gram
Gal	Galactose
GFP	Green fluorescent protein
Glc	Glucose
Gly, G	Glycine
h	Hour
HA	Haemaglutinin
HCl	Hydrochloric acid
Hect	homologous to E6-AP C-terminus
His	Histidine
HOAc	Acetic acid
HRPO	Horse radish peroxidase
kb	Kilobase pairs
kDa	Kilodalton
l	Liter
LB	Luria Broth
Lys	Lysine
M	Molar
MCS	Multi cloning site
mg	Milligram
min	Minute
ml	Millilitres
mM	Millimolar
MV	Mineral medium
NEB	New England Biolabs
nm	Nanometer
OD_{600}	Optical density at 600 nm
ORF	Open reading frame
PBS	Phosphate buffer saline
PCR	Polymerase chain reaction
PEG	Polyethylenglycol

pH	-log 10 $^{[H+]}$
pmol	Picomole
RNA	Ribonucleic acid
RNase	Ribonuclease
rpm	Rotations per minute
RT	Room temperature
s	Seconds
S .cerevisiae	*Saccharomyces cerevisiae*
SDS	Sodium-Dodecyl-Sulfate
SDS-PAGE	SDS-Polyacrylamide Gel Electrophoresis
Ser, S	Serine
T	Tyrosine, thymin
T4-Ligase	Bacteriophage T4 Ligase
TAE	Tris acetate EDTA
TCA	Trichloroaceticacid
TE	Tris EDTA
TEMED	Tetramethylethyldiamine
Tris	Tris(hydroxymethyl)aminomethane
Triton X 100	Alkylpehnylpolyethylenglycol
Tween 20	Polyoxyethylensorbitolmonolaurate
U	Units
Ub	Ubiquitin
UBP/USP	Ubiquitin specific protease
UCH	Ubiquitin carboxyl hydrolase
Ura	Uracil
UV	Ultra violet
V	Volts
v/v	Volume/ Volume
w/v	Weight/ Volume
WT	Wild type
X-Gal	5-brom-4-chloro-3-indolyl-beta-D-galactopyranoside
YPD	Yeast complete media with 2% glucose

YPEtOH	Yeast complete media with 2% ethanol
B-ME	2-Mercaptoethanol

1 ABSTRACT

Glycolysis and gluconeogenesis are reciprocally controlled central metabolic pathways in cells. Catabolite degradation of fructose-1,6-bisphosphatase (FBPase) is a key regulatory step, when *Saccharomyces cerevisiae* cells switch from anabolic gluconeogenesis to catabolic glycolysis. Addition of glucose to cells growing on a non-fermentable carbon source causes FBPase phosphorylation resulting in a decrease of enzymatic activity. This is followed by a proteolytic breakdown of the enzyme via the ubiquitin-proteasome system with a half-life of 20-30 min. In a genome wide screen nine so called *gid* mutants (glucose induced degradation deficient) defective in proteasome-dependent catabolite degradation of FBPase were identified. Analysis of Gid2 revealed that this protein is a part of a soluble, cytosolic protein complex with a molecular mass of at least 600kDa (Regelmann et al., 2003).

The work of this thesis focuses on the analysis of the novel Gid proteins and their possible role in a higher molecular mass protein complex. To be able to detect Gid proteins immunologically, functional chromosomally HA eptitope tagged versions of Gid5, Gid6, Gid7, Gid8 and Gid9 proteins were generated.

Using step glycerol gradient centrifugation it could be shown that Gid5/Vid28, Gid7, Gid8 and Gid9 are also components of a higher molecular mass complex of about 600kDa. Gid1/Vid30, Gid/Ubc8 and Gid4/Vid24 exhibit a sedimentation profile of lower molecular mass slightly overlapping with 600kDa aminopeptidase I. Gid6/Ubp14 is only present in its monomeric form. Use of Gid7 as a bait protein in a co-immunoprecipitation experiment, led to the identification of Gid1/Vid30, Gid2, Gid4/Vid24, Gid5/Vid28, Gid7, Gid8 and Gid9 as interacting components. The protein Gid6/Ubp14 is not part of this protein complex. The direct interaction of Gid4 with Gid5 could be shown via the two hybrid method.

Expression profiles on ethanol or glucose of Gid1, Gid2, Gid5, Gid6, Gid7, Gid8 and Gid9 were similar. Gid4/Vid24 was not expressed on ethanol but appears when cells are treated with glucose. As found for Gid3/Ubc8 (Schüle et al., 2000), Gid4/Vid24 seems to disappear during incubation on glucose in a time-dependent fashion.

Fructose-1,6-bisphosphatase was found to interact with Gid1 and Gid7 protein. As shown for *GID2* (Regelmann et al., 2003) deletion of *GID1* and *GID7* leads to a block in fructose-1,6-bisphosphatase polyubiquitination. This shows that Gid proteins are directly involved in the ubiquitination process which preceeds proteasome degradation. Two discovered short RING domains in Gid2 and Gid9 (ShRING domains) as well as the discovery of 5 WD40 domains within Gid7 suggest a role of the Gid complex as a novel E3 ubiquitin ligase. The targeted

mutation of conserved cysteine residues within the shRING domain of Gid2 could support this theory.

Biochemical and molecular methods were used to identify the localization of Gid1, Gid6, Gid7 and Gid8. Interestingly all four Gid proteins were found to be localized in the nucleus. The direct interaction of FBPase with these Gid proteins raised the question of whether FBPase itself had a function in the nucleus of the cell or not. To investigate this question GFP-fusions with FBPase were constructed and localisation studies were performed. An increasing signal of FBPase within the nucleus after onset of catabolite degradation gave proof of the existence of this enzyme in the nucleus as well. Several mutants known to have a defect in nuclear import were tested for the catabolite degradation of FBPase.

The protein kinaseA pathway was shown to be the signal transduction pathway triggering FBPase degradation. This led to the discovery of novel putative phosphorylation sites within FBPase by bioinformatics.

Die Glykolyse und die Gluconeogenese sind reziprok gesteuerte, zentrale Stochwechselwege in der Zelle. Die Katabolitdegradation des Enzyms Fructose-1,6-bisphosphatase (FBPase) ist dabei ein zentraler Regulationsmechanismus, um von der anabolen Glukoneogenese zur katabolen Glykolyse zu wechseln. Durch die Zugabe von Glukose zu Zellen, die auf nicht fermentierbaren Kohlenstoffquellen wachsen, erfolgt eine reversible Phosphorylierung der FBPase mit einer daraus resultierenden Verringerung der enzymatischen Aktivität. Anschließend wird das Enzym, mit einer Halbwertszeit von 20-30 min, über das Ubiquitin-Proteasom System proteolytisch abgebaut. In einem genomweiten Screen wurden neun sogenannte *gid* Mutanten (glucose induced degradation deficient) identifiziert, die einen Defekt in der proteasomalen Katabolitdegradation der FBPase aufweisen. Die Analyse von Gid2 zeigte, daß dieses Protein Teil eines löslichen, zytosolischen Proteinkomplexes mit einer molekularen Masse von wenigstens 600kDa darstellt (Regelmann et al., 2003).

Die Thematik dieser Dissertation war es, die neuen Gid Proteine in Hinsicht auf ihre Funktion und ihre mögliche Rolle in einem hochmolekularen Proteinkomplex zu analysieren. Um eine immunologische Detektion der Gid Proteine zu ermöglichen, war es notwendig, chromosomale HA epitopmarkierte Gid5, Gid6, Gid7, Gid8 und Gid9 Proteine zu erzeugen.

Mit Hilfe der massenabhängigen Auftrennung dieser Proteine in einem Glyceringradienten war es möglich zu zeigen, dass neben Gid2 auch Gid5, Gid7, Gid8 und Gid9 ausschließlich in den hochmolekularen Fraktionen um 600kDa vorliegen. Gid1, Gid4 und Gid3/Ubc8 sedimentierten hauptsächlich in den niedermolekularen Fraktionen mit einer leichten Überlappung mit den Fraktionen des 600kDa Markerproteins AminopeptidaseI. Gid6/Ubp14 konnte ausschließlich in den niedermolekularen Fraktionen nachgewiesen werden. Durch Co-Immunopräzipitationen konnten mit Hilfe von Gid7 als ‘bait’ Protein Gid1, Gid2, Gid4, Gid5, Gid8 und Gid9 als interagierende Proteine gefunden werden. Das Protein Gid6/Ubp14 war nicht mit Gid7 assoziiert und scheint daher keine Komponente des Gid-Komplexes zu sein. In einem two hybrid Versuch wurde die direkte Interaktion des Proteins Gid4 mit dem Protein Gid5 gezeigt.

Die Expressionsprofile auf ethanol- bzw. glucosehaltigem Medium von Gid1, Gid2, Gid5, Gid6, Gid7, Gid8 und Gid9 waren vergleichbar. Gid4 wird unter Derepressionsbedingungen nicht exprimiert und erscheint erst unter Repression nach Glucosegabe. Ähnlich wie Gid3/Ubc8 scheint Gid4 nach seiner Hochregulation wieder abgebaut zu werden. Fruktose-1,6-bisphosphatase konnte durch Coimmunopräzipitationsexperimente als Interaktionspartner von Gid1 und Gid7 nachgewiesen werden. Wie in früheren Arbeiten gezeigt wurde, ist ein Hefestamm, der im *GID2* Gen deletiert ist, nicht mehr in der Lage, FBPase zu

polyubiquitinieren (Regelmann et al., 2003). Solche Phänotypen konnten auch für *GID1* und *GID7* Deletionen gezeigt werden. Dies beweist den direkten Einfluß dieser Gid Proteine im Prozeß der proteasomalen Katabolitdegradation von FBPase. Zwei rudimentäre (short) RING Domänen (ShRING) konnten in dieser Arbeit in den Proteinen Gid2 und Gid9 gefunden werden. Die zusätzlich auftretenden fünf WD40 Domänen in Gid7 sind gute Hinweise für die Funktion des Gid Komplexes als neue FBPase spezifische Ubiquitin Ligase. Durch gezielte Mutation der konservierten Cysteinreste der RING Domänen konnte eine solche Theorie im Ansatz bestätigt werden.

Durch biochemische und molekularbiologische Versuche konnte gezeigt werden, dass die Proteine Gid1, Gid6, Gid7 und Gid8 zum größten Teil im Zellkern vorzufinden sind. Durch die direkte Interaktion von FBPase mit Gid Proteinen stellte sich nun die Frage, ob FBPase selbst auch im Zellkern nachgewiesen werden kann. Durch die Konstruktion von GFP Fusionen wurde gezeigt, dass FBPase unter Derepressionsbedingungen größtenteils im Cytosol der Zelle vorzufinden ist. Nach Zugabe von Glucose hingegen erscheint ein FBPase spezifisches Signal auch im Zellkern. Eine eventuelle Katabolitdegradation der FBPase im Zellkern wurde daraufhin durch diverse nukleäre Importmutanten getestet.

Es konnte auch ein Zusammenhang zwischen der Protein KinaseA abhängigen Phosphorylierung der FBPase und ihrer anschließenden Katabolitdegradation gezeigt werden. Mehrere zusätzliche potentielle Phosphorylierungstellen der FBPase wurden *in silico* gefunden.

2 INTRODUCTION

The protein level of each cell has to be in a dynamic state so that the cell is able to adapt to environmental changes. This balance is regulated by numerous regulatory mechanisms that measure the environmental conditions in order to transduce specific signals to downstream targets. For years these signals were thought to control protein homeostasis on a transcriptional level only. The importance of protein degradation as its logical antagonist has been neglected. Nowadays it is widely accepted that protein degradation is a powerful and highly specific mechanism to control protein levels (Wilkinson, 2004; Wolf, 2004). Compared to other kinds of regulatory mechanisms, degradation is a relatively fast process. The most important advantage of protein degradation however is the irreversibility of this process. Elimination of a protein removes any chance of it being reactivated inappropriately.

In eukaryotic cells there exist two possible protein degradation pathways. The lysosome or vacuole is a compartmentalized organelle containing different unspecific acidic hydrolases. Although these are important degradative organelles particularly under stress conditions, most of the proteolysis that occurs in lysosomes/vacuoles is relatively non-specific and slow (Knop et al., 1993; Thumm, 2000). In contrast, the specific and fast degradation of most soluble eukaryotic proteins is carried out by the ubiquitin-proteasome pathway. In this pathway a set of three enzymes catalyses and covalently links a multi-ubiquitin chain to an acceptor protein by this acting as a general degradation signal (2.1). This sequential polyubiquitination reaction is catalysed by a so called ubiquitin-activating enzyme (E1), an ubiquitin-conjugating enzyme (E2) and an ubiquitin protein ligase (E3) (2.1). A polyubiquitinated substrate binds with high affinity to a multisubunit protease, called the 26S proteasome (2.2) and gets degraded there.

2.1 THE UBIQUITIN SYSTEM

When the small 76-residue protein called ubiquitin was first described in the early seventies no one expected it to be one of the most important posttranslational protein modifiers within all higher organisms (Goldstein et al., 1975). It was named ‘ubiquitin’ because it is ubiquitously present and highly conserved throughout the eukaryotic kingdom. The amino acid sequence of ubiquitin is almost identical among animals and ubiquitin from *S. cerevisiae* differs in only three amino acids from the animal form. This strong conservation is of course the result of strong selective pressure and reflects its importance throughout evolution.

In yeast ubiquitin is encoded by four genes: *UBI1, UBI2,* and *UBI3* code for fusions of ubiquitin to ribosomal subunit proteins, while *UBI4* encodes a stress induced head to tail

fusion of five ubiquitin molecules with a C-terminal additional aminoacid on the last ubiquitin monomer (Ozkaynak et al., 1987). Propeptide processing is therefore an inevitable process to sustain the pool of free ubiquitin molecules. Different so called DUBs are involved in this process (Amerik and Hochstrasser, 2004; Amerik et al., 2000). Ubiquitin was first found to be bound with its C-terminal glycine to a lysine residue within H2A histone forming an isopeptide bond (Goldknopf and Busch, 1977). This established that ubiquitin could be conjugated to other proteins. Later, in most cases polyubiquitination of a substrate was described to lead to a fast degradation of these proteins by the so called 26S proteasome (see 2.2) (Ciechanover et al., 1984). Most recently, monoubiquitination was described leading to endocytosis and a subsequent vacuolar degradation of target proteins (Dupre et al., 2004). The final solution of both processes is the destruction of regulatory and malfolded proteins. Compared to classical regulatory mechansims like phosphorylation the degradation of proteins is irreversible and leads to complete loss of activity. Although this process is highly energy dependent, the covalent modification of proteins by ubiquitin and their subsequent destruction was found to be involved in many aspects of protein metabolism and cell function. Among the cellular processes affected by ubiquitin dependent reactions are cell cycle control and progression, signal transduction, chromosome structure and segregation, transcriptional regulation, endocytosis, organelle biogenesis, viral pathogenesis and the stress response, to just mention a few (Hershko, 2005; Hershko and Ciechanover, 1998).

Two major functional sites important for proteasomal degradation have been discovered in ubiquitin. The C-terminal glycine of ubiquitin (G76) was long known to be sensitive to mutations. Ubiquitination of target proteins results in the formation of an isopeptide bond between the carboxygroup of glycine 76 and the ε-amino group of a substrate lysine residue or the aminoterminus of lysine-less proteins (Breitschopf et al., 1998). A second critical residue within ubiquitin is lysine48 (K48). This residue can serve as an acceptor site for further ubiquitination in the same way as lysine residues in target proteins. A polyubiquitin chain attached to a substrate protein is the result (Finley and Chau, 1991; Pickart, 1997). K48 linked polyubiquitin chains constitute the predominant signal for targeting substrates to the 26S proteasome for their following degradation (Pickart, 1997). *In vitro* binding assays demonstrated that four ubiquitin moieties conjugated via the K48 residue to a target protein provide the minimal degradation signal. Affinity to the 26S proteasome increases more than 100-fold when the chain is lengthened from two to four ubiquitin molecules. However affinity increases only threefold when four more ubiquitins are added to the chain (Thrower et al., 2000). The half life of a protein is therefore determined by its affinity to the 26S proteasome

which is regulated by controlled addition and detachment of ubiquitin molecules to the substrate.

A multitude of other ubiquitination functions apart from proteasomal degradation were described. For example many cell surface proteins are degraded by a different ubiquitin-dependent mechanism (Hicke and Dunn, 2003). A single ubiquitin can efficiently signal endocytosis, leading to proteolysis of a membrane protein in the vacuole or lysosome (Hicke and Riezman, 1996; Horak and Wolf, 2001; Kolling and Hollenberg, 1994). It gets even more complicated considering that ubiquitin has seven internal lysines. Because of this a multi-ubiquitin chain could have a huge number of different topologies and conformations with different functions within the cell if the different lysines were used. However not much is known about this yet. But a yeast strain that is blocked for chain assembly via lysine63 (K63), for example, shows defects in post replicative DNA repair, stress response and various other intracellular mechanisms. Therefore K63 linked chains seem to have a function that does not involve proteasomal proteolysis at all (Dubiel and Gordon, 1999).

To make it even more complicated a class of proteins called ubiquitin-like proteins (UBLs) share the same fold as ubiquitin but have a rather low sequence similarity. Comparable to ubiquitin they are also covalently linked to a number of cellular proteins (Walters et al., 2004).

To be able to control the huge diversity of possible substrates for ubiquitination, conjugation of ubiquitin and of most UBLs onto target proteins is dependent on the successive action of three different classes of enzymes. In an initial activation step a single ubiquitin moiety is catalysed by a so called E1 or 'ubiquitin activating enzyme'. In the following step ubiquitin is transferred and covalently linked to an 'ubiquitin conjugating enzyme' also called E2. The final step includes the transfer of ubiquitin to its specific substrate. This step is usually conducted by a so called ubiquitin ligase or E3 which is highly substrate specific (Hershko and Ciechanover, 1998).

Before an isopeptide bond between the C-terminal glycine of ubiquitin and an amino group of a target protein can be formed, ubiquitin has to be activated at its C-terminus. In this initial reaction ubiquitin becomes covalently linked to a ubiquitin activating enzyme (E1) at the expense of ATP cleavage forming a thioester bond between its C-terminal carboxyl group and a cysteine residue of E1 (Ciechanover et al., 1982). This reaction involves the hydrolysis of the β-anhydride bond of ATP yielding AMP and PP_i with the intermediate formation of an E1 bound ubiquitinyladenylate (Finley and Chau, 1991). Interestingly *UBA1* is the only gene in *S. cerevisiae* encoding an ubiquitin activating enzyme and it was described to be essential

for growth (McGrath et al., 1991). Uba1 forms a homodimer with an apparent mass of 210kDa (Hershko and Ciechanover, 1992). Several other enzymes sharing a conserved Cys residue essential to form a thiolester bond with ubiquitin have been discovered in *S.cerevisiae*. They were described to be E1 activating enzymes for ubiquitin-like proteins (Dohmen et al., 1995; Johnson et al., 1997; Liakopoulos et al., 1998).

In a second step the E1 linked ubiquitin moiety is transferred, in a transesterification reaction, from E1 to a cysteine residue of an ubiquitin-conjugating enzyme (E2). This active site cysteine is also required for the formation of a thiol ester bond with ubiquitin. It is localized in a highly conserved core domain of approximately 150 amino acids. This domain is present in all 13 E2s discovered in *S.cerevisiae*. Specific N- or C-terminal extensions of some E2s are proposed to be responsible for the interaction with their cognate E3 or for substrate specificity (Pickart and Eddins, 2004). Considering that only Ubc9p and Ubc3p are essential genes, a large redundancy within the E2 enzymes is expected. For example, the degradation of the yeast Matα2 transcriptional repressor depends on four different E2s (Chen et al., 1993).

In the last step the ubiquitin conjugating enzyme catalyses the formation of an isopeptide bond between the G76 residue of the activated ubiquitin and a lysine residue of the target protein. The internal K48 of the attached ubiquitin can form an isopeptide bond with the G76 of another ubiquitin to form a multiubiquitin chain, which serves as a proteasome targeting signal (Pickart, 1997). However, for substrate specificity this reaction requires the participation of another component, called E3 or ubiquitin protein ligase. The enormous quantity of different proteasomal substrates therefore led to a huge amount of different E3s (Hershko and Ciechanover, 1998). Ubiquitin ligases select their specific substrate protein for ubiquitination via an interaction with a degradation signal within the substrate. By binding to this so called degron and to the E2 enzyme a ternary E2-E3-substrate complex is formed (Finley and Chau, 1991). Regardless of the vast amount of different E3 enzymes all described ubiquitin ligases contain one of three possible E2 binding domains. They can be classified as HECT (homologous to E6AP Carboxy Terminus), RING (Really Interesting New Gene) or U-box protein family members.

HECT domain ubiquitin ligases have a unique feature among E3s. They do not only serve as a bridging factor between the substrate and the appendant E2 but they form a thiolester intermediate with ubiquitin before it finally gets attached to the substrate protein. The HECT domain is a ~350 residue region that includes a strictly conserved cysteine residue ~35 residue upstream of the C-terminus. This residue acts as the site of thiol ester formation

with ubiquitin. It is proposed that the unique N-terminus of each family member interacts with specific substrates while the HECT domain is responsible for E2 binding and ubiquitination (Kumar et al., 1997). With five potential HECT domain E3s this family is a rather small group within yeast E3s (Wang et al., 1999). Examples for E3s with HECT domains in *S. cerevisiae* are Rsp5 or Ufd4 (Pickart, 2001).

The other structural element in ubiquitin ligases is the RING finger domain. The protein sequence of this domain is defined by eight conserved cysteine and histidine residues that together are able to complex two zinc ions in a cross brassed structure. Two classical subtypes of RING domains are described. One with seven cyteines and a histidine at position 4 (RING-HC) and one with six cyteines and two histidines at position 4 and 5 (RING-H2). The biological function of RING domains is to directly bind E2s. But in contrast to the HECT domain ubiquitin ligases this class of E3s does not form thioester intermediates with ubiquitin prior to transfer to the bound substrate. RING ubiquitin ligases rather mediate the contact between substrate and bound E2 for the direct transfer of ubiquitin to the substrate. Strikingly RING E3s exist as single-subunit enzymes but also as multi-subunit E3 ligase complexes (Freemont, 2000; Jackson et al., 2000). The yeast genome codes for at least 45 canonical RING containing proteins (www.smart-embl.de). However, the range of substrates is widened by interchangeable substrate specific modules in some multi-subunit ubiquitin ligases like the SCF complex. It is interesting that a novel family of ubiquitin ligases called U-box E3s are structurally related to RING E3s but lack the conserved cysteine and histidine residues (Hatakeyama and Nakayama, 2003; Ohi et al., 2003).

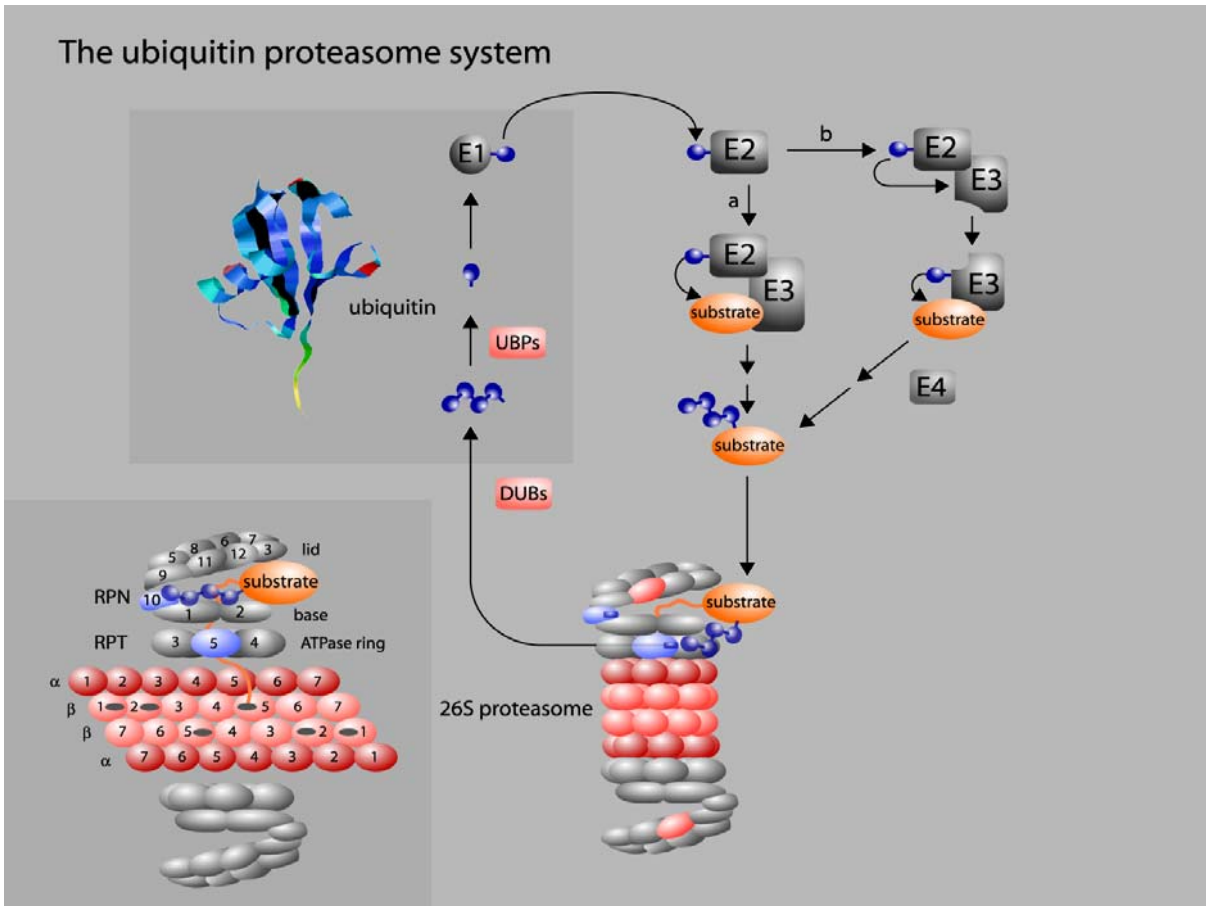

Figure 1: Schematic representation of the ubiquitin dependent protein degradation pathway in *S.cerevisae*. Ubiquitin is conjugated to the target protein via a set of three enzymes which are called E1, E2 and E3. The C-terminal glycine 76 residue of ubiquitin is attached to a cysteine residue of E1 (ubiquitin-activating enzyme) forming a thioester bond. This step is ATP dependent. Then ubiquitin is transferred to E2, the ubiquitin-conjugating enzyme. Ubiquitin is finally linked to the target protein via an isopeptide bond between glycine 76 and a lysine residue of the substrate protein. In pathway (a) a RING ubiquitin ligase (E3) functions as a mediator between the substrate and the specific ubiquitin conjugating enzyme. Pathway (b) describes how ubiquitin is transferred to a cysteine residue within a HECT ubiquitin ligase and finally attached to a lysine residue in the substrate. So called deubiquitinating enzymes cleave off the polyubiquitin chain from the substrate (DUBs) or cleave polyubiquitin chains into their single moiety units (Ubps). Ubiquitin binding subunits of the proteasome are highlighted in blue, catalytic sites in bright red. The crystal structure of ubiquitin is shown in the left upper corner. (adapted from Wolf and Hilt, 2004)

2.2 THE PROTEASOME

The proteasome is a multicatalytic proteinase that degrades proteins into oligopeptides of about 3-15 amino acids (Ehring et al., 1996; Kisselev et al., 1998; Nussbaum et al., 1998). It appears to be the major protease of the nuclear and cytoplasmic compartments of the eukaryotic cell (Baumeister et al., 1998; Rock et al., 1994). Studies with proteasome inhibitors have shown that the bulk of cellular proteins, 80-90%, are degraded by the proteasome (Rock et al., 1994). Some of the various roles of the 26S proteasome are the degradation of misfolded or damaged proteins, of cell cycle regulators, the processing of antigens and the activation or degradation of transcription factors (Hershko and Ciechanover, 1998). 26S proteasomes are composed of proteolytically active complexes, known as 20S core particles and regulatory complexes, called 19S cap complexes.

The 20S proteasome is a multicatalytic and multisubunit protease complex existing in all eukaryotic cells (Achstetter et al., 1984; Kleinschmidt et al., 1988; Wolf and Hilt, 2004). However, these proteases are not only found throughout the eukaryotic kingdom but related complexes with a much simpler subunit composition have also been purified from some archaea and some bacteria (Dahlmann et al., 1989). The proteasome is arranged of four heptameric rings, which are stacked together to form a hollow cylinder. The proteolytically active ß-type subunits form the two inner rings, while the non-active α-type subunits form the two outer rings. As in other eukaryotes, the three *S. cerevisiae* β subunits Pre2/β5, Pre3/β1 and Pup1/β2 carry the active sites and face the central cavity in the interior of the complex. These active sites have chymotrypsin-like, trypsin-like and peptidyl-glutamyl-peptide hydrolizing activity, respectively, bearing an N-terminal threonine residue as the active site nucleophile. The proteasome thus defines a new class of protease, the N-terminal threonine protease (Fenteany et al., 1995; Heinemeyer et al., 2004; Hilt and Wolf, 1995; Wolf and Hilt, 2004). In mammals three additional γ interferon inducible active site subunit variants exist. They can be incorporated into the 20S proteasome instead of the constitutive β1, β2 and β5 subunits forming a proteasome subtype. This so called immunoproteasome is involved in the formation of antigenic peptides presented by the MHC class 1 complex (Kloetzel, 2004).

The active sites are accessible only through a narrow pore on both ends of the cylinder. This architecture prevents uncontrolled degradation of cellular proteins and allows controlled protein degradation. The proteasome is a good example for self compartmentalization within the eukaryotic and prokaryotic cell (Baumeister et al., 1998). Crystallographic analysis of the 20S proteasome demonstrated that proteasomes are hollow structures with the interior divided

into three compartments, two antechambers and a central chamber with the catalytic activity (Heinemeyer et al., 2004; Lowe et al., 1995). This chamber can only be accessed by two narrow pores on each end of the cylindrical barrel. With a size of only 2 nm the pores ensure that only unfolded proteins or short peptides can access the interior of the 20S proteasome. An additional barrier is formed by the N-termini of the α subunits forming an almost inaccessible gate (Bajorek and Glickman, 2004).

Usually the degradation of a target substrate is dependent on its polyubiquitination and the presence of ATP. However there are some exceptions, the degradation of small oligopeptides neither requires ATP nor polyubiquitination (Rubin and Finley, 1995). This leads to the conclusion that proteins in their native state are too large to enter the inner cavity of the 20S proteasome. Polyubiquitinated proteins have to be unfolded before entering the proteolytic core. The 20S core alone is neither able to bind polyubiquitinated substrates nor to unfold them. Substrate unfolding and recognition of the polyubiquitin tag are carried out by the 19S regulator cap complex that is located at both ends of the 20S core complex. The unfolding process is described as a reverse chaperone activity and is therefore ATP dependent (Ferrell et al., 2000). The so called 19S cap is composed of at least 17 subunits and it is directly associated with the 20S core complex to form the fully functional 26S proteasome. The 19S cap complex itself can be dissociated into two subcomplexes which are called the base and the lid (Glickman et al., 1998b) .

The base consists of six different ATPase subunits Rpt1 to Rpt6 (for Regulatory particle Triple-ATPase protein) and three non-ATPases Rpn2, Rpn3 and Rpn10 (for Regulatory particle Non-ATPase). It has been shown that the base has chaperone like activity *in vitro* (Braun et al., 1999). This is consistent with the theory that it could function as a reverse chaperone *in vivo*. The six ATPases form a ring that directly interacts with the α–subunits of the 20S core. Substrate unfolding therefore is catalysed by the six ATPases of the base complex. The importance of these subunits becomes evident when considering the fact that all Rpt subunits are essential genes (Rubin et al., 1998). Also a striking conservation between yeast and human Rpt subunits from 66-76% identity show their importance. The interaction of Rpt subunits with the N-terminal extensions of 20S α-subunits seems to induce the opening of the pore to the inner cavity of the 20S proteasome (Kohler et al., 2001), thus making protein degradation possible.

Prior to unfolding of a substrate, however, proteins destined for degradation need to be selected as proteasomal substrates. A polyubiquitin chain attached to a lysine residue within the target protein or to the aminoterminus is known to be the signal for degradation of most

proteins. In some rare cases this modification is not necessary (Hoyt and Coffino, 2004). However all substrates need an increased affinity to the proteasome in order to be unfolded and subsequently degraded. A subunit of the 19S cap, Rpn10, was found to directly interact with polyubiquitin chains. But the fact that a *rpn10* deletion strain is viable and doesn't inhibit protein degradation drastically, soon led to the conclusion that there had to be redundant subunits (Fu et al., 1998; van Nocker et al., 1996). A more recent study showed the involvement of Rpt5, one of the six base ATPases in binding polyubiquitinated substrates (Lam et al., 2002) as well as non-ubiquitinated substrates (Hoyt and Coffino, 2004). Rpn1 and Rpn2 have been described to possess sequence similarities to the chain binding site of Rpn10 (Young et al., 1998). Recent observations showed a direct interaction of the UBA-UBL domain proteins Rad23 and Dsk2 to the leucine rich repeats of Rpn1 and Rpn2. Their role in transport of polyubiquitinated proteins to the 26S proteasomes has been shown (Elsasser and Finley, 2005; Medicherla et al., 2004).

In *rpn10* deletion strains a ~400 kDa subcomplex of the 19S cap could be copurified which corresponds to the distal part of the 19S cap and has been called the lid. The lid of the 19S cap consists of at least eight different subunits, Rpn3 and Rpn5 to Rpn11. It is linked to the base of the 19S cap via Rpn10 (Glickman et al., 1998a). Except for a similar domain distribution within these subunits not much is known about them. Rpn11 has been described to carry intrinsic isopeptidase activity and is necessary for the cleavage of polyubiquitin chains from proteasomal substrates. Mutations in the active sites of Rpn11 are lethal (Verma et al., 2002; Yao and Cohen, 2002). Another interesting candidate among the lid subunits is Rpn4. Not associated to the proteasome this protein controls the transcription of proteasomal subunits and is a proteasomal substrate itself. Thereby it regulates the amount of active proteasomes in a negative feedback circuit (Jelinsky et al., 2000; London et al., 2004; Xie and Varshavsky, 2001).

Interestingly in yeast 80% of the 26S proteasomes are localized inside the nucleus (Enenkel et al., 1998; Enenkel et al., 1999; Russell et al., 1999). Recently it was shown that 26S proteasomes are imported into the nucleus as inactive precursor complexes by the classical karyopherin αβ pathway. A classical bipartite nuclear localization sequence of Rpn2 is necessary for proper translocation. The deletion of Rpn2 NLS leads to improper nuclear proteasome localization (Wendler et al., 2004).

The various described proteasomal *in vivo* substrates range from a misfolded variant of carboxypeptidase (CPY^*), tumor suppressor proteins like p53, transcriptional repressors like Matα2, cell cycle control proteins like cyclins up to metabolic enzymes like the

gluconeogenetic fructose-1,6-bisphophatase (Egner et al., 1993; Kostova and Wolf, 2003; Saville et al., 2004; Schork et al., 1995; Willems et al., 1999; Wolf and Hilt, 2004).

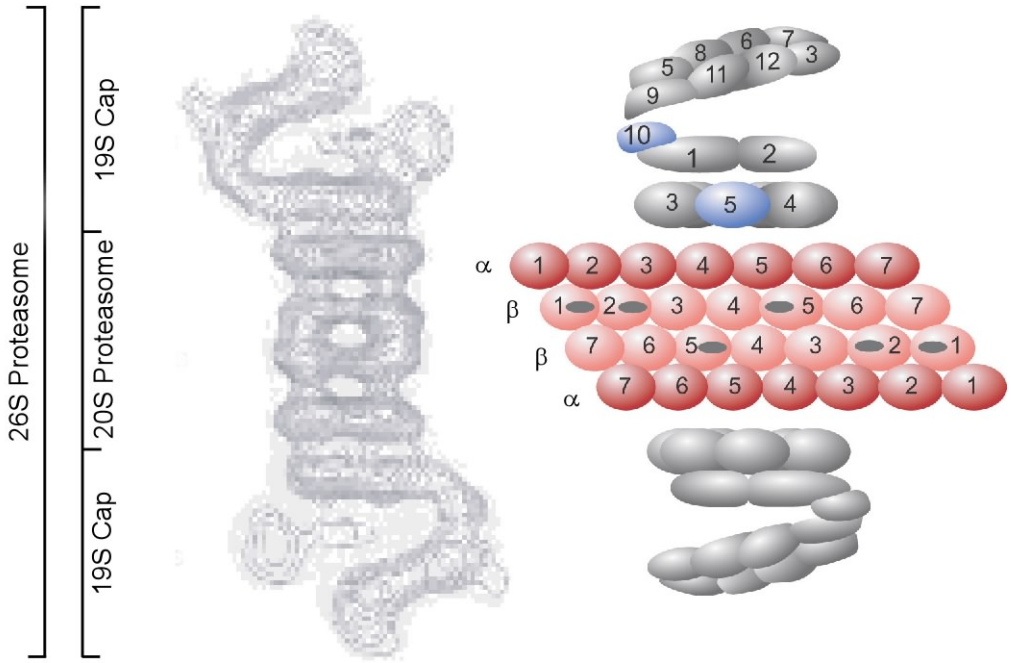

Figure 2: EM contour plot of the 26S Proteasome (left) and its known subunit distribution (right). All known subunits of the 26S Proteasome from *S.cerevisiae* are shown in the right image. The 20S Proteasome is arranged of four heptameric rings, which are stacked together to form a hollow cylinder. The proteolytically active ß-type subunits form the two inner rings, while the non-active α-type subunits form the two outer rings. Active site subunits are highlighted with a black line. The so called 19S cap is composed of at least 17 subunits and it is directly associated with the 20S core complex to form the fully functional 26S proteasome. Subunits known to bind polyubiquitin chains are highlighted in blue. (adapted from Wolf and Hilt, 2004)

2.3 GLUCONEOGENESIS AND FRUCTOSE-1,6-BISPHOPHATASE

Free living single cell organisms have to face an ever changing environment in terms of temperature, pH, moisture, availability of trace elements and most important of carbon and nitrogen sources. A proper and quick adaptation to these changes is essential for cellular viability. Therefore cells tightly control and regulate their answers to these changes. Every change in living conditions leads to a change in the activity of enzymes within each cell. These changes take place by altering the activity of enzymes via activation and inhibition by metabolites, by posttranslational modifications, by switching genes on and off or by enzyme disposal. All these regulatory steps are dependent on a sophisticated ‘sensing system’ that constantly measures all environmental parameters to send a signal to downstream targets. In the case of glucose these sensing and signalling systems are extremely advanced and sensitive

because glucose is the preferred carbon and energy source for all cells. Addition of glucose changes gene expression at the transcriptional, posttranscriptional, translational and posttranslational level to ensure the efficient and elusive catabolism of this sugar to yield energy and cellular building blocks (Kaniak et al., 2004; Rolland et al., 2002). In a pathway called glycolysis glucose is metabolized to pyruvate under aerobic conditions or to ethanol under anaerobic conditions. Due to its requirement as a donor for building blocks, under glucose depletion this molecule has to be synthesized *de novo* in a reverse process called gluconeogenesis. Both antagonistic pathways are reciprocally controlled to prevent a futile cycle of ATP hydrolysis by simultaneous action of glycolysis and gluconeogenesis (Purwin et al., 1982). Although both pathways share a major part of their enzymatic equipment, some of the reactions are thermodynamically irreversible and therefore need a different subset of enzymes. These irreversible steps are potential sites of control (Stryer, 2002).

One striking example of such control is the regulation of the key gluconeogenetic enzyme fructose-1,6-bisphosphatase (FBPase). It catalyses the dephosphorylation step of fructose-1,6-bisphosphate to fructose-6-phosphate. The antagonist in glycolysis is the enzyme phosphofructokinase, it catalyses the ATP dependent phosphorylation of fructose-6-phosphate (Stryer, 2002) (Figure 3).

FBPase is expressed only when cells are grown on a non-fermentable carbon source, like ethanol. It is rather long lived with an approximate half-life of about 90h (Funayama et al., 1980). However, FBPase is extremely sensitive to glucose and its addition to the medium leads to a set of different actions to shut down the activity of this enzyme. Initially, the transcription rate of FBPase is repressed by Mig1p to stop the new synthesis (Klein et al., 1998; Rolland et al., 2002). In a second step FBPase becomes inactivated by the protein kinaseA (PKA) dependent phosphorylation of serine11 within the enzyme. This modification is described to shift the pH optimum of FBPase to pH 8.8, by this decreasing the enzymatic activity (Funayama et al., 1980). An additional process described as catabolite degradation finally leads to the proteolytic breakdown of FBPase with a half life of 20-30 minutes. All these processes are important to switch metabolism from gluconeogenesis to glycolysis.

The site of FBPase degradation was first described to take place in the vacuole by vacuolar proteinases (Holzer, 1976; Molano, 1974). Studies on vacuolar proteinase mutants, however, did not give any indication for vacuolar proteinase involvement in this process (Wolf, 1982; Wolf, 2004). Upon discovery of the 26S proteasome, specific FBPase degradation by the ubiquitin proteasome system was found experimentally (Schork et al., 1994a; Schork et al., 1994b; Schork et al., 1995). Despite these facts the model of a vacuolar degradation of

FBPase is still under investigation (Chiang and Schekman, 1991). A recent publication however, discusses both pathways to be dependent on the derepression time (Hung et al., 2004). When following proteasomal degradation, a complete stabilisation of FBPase can be observed in different proteasomal mutants as well as in strains with defects in polyubiquitin chain formation (Schork et al., 1995). Also the involvement of the ubiquitin conjugating enzyme Ubc8/Gid3 in catabolite degradation of FBPase is described and supports the theory of proteasomal degradation (Schüle et al., 2000). This enzyme is catalysing the ubiquitination of histones *in vitro* and is an orthologue of the human ubiquitin conjugating enzyme UbcH2 (Kaiser et al., 1994).

In a recently performed genome wide screen eight new genes important for proteasomal catabolite degradation of FBPase have been discovered. These genes were named *GID1*, *GID2* and *GID4* to *GID9* standing for glucose induced degradation deficient (Regelmann et al., 2003). Among them was *GID6* encoding a well analyzed enzyme of the deubiquitinating enzyme family: *UBP14*. This enzyme is described to be involved in the detachment of polyubiquitin chains to their single moities. Deletion of this gene is proposed to lead to an accumulation of free polyubiquitin chains that competitively inhibit the ubiquitin binding sites in the 26S proteasome (Amerik et al., 1997; Amerik and Hochstrasser, 2004).

The protein Gid2 is described to be important for the polyubiquitination of FBPase and it was found to sediment in the 600 kDa fractions in a glycerol density gradient. This might indicate that Gid2p is a component of a high molecular mass protein complex (Regelmann et al., 2003).

Most interestingly three of the newly discovered GID genes were described earlier to be necessary for a vacuolar degradation of FBPase (*VID* genes). This strongly suggests an overlapping role of *GID1/VID30*, *GID4/VID24* and *GID5/VID28* in both pathways (Chiang and Chiang, 1998; Regelmann et al., 2003). PKA dependent phosphorylation of FBPase is described to reduce its activity at pH7. A site directed mutagenesis of serine11 to an alanine residue however showed that this mutation does not seem to affect the degradation of fructose-1,6-bisphosphatase via the proteasome. Phosphorylation and polyubiquitination therefore seem to be independent processes. Interestingly the N-terminal proline in the yeast FBPase sequence is indispensable for catabolite degradation and suggests a role as a degradation signal (Hämmerle et al., 1998).

All results from our laboratory show that glucose induced catabolite degradation of FBPase is dependent on the ubiquitin proteasome pathway. Why the working group of Chiang et al. favours vacuole dependent catabolite degradation of FBPase is still a matter of dicussion. A

recent publication confirmed our results and suggests two independent catabolite degradation pathways, which are dependent on the derepression time of FBPase and the derepression media (Hung et al., 2004). While in our working protocols cells are derepressed for 16h on ethanol containing media, cells are derepressed for 48h and more on acetate containing media in protocols used by H. L. Chiang and coworkers. A possible explanation for this time dependent phenomenon is probably due to the fact that starvation of yeast cells on non fermentable carbon sources longer than 48h leads to unspecific uptake of cytosolic proteins via autophagocytosis (Thumm, 2000).

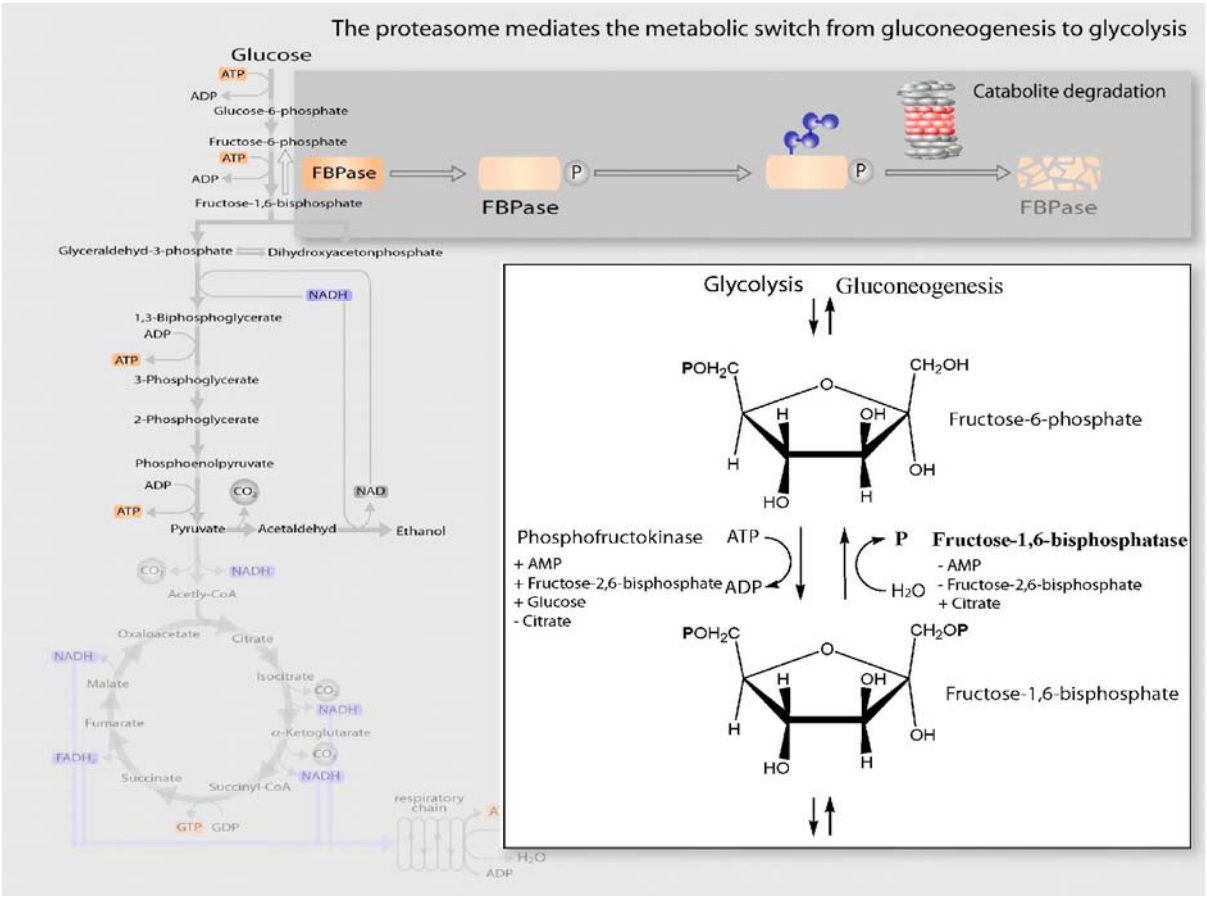

Figure 3: The gluconeogenic enzyme Fructose-1,6-bisphosphate and catabolite degradation. FBPase is a key gluconeogenic enzyme. It catalyses the dephosphorylation of the sugar fructose-1,6-bisphosphate to fructose-6-phosphate. After glucose shift this enzyme becomes inactivated by phosphorylation with subsequent polyubiquitination and degradation by the 26S proteasome. This process is called catabolite degradation and is the major switch from anabolic gluconeogenesis and catabolic glycolysis.

2.4 OBJECTIVES

Fructose-1,6-bisphosphatase is a gluconeogenetic enzyme. Upon shift of cells to glucose it is rapidly phosphorylated. In an independent process it is subsequently polyubiquitinated and degraded by the 26S proteasome. These processes prevent a ‘futile cycle’ of ATP hydrolysis.

This so called catabolite degradation is an excellent model system to study signal transmitted degradation of an enzyme by the ubiquitin system and the 26S proteasome.

In a recent genome wide screen for components involved in catabolite degradation of FBPase, 9 *GID* genes (glucose induced degradation deficient) were identified. It was the aim of this work to shed light onto the function of the Gid proteins in degradation of FBPase. One part of this work was devoted to the creation of chromosomally integrated epitope tagged versions of Gid5, Gid6, Gid7, Gid8 and Gid9 to be able to detect these proteins immunologically. This was important to be able to further characterize these proteins and get a hold on their function. Gid2 was shown to cofractionate with a 600 kDa marker protein suggesting the existence of a high molecular mass protein complex. To show the possible involvement of Gid2 and other Gid components in such a protein complex, interaction studies had to be done. First, the fractionation pattern of other Gid components in a glycerol gradient should give hints for the existence of such a 'Gid complex'. Thereafter co-immunoprecipitation experiments and two hybrid studies were planned to confirm this hypothesis.

The characterization of *gid* deletion strains should give insights in the place of action of Gid-proteins with a focus on the ubiquitin proteasome pathway. Of particular interest was the question whether Gid proteins are important for polyubiquitination of FBPase. To answer this question polyubiquitination experiments in *gid* mutant strains were planned.

Extensive sequence analysis unravelled the existence of rudimentary short RING domains (ShRING domains) in the sequence of Gid2 and Gid9. RING domains were shown to be signatures in ubiquitin ligases (E3 enzymes). Point mutations of the conserved cysteine residues within these typical E3 domains should help to prove the existence of a new E3 complex. The direct interaction of FBPase with subunits of the Gid complex should support this idea.

To be able to localize Gid proteins in the living cell, GFP fusions were planned for Gid1, Gid6, Gid7 and Gid8. The localization of the Gid fusion proteins within the cell should be confirmed with biochemical cell fractionation experiments. Another point was to clarify the intracellular localization of FBPase itself. Fusions of FBPase to the green fluorescent protein should help to do so.

3 RESULTS

In a recent genome wide screen 9 so called *GID* genes were uncovered. The deletion of any *GID* gene (glucose induced degradation deficient) leads to a disturbed catabolite degradation of FBPase by the 26S proteasome and is therefore an important component of this process (Achstetter et al., 1984; Regelmann et al., 2003). The further characterization of these components is crucial to understand the entire process in more detail. To be able to immunologically detect the Gid-proteins it was necessary to create epitope tagged versions or to produce polyclonal antibodies. Polyclonal antisera were produced against FBPase (Regelmann, 2005) and Gid4 (Josupeit, 2003). However the very weak specificity of both rabbit sera made it necessary to further purify both antibodies.

3.1 EXPRESSION PROFILES OF THE GID PROTEINS

3.1.1 Construction of C-terminal HA fusion proteins

To be able to immunologically detect Gid5, Gid6, Gid7, Gid8 and Gid9 it was important to create C-terminal fusions with a triple HA epitope from influenza virus (Gid5-HA_3 to Gid9-HA_3). The nine amino acid epitope is relatively small and antibodies against it are commercially available. A method based on homologous recombination and integration of a PCR generated integration cassette into the genome was used (Longtine et al., 1998). Integration of the tag into the genome by this method has the advantage to be able to express the studied protein under its native promoter.

The existence of HA_3 tagged versions of Gid1 (Regelmann, 2005), Gid2 (Regelmann et al., 2003) and Gid3 (Schüle et al., 2000) in a W303 background led to the choice to use the same yeast strain to produce these novel strains.

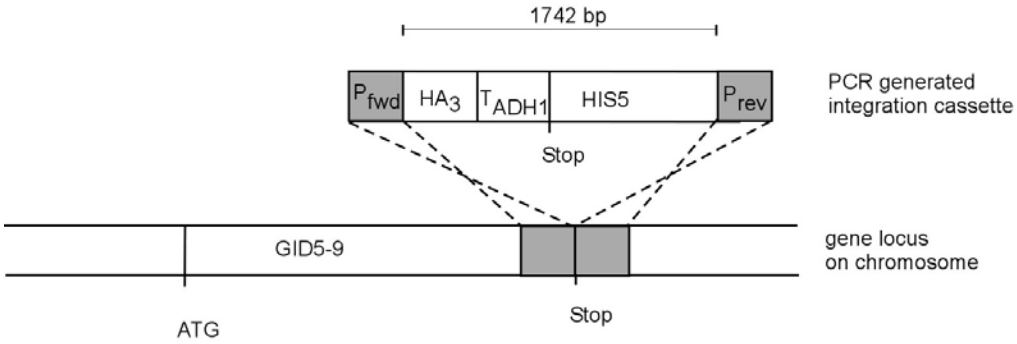

Figure 4: Construction of C-terminal HA_3 tagged Gid proteins in yeast strain W303. A 1742 bp PCR fragment containing a triple HA epitope (HA_3), the *ADH1* terminator and the *HIS5 S. pombe* auxotrophy marker was used to generate C-terminal HA_3 tagged Gid proteins by homologous recombination with the yeast genome. PCR primers were designed to be homologous to the region 40 bp in front of (P_{fwd}) and 40 bp after the stop codon (P_{rev}). This method allows expression of the integrated gene from the endogenous promotor.

Figure 4 shows a PCR generated integration cassette to produce triple HA tagged Gid proteins and its homologous recombination into the yeast genome. All primers used for the generation of such HA tagged strains are listed in 5.1.8 and named 'GidX fwd' for the forward primer and 'GidX rev' for the reverse primer of the respective Gid protein. The PCR to generate the integration cassette was done as described before (Longtine et al., 1998) and transformed into the yeast strain W303 as described in 5.3.4.3. Afterwards, the correct integration of a single cassette at the authentic locus was verified by Southern blot analysis (5.3.5).

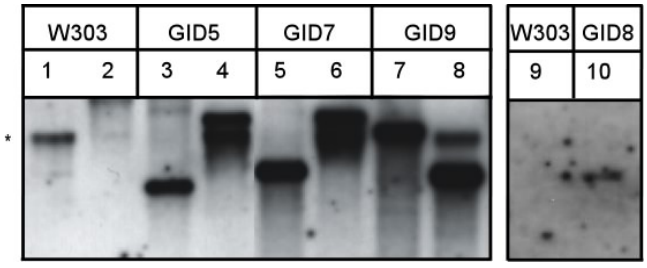

Figure 5: Southern blot analysis of the strains containing the tagged proteins Gid5-HA_3 and Gid7-HA_3 to Gid9-HA_3. For Southern blot analysis chromosomal DNA of the novel triple HA tagged Gid strains was isolated and digested. After gel electrophoresis DNA fragments were blotted onto a nylon membrane. Fragments containing the novel *HIS5* marker gene were visualized with a *HIS5* specific probe. Wild type DNA was digested with EcoRV (lane1), EcoRI (lane 2) and NcoI (lane 9) and served as a negative control. *GID5-HA_3* DNA was digested with EcoRI (lane3) and EcorV (lane 4). In lane 3 a 3897 bp and in lane 4 a 5958 bp fragment could be visualized. *GID7-HA_3* DNA was digested with EcoRI (lane5) and EcoRV (lane6). A 3740 bps in lane 5 and a 6416 bps fragment in lane 6 can be seen. In lane 7 and 8 DNA from *GID9-HA_3* was also digested with EcoRI (lane7) and EcoRV (lane8). The fragment sizes were 5931 and 2541 bps. DNA from *GID8-HA_3* was digested with Nco1 (lane10) and a 4360 bp fragment could be revealed. All fragments corresponded to the calculated sizes. The asterisk marks a cross reaction band in EcoRV digests that appears also in the negative control. Southern blots for *GID8-HA_3* were performed together with Sven Alberts (Alberts, 2005), for *GID6-HA_3* together with Bernhard Braun (Braun, 2006).

All strains show a Southern restriction pattern at the expected sizes and therefore carry the integration cassette at the authentic GID-gene locus. For further verification of the novel strains it was necessary to check the biological activity of the modified Gid proteins.

Non functional Gid proteins lead to a disturbed catabolite degradation of FBPase (Regelmann et al., 2003) hence the name glucose induced degradation deficient (GID). Therefore it was important to check whether the triple HA epitope disturbed the biological functionality or not. This was done by testing the ability of the modified strains to still be able to promote degradation of FBPase.

Figure 6A-E shows that all HA tagged Gid proteins are functional with an FBPase degradation pattern comparable to the wild type strain. A somewhat reduced capability of catabolite degradation can be observed in Figure 6E for cells expressing the Gid9-HA_3 fusion protein. However, although slightly slower, the catabolite degradation of FBPase can still take place and the strain was used for further studies.

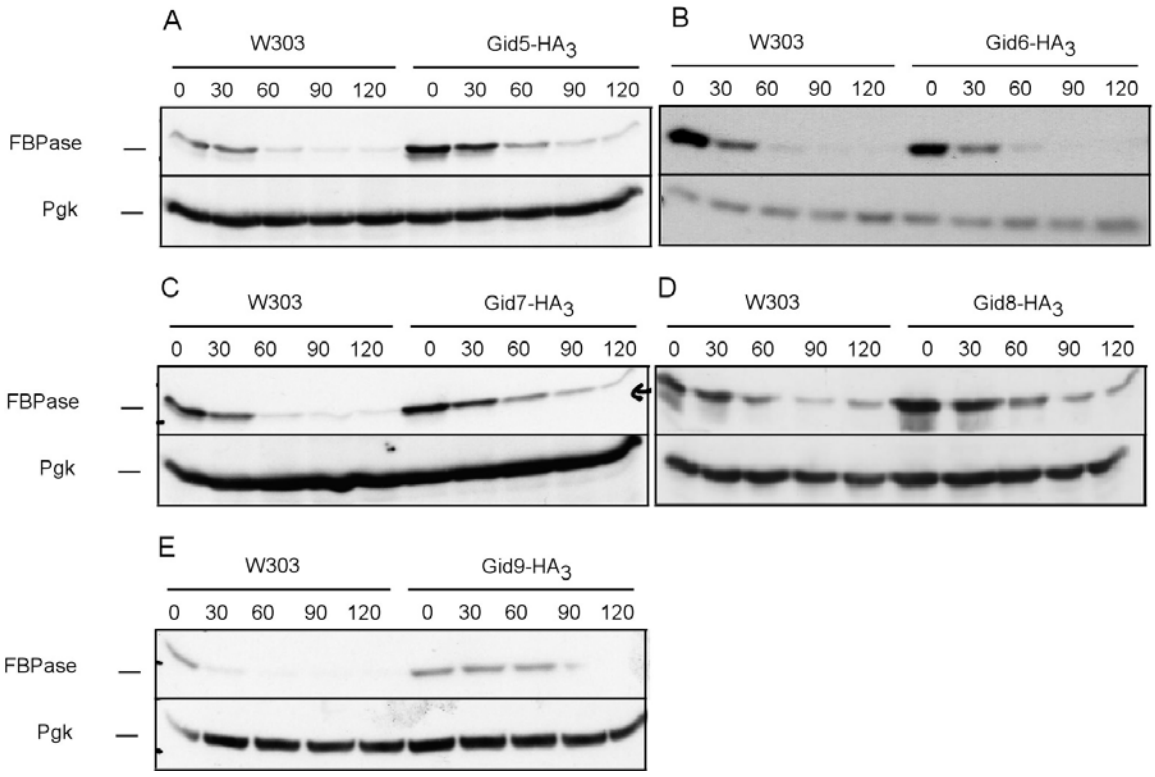

Figure 6: Functionality of HA_3 tagged Gid proteins. All strains with a C-terminal Gid-HA_3 fusion were cultured in YPEtOH for 16 h to induce gluconeogenesis. W303 was used as a positive control. Samples were taken after 16 h of derepression (0) and thereafter every 30 minutes after addition of 2% glucose, up to 120 min (30- 120). After lysis of cells and subsequent electrophoresis of cell extracts, protein was transferred onto a nitrocellulose membrane. The fate of FBPase was traced by visualization with FBPase specific antibody. Pgk1 specific antibody was used to show homogenous loading of protein. In (A) strain YTP11 (Gid5-HA_3), in B strain Gid6-HA_3, in C strain YTP10 (Gid7-HA_3), in D strain YSA1 (Gid8-HA_3) and in D strain YTP12 was tested for the functional catabolite degradation of FBPase. The Gid6-HA_3 (B) fusion protein was made together with Bernhard Braun (Braun, 2006) and the Gid8-HA_3 fusion protein (D) was made together with Sven Alberts (Alberts, 2005).

3.1.2 Expression patterns of the Gid fusion proteins

According to the expression pattern of Gid2 and Gid3/Ubc8 (Regelmann et al., 2003; Schüle et al., 2000) it was interesting to see whether other Gid proteins involved in catabolite degradation of FBPase followed a similar regulation and expression pattern. Gid2 and Gid3/Ubc8 are not present in logarithmic grown cells in a rich glucose medium. However after derepression of FBPase in medium with non-fermentable carbon sources both proteins are upregulated. Interestingly Gid2 is rather stable after the onset of catabolite inactivation while Gid3/Ubc8 is rapidly degraded. Two hours after addition of glucose to derepressed cells the protein level of Gid3/Ubc8 is not detectable anymore (Regelmann et al., 2003; Schüle et al., 2000). Both results match the measured mRNA levels of *GID2* and *GID3/UBC8* during a diauxic shift. Under glucose depleted conditions the mRNA level of *GID2* and *GID3/UBC8* is strongly upregulated (DeRisi et al., 1997). It is also interesting to mention that the addition of cycloheximide strongly disturbs the catabolite degradation of FBPase (Chiang and Chiang, 1998; Pfirrmann et al., 2006) and leads to a block of polyubiquitination of FBPase (Schork, 1995). Cycloheximide is known to inhibit translation elongation and therefore stops new protein synthesis. This shows that protein *de novo* synthesis is required for the successful completion of catabolite degradation.

To look if one of the newly discovered Gid proteins is such an upregulated *de novo* synthesized protein responsible for the degradation of FBPase, expression patterns had to be determined. This was done similar to the elucidation of the expression patterns of Gid2 and Gid3/Ubc8 (Regelmann et al., 2003; Schüle et al., 2000).

As can be seen in Figure 7 all tested Gid proteins are present under derepression conditions already (0) and none of them is upregulated during activation of catabolite degradation. A constant decrease of Gid5-HA_3 protein can be observed and after 120 min glucose shift the signal almost disappears (Figure 7B). However all other Gid proteins are rather stable and seem to be constitutively present during the catabolite degradation process. In Figure 7A the protein pattern of Gid1-HA_3 shows a double band. It could be shown that Gid1 underlies phosphorylation (Jochen Regelmann, unpublished data). However no particular role for this posttranslational modification could be revealed yet. It is interesting that no fluctuations of this modification can be observed during catabolite degradation.

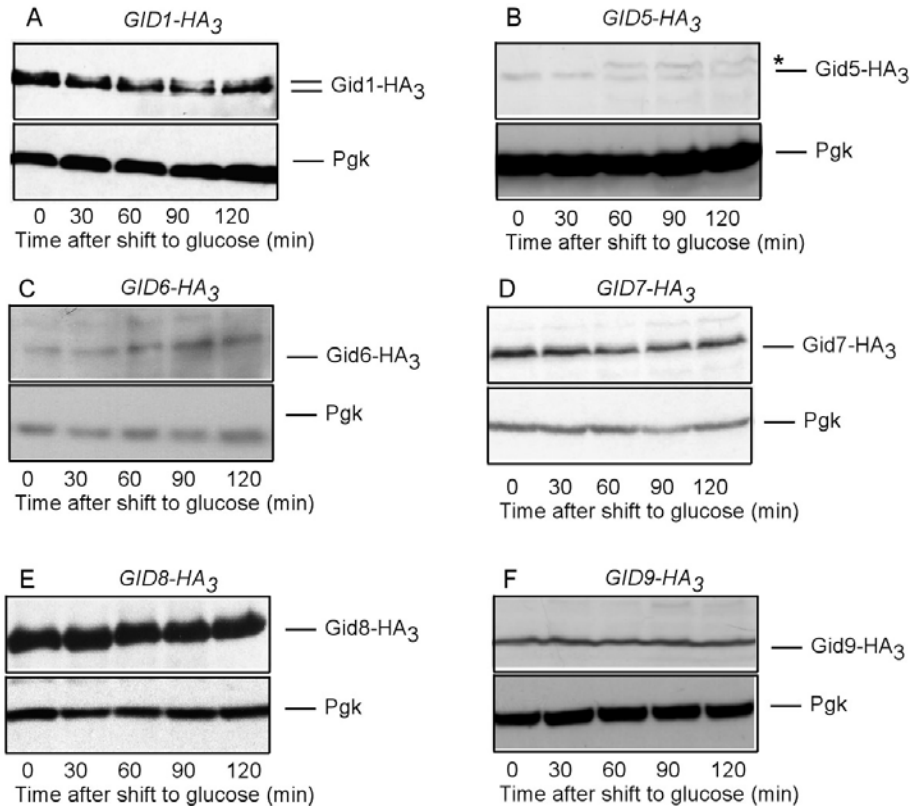

Figure 7: Expression profiles of Gid proteins. To see if Gid proteins are upregulated during the onset of catabolite degradation the strains *GID1-HA$_3$* (A) and *GID5* to *GID9-HA$_3$* (B-F) were grown on YPEtOH for 16h to induce gluconeogenesis. 1.5 OD of cells were taken (0) and thereafter samples were taken every 30 min after glucose addition to cells (30-120). To visualize Gid proteins, cells were lysed, cell extracts were separated by electrophoresis with subsequent Western blotting and decoration with antibody against the HA epitope. Antibody against Pgk was used to check for homogenous protein concentration in all lanes. The asterisk marks a cross reaction band.

None of the up to now investigated Gid proteins is upregulated after glucose shift. Therefore these components of the catabolite degradation machinery cannot be responsible for the earlier described dependency of the catabolite degradation of FBPase on new protein synthesis. To be able to immunologically detect Gid4/Vid24 it was necessary to affinity purify a polyclonal antiserum raised against Gid4/Vid24.

3.1.3 Purification of polyclonal antiserum against Gid4 and Western blot analysis

Gid4/Vid24 is a 42 kDa protein which has been described to be essential for the vacuolar degradation of FBPase. There it is proposed to be a peripheral membrane protein that is needed for the specific transportation of FBPase containing vesicles to the vacuole (Chiang

and Chiang, 1998). Interestingly Vid24 is also important for the proteasomal degradation of FBPase and has been named Gid4 in this context (Regelmann et al., 2003). Gid4/Vid24 is described to be upregulated after glucose shift for the vacuolar degradation of FBPase (Chiang and Chiang, 1998; Kaniak et al., 2004). To further study the influence of Gid4 on proteasomal catabolite degradation it was important to purify an antiserum that was produced in earlier studies (Josupeit, 2003). This was done as described in chapter 5.4.8.

As can be seen in Figure 8, a Gid4 specific signal appears 30 min after the cells were shifted to glucose (30) in wild type cells (W303) and almost disappears 120 min after glucose shift (120). In the sample taken after 16h of derepression (0) however no signal can be seen. The *gid4* deletion strain shows no Gid4 specific signal as it serves as a negative control. A strong cross reaction band of the purified Gid4 specific antiserum appears right over the Gid4 signal and is marked with an asterisk. Eluted antibody could only be used right after elution and lost its specificity afterwards.

Gid4 is the only Gid protein that is upregulated after glucose shift. The result above was verified by a co-worker (Olivier Santt) with an epitope tagged version of Gid4. Both results show a strong upregulation of Gid4 during activation of catabolite degradation with a subsequent degradation. This result is controversial to data published by Chiang and coworkers. This work shows Gid4 which is upregulated but remains constant in protein concentration during the process of catabolite degradation (Chiang and Chiang, 1998).

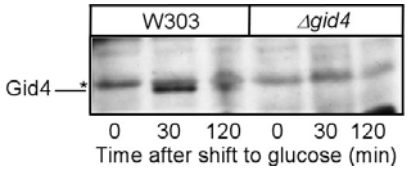

Figure 8: Expression profile of Gid4. Cells of the wild type strain W303 and of a strain deleted in *GID4* (*Δgid4*) were taken after 16h growth on YPEtOH (0) and 30 and 120 min after glucose shift (30, 120). Cell lysates were separated by electrophoresis with subsequent Western blotting and decorated with purified Gid4 specific antiserum. The asterisk marks a cross reaction band.

3.2 SUBCELLULAR LOCALIZATION OF THE GID PROTEINS

The majority of the enzymes responsible for gluconeogenesis are found in the cytoplasm. Among them is the key enzyme of this process, fructose-1,6-bisphosphatase (Stryer, 2002). However the site of catabolite degradation of FBPase in *S.cerevisiae* is still a matter of discussion. A model based on proteasomal degradation of FBPase would support a degradation process also located in the cytosol of the cell, while a model based on the vacuolar degradation proposes an uptake of cytosolic FBPase into vesicles that fuse with the

vacuole to degrade their cargo. A direct involvement of the recently discovered Gid proteins in proteasomal catabolite degradation would therefore also suggest their role in the cytosol of the cell. Supporting this idea cell fractionation experiments showed that Gid2 and Gid3 are soluble cytosolic roteins (Regelmann et al., 2003; Schüle et al., 2000). It was interesting to follow the localisation of the additional Gid proteins. In this thesis the focus was put on the distribution of Gid1, Gid6, Gid7 and Gid8.

3.2.1 Construction of C-terminal GFP fusion proteins

The green fluorescent protein (GFP) is a 27 kDa protein isolated from the jellyfish *Aequorea victoria* which has intrinsic fluorescence with an emission wavelength of 508 nm. Fused to the protein of interest, GFP is a very useful tool to study the localization and site of action of a protein within the living cell (Huh et al., 2003). To ensure that overexpression of such a fusion protein does not lead to mislocalizations in the cell it is important to keep the protein under its native promoter. Therefore a method similar to the one described in chapter 3.1.1 was chosen. Instead of a triple HA tag a green fluorescent protein (GFP) was C-terminally fused to Gid1, Gid6, Gid7 and Gid8. A PCR generated integration cassette for homologous recombination was constructed using the same primers as described before (5.1.8) with the use of the template plasmid pFA6a-GFP(S65T)-His3MX6 instead (Wach et al., 1997).

Furthermore it was important to check the newly generated yeast strains for the expression of the respective GFP fusion protein. In Figure 9 the functionality and the expression patterns of Gid1-GFP and Gid7-GFP fusion proteins can be seen. After SDS electrophoresis Gid7-GFP shows a signal at the expected size of 112 kDa (85 kDa + 27 kDa), while Gid1 runs at 130 kDa (108 kDa + 27 kDa). The wild type proteins do not show a signal at the described sizes. Compared to the wild type strain (BY), FBPase degradation in a Gid7-GFP and a Gid1-GFP strain are disturbed with no or little deradation up to 90 min after glucose shift. Strain Gid6-GFP and Gid8-GFP were constructed and tested in cooperation with Braun and Alberts. All strains were used to localize respective proteins within the cell.

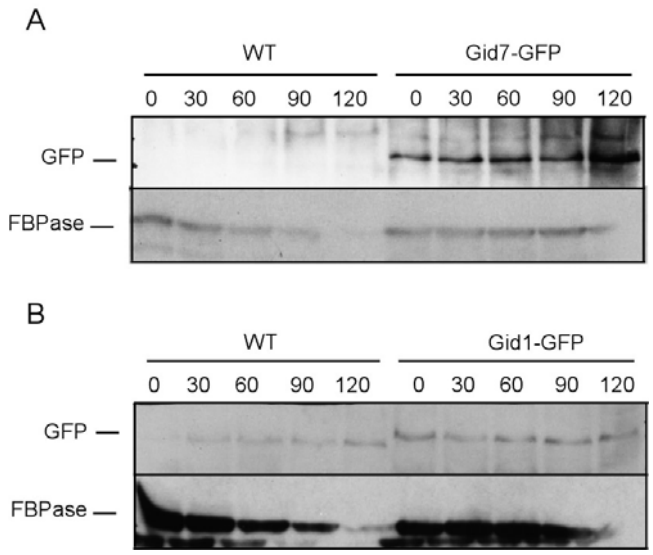

Figure 9: Functionality and expression patterns of Gid1-GFP and Gid7-GFP fusion proteins. Cells of the strains Gid1-GFP (A), Gid7-GFP (B) and BY were taken after 16h growth on YPEtOH (0 min) and every 30 min after glucose shift (30-120 min). The lysates were subjected to SDS-PAGE with subsequent Western blot analysis. GFP fusion proteins were detected with GFP specific antibodies, while the fate of FBPase was followed with FBPase specific antibody.

The localization of Gid-GFP fusion proteins was performed as described in Figure 10. Hoechst33342 stained nuclei can be seen in all investigated strains in the right column (Hoechst33342). Nomarski filter was used to watch whole cells shown in the middle column (Nomarski). The GFP signal can be seen in the left column. A BY4741 strain without a GFP fusion was used as a negative control and as expected no GFP signal can be seen. Unexpectedly all observed Gid proteins are mainly localized in the nucleus of the cell. The punctuated GFP signal clearly overlaps with the signal obtained by the nuclear Hoechst33342 staining. This rather unexpected result raises the question if Gid proteins always localize to the nucleus or if shuttling of some components occurs dependent on the growth conditions. A certain portion of Gid1 and Gid7 distributed in the cytosol cannot be excluded at this stage because a slight GFP signal also appears in the cytosol of the cell.

Cells grown under derepression conditions in SD-CA-EtOH medium showed a stronger background signal, which made it impossible to detect any GFP signal.

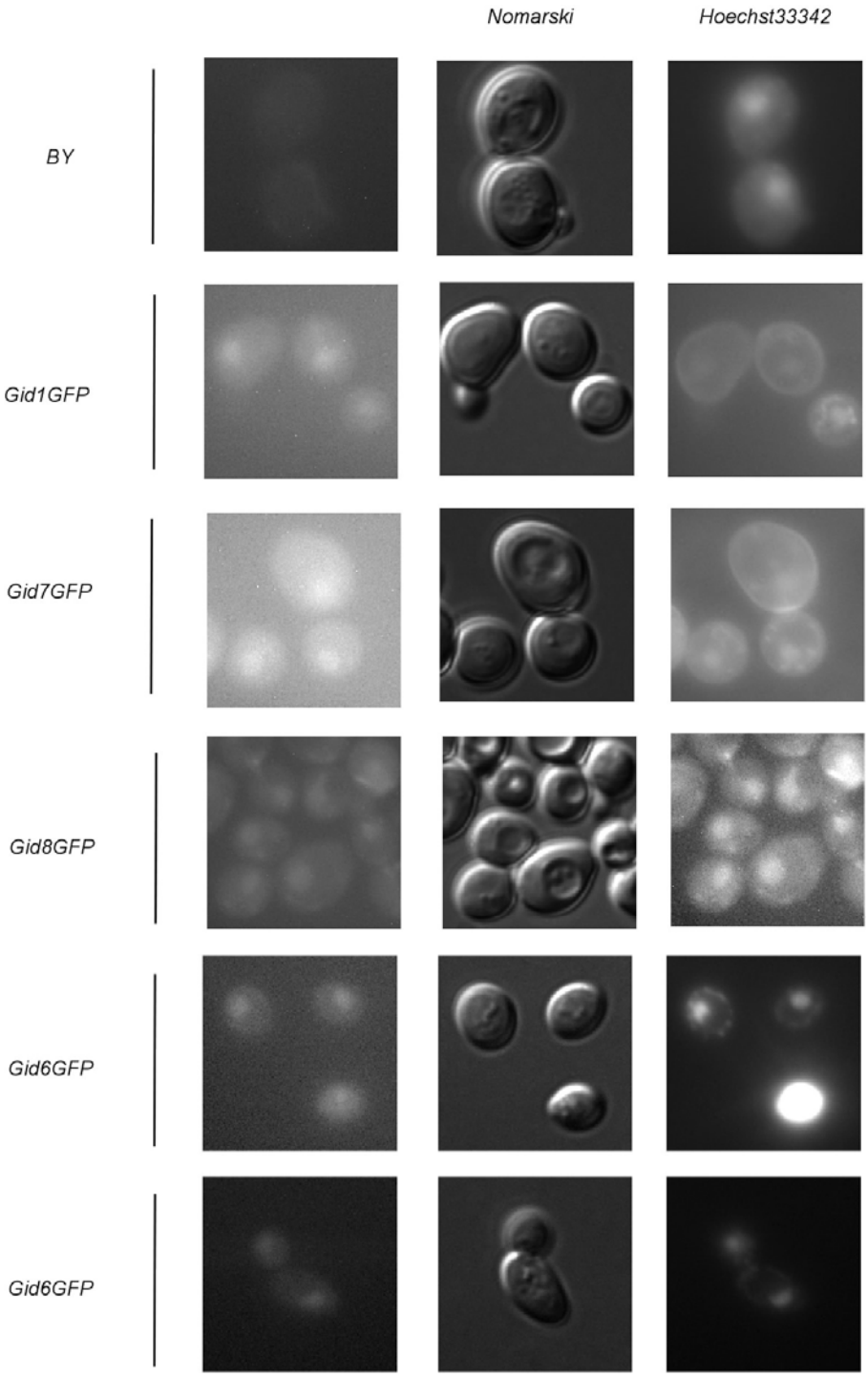

Figure 10: Localization of Gid1, Gid6, Gid7 and Gid8 in the yeast cell. Strains with the green fluorescent protein fused to Gid1, Gid6, Gid7 and Gid8 (Gid1GFP, Gid6GFP, Gid7GFP and Gid8GFP) were grown to the logarithmic phase on SD-CA-Glc medium and watched under the microscope. Nuclei were stained with Hoechst33342 (right column). GFP signals can be seen in the left column and whole yeast cells in the middle column (Nomarski). BY 4741 was used as a negative control.

3.2.2 Biochemical localization studies of Gid proteins

The result in Figure 10 indicates that Gid1, Gid6, Gid7 and Gid9 are at least partly localised in the nucleus under repression conditions. To make a clear statement about the localisation of Gid proteins before and after the onset of catabolite degradation, an additional experiment had to be designed. The method of choice was a cell fractionation experiment to isolate the nucleus from other organelles and soluble proteins (Ausubel et al., 1992). Corresponding experiments were performed for Gid7 and Gid8 in cooperation with Lise Barbin.

Figure 11 shows the distribution of Gid7 (Figure 11 A) and Gid8 (Figure 11 B) after a cell fractionation experiment designed to separate nuclei from other organelles and soluble proteins. In lane1 and 2 whole cell extracts can be seen with all marker proteins present. A comparable amount of protein was loaded for samples taken after 16h of derepression (lane 1) and 30 minutes after the onset of catabolite degradation (lane 2). Cytosolic fractions were separated after differential centrifugation (lane 3, derepressed cells; lane 4, catabolite degradation induced cells). A strong signal can be seen for the cytosolic marker protein Pgk1 and for the cytosolic protein FBPase in both samples. No or little signal can be seen for Nop1, Gid7 and Gid8 respectively. However, in the nuclear fraction (lane 5 and 6) the nuclear marker protein Nop1 shows a strong signal before (lane 5) and after (lane 6) the onset of catabolite degradation. This shows that nuclei were separated properly. Interestingly the strongest HA signals were also observed in the nuclear fractions. Gid7 and Gid8 are mainly localised to the nucleus of the cell. Minor distribution in the cytosolic fractions cannot be excluded but the low signal in the cytosolic fractions might also appear because of partially lysed nuclei. However, a relatively strong signal of Gid8 in lane 3 (Figure 11B) in the cytosolic fraction with no Nop1 signal supports a partial localisation of Gid8 in the cytosol under derepression conditions.

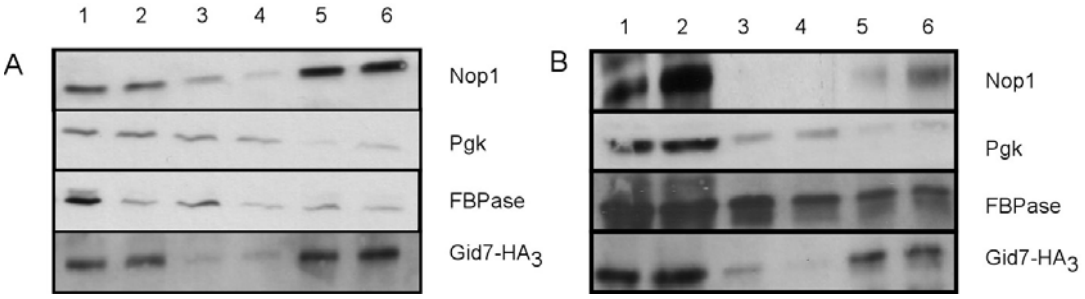

Figure 11: Distribution of the protein Gid7-HA$_3$ and Gid8-HA$_3$ in a cell fractionation experiment. To separate nuclei from total cell lysates a protocol described by Ausubel was used (Ausubel et al., 1992). Cells were taken after 16h of derepression (lane 1, 3, 5) or after the onset of catabolite degradation (lane 2, 4, 6). Lysates were subjected to differential centrifugation to separate nuclei from soluble proteins and other organelles. Samples were taken from the whole yeast extract (lane 1 and 2), from the corresponding supernatants after differential centrifugation (lane 3 and 4) and from the nuclear pellet (lane 5 and 6). All samples were subjected to SDS-PAGE and subsequent Western blot analysis. Nop1 specific antibody was used as a nuclear marker protein, Pgk1 specific antibody as a cytosolic marker protein and HA specific antibody was used to visualise Gid7 (A) and Gid8 (B).

3.3 GLYCEROL GRADIENT DENSITY CENTRIFUGATION

In recent studies the protein Gid2 was shown to co-fractionate in higher molecular mass fractions than expected from its molecular mass. Gid2 is a 49 kDa protein and was expected to co-fractionate with the 45 kDa Pgk1 in a glycerol density centrifugation experiment. However it was found in the high molecular mass fraction of yeast vacuolar aminopeptidaseI of about 600kDa instead (Regelmann et al., 2003). This result raised the question of whether other Gid proteins follow the same molecular mass distribution in a glycerol density centrifugation experiment. We therefore analysed the sedimentation behaviour of epitope tagged Gid1, Gid3, Gid4, Gid5, Gid6, Gid7, Gid8 and Gid9 (3.1.1) using the same experimental design.

As seen in Figure 12 Gid5-HA$_3$ (A; 108kDa), Gid7-HA$_3$ (B; 88kDa), Gid8-HA$_3$ (C; 53kDa) and Gid9-HA$_3$ (D; 63kDa) mainly sediment in fraction 7 and 8 together with the 600 kDa marker protein aminopeptidase I (Ape1). The 45 kDa marker protein Pgk1 is only present in fraction 2 and 3, while the 2.4 MDa marker fatty acid synthetase (Fas) is mostly present in fraction 9-10. The gluconeogenetic FBPase sediments in fraction 4-5 but is also present in the higher molecular mass fraction to a lower extent. All shown Gid proteins do not fractionate at their expected molecular masses but show a similar fractionation pattern as described for Gid2 (Regelmann et al., 2003). A possible `Gid complex` seems to be present under derepression conditions (not shown) as well as after the onset of catabolite degradation (Figure 12).

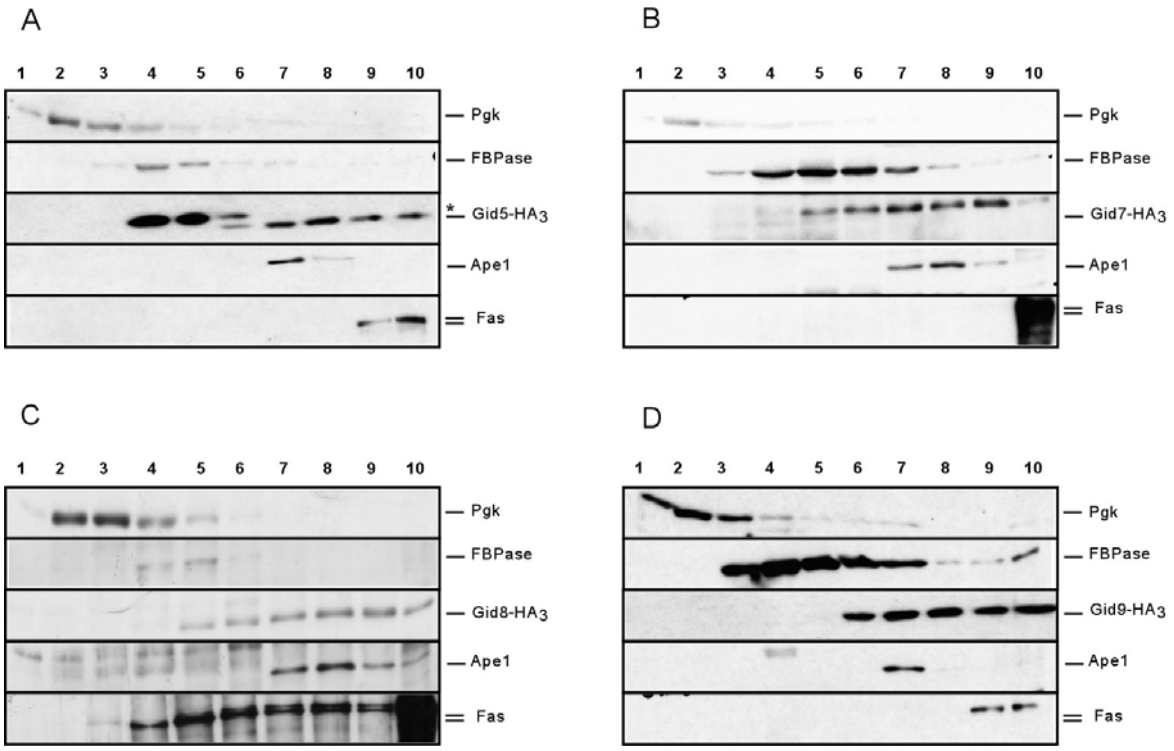

Figure 12: Distribution of Gid5 (A), Gid7 (B), Gid8 (C) and Gid9 (D) in a glycerol gradient 20 min after onset of catabolite degradation: Strains YTP11 (GID5-HA_3), YTP10 (GID7-HA_3), YSA1 (GID8-HA_3) and YTP12 (GID9-HA_3) were grown in YPEtOH and shifted to glucose containing YPD medium for 20 min. Proteins in cell extracts were separated by centrifugation in a glycerol step gradient. Fractions were collected and proteins were visualized by immunoblotting using specific antibodies. Gid proteins were visualized with HA antibody. Pgk, phosphoglycerokinase, M_r=42kDa, FBPase, fructose-1,6-bisphosphatase, M_r=148kDa, ApeI, amonipeptidaseI, M_r=600kDa; Fas, fatty acid synthase, M_r=2.4Mda. The asterisks marks a contaminating band.

Somewhat different sedimentation behaviours were observed for Gid1 (A; 108 kDa), Gid3 (C; 25 kDa), Gid4 (B; 41 kDa) and Gid6 (D; 89 kDa) (Figure 13). Epitope tagged strains were cultivated and treated the same way as described above and subjected to glycerol step gradient centrifugation (5.4.12). Interestingly Gid6 only appears in the low molecular mass fractions 3 and 4. This shows that Gid6 only exists in its monomeric state, not associated with other proteins. Gid3 (25 kDa) shows up in fraction 2 and 3 with a maximum signal in fractions 4 and 5. Gid3 however is appearing in higher mass fractions than expected (fraction 4 and 5) with a rather small amount in the expected low molecular mass fractions (fraction 2 and 3). Gid3 seems to be associated with other proteins but does not share the same distribution as other Gid proteins in Figure 12. Gid1 and Gid4 differ from other Gid proteins in Figure 12 as well. The major part of protein seems to fractionate in the low molecular mass fractions (fraction 4-5 for Gid1; fraction 3-4 for Gid4). However, a considerable amount of each protein is also present in the high molecular mass fractions up to fraction 7 (Gid4) and fraction 10 (Gid1). This shows that both proteins could also be part of a putative high

molecular mass Gid complex. Interestingly the phosphorylated version of Gid1 can only be seen in fraction 5-7. In fraction 4 only the unmodified species seems to exist.

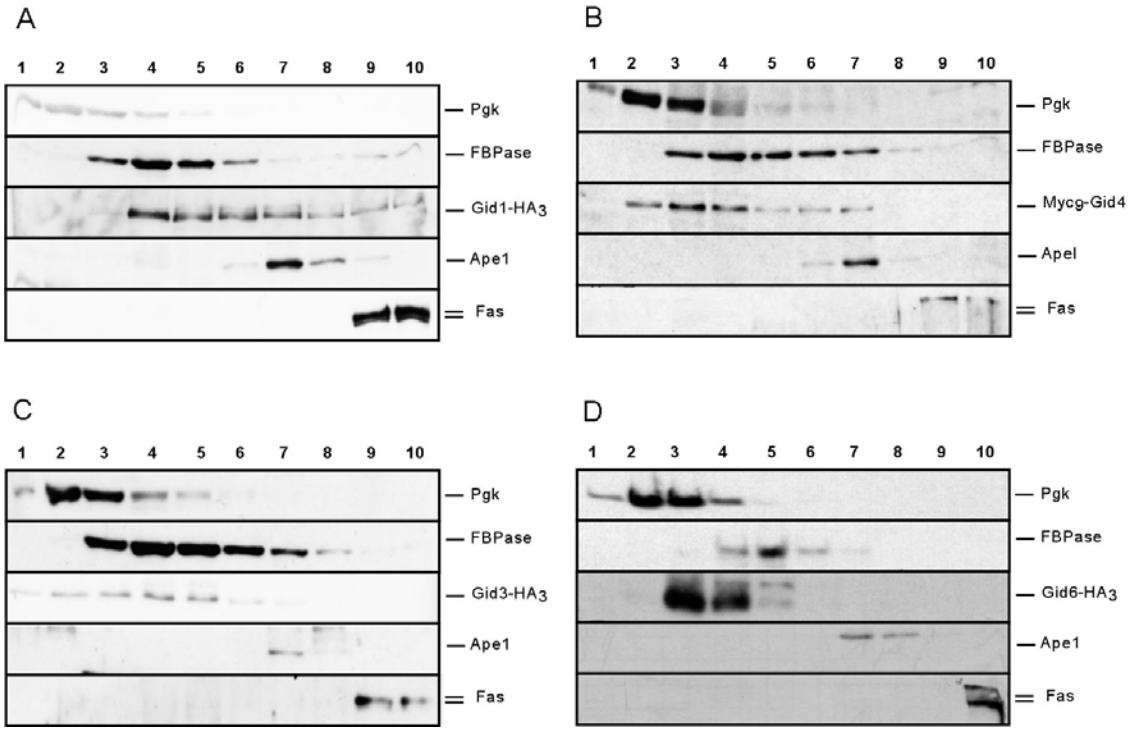

Figure 13: Distribution of Gid1 (A), Gid3 (C), Gid4 (B) and Gid6 (D) in a glycerol step gradient 20 min after onset of catabolite degradation: Gid1-HA_3, Myc_9-Gid4, Gid3-HA_3 and Gid6-HA_3 were grown in YPEtOH and shifted to glucose containing YPD medium for 20 min. Proteins in cell extracts were separated by centrifugation in a glycerol step gradient. Fractions were collected and proteins were visualized by immunoblotting using specific antibodies. Gid proteins were visualized with HA antibody, Gid4 with myc antibody. Pgk, phosphoglycerokinase, M_r=42kDa, FBPase, fructose-1,6-bisphosphatase, M_r=148kDa, ApeI, amonipeptidaseI, M_r=600kDa; Fas, fatty acid synthase, M_r=2.4Mda.

The protein Gid7 is known to contain 5 so called WD40 domains. A minimum of 5 domains are described to form a circularised beta-propeller structure which is known to coordinate multi-protein complex assemblies to serve as a scaffold for protein interactions (Smith et al., 1999). It was of crucial interest to look if the WD40 domains in the Gid7 protein would function as a scaffold for a Gid protein complex. Based on this idea the deletion of the *GID7* gene should lead to the collapse of the Gid complex. To test this, a strain Y31488 carrying a *gid7* deletion in the BY background was transformed with a 2µ plasmid that allows the expression of HA_3 tagged Gid1 (pJR15). As a control the same plasmid was transformed into Y34594 a yeast strain with a *gid1* deletion in the same background. These cells were treated as described above and centrifuged on a glycerol density gradient.

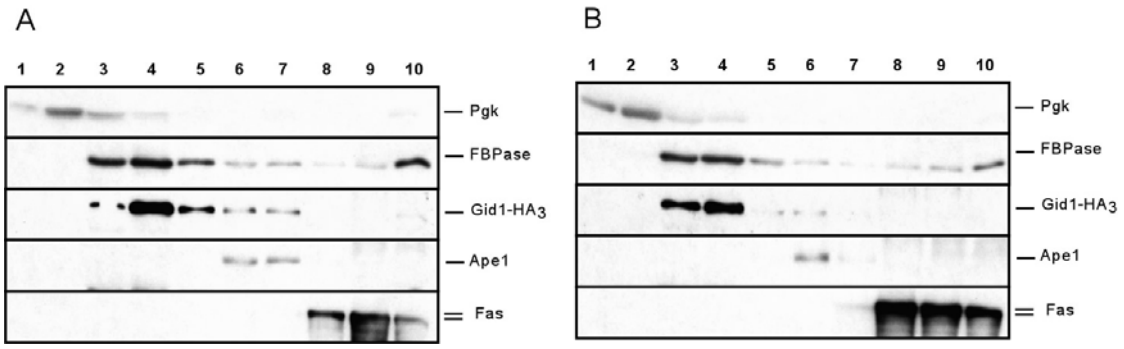

Figure 14: Distribution of Gid1 in a *gid1* deletion (A) and in a *gid7* deletion (B) in a glycerol step gradient 20 min after onset of catabolite degradation: The strain Y31488 carrying a *gid7* deletion and Y34594 carrying a *gid1* deletion was transformed with a 2µ plasmid that allows the expression of HA_3 tagged Gid1p (pJR15). Proteins in cell extracts were separated by centrifugation in a glycerol step gradient. Fractions were collected and proteins were visualized by immunoblotting using specific antibodies. Gid1 protein was visualized with HA antibody. Pgk, phosphoglycerokinase, M_r=42kDa, FBPase, fructose-1,6-bisphosphatase, M_r=148kDa, ApeI, amonipeptidaseI, M_r=600kDa; Fas, fatty acid synthase, M_r=2.4Mda.

Figure 14 shows the distribution of Gid1-HA_3 expressed from the 2µ plasmid pJR15 in a *gid1* deletion strain. The distribution is comparable to Gid1-HA_3 expressed from its endogenous promotor in Figure 13A. The distribution of Gid1-HA_3 expressed from pJR15 in a *gid7* deletion strain looks similar. The extension of Gid1 to the high molecular mass fractions 5, 6 and 7 is slightly reduced. This could indicate the collapse of the Gid complex in a *gid7* deletion strain. However, such a hypothesis needs further experimental evidence.

3.4 THE GID PROTEIN COMPLEX

As shown in Figure 12 five out of nine Gid proteins are cofractionating in the high molecular mass fractions with the 600 kDa marker protein Ape1 and higher. Somewhat different sedimentation behaviours can be observed for Gid1 and Gid4 (Figure 13). The major part of both proteins seems to exist in the low molecular mass fractions of their calculated mass. However a minor distribution of both proteins also cofractionates with Ape1. These results raised the question of whether all the examined Gid proteins except Gid3 and Gid6 do function together in a protein complex. To prove the existence of such a 'Gid complex' further experiments had to be done. A state of the art experiment to look for *in vivo* interactions of proteins in the cell is the so called co-immunoprecipitation (Co-IP) (3.4.1). The so called two hybrid system was chosen to verify results in a genetic screen (3.4.2) (Fields and Song, 1989). To study the behaviour of the Gid complex during catabolite degradation protein complexes were electrophoretically separated under native conditions (3.4.3). Finally the presence of FBPase itself in the Gid complex had to be investigated (3.4.4).

3.4.1 Interaction studies of Gid proteins using co-immunoprecipitation

Co-immunoprecipitation (Co-IP) is an *in vitro* method used to study protein-protein interactions. For Co-IP a specific antibody is used to immunoprecipitate a target antigen. Associated proteins are then detected by Western blot analysis using the respective antibodies against these proteins (5.4.11).

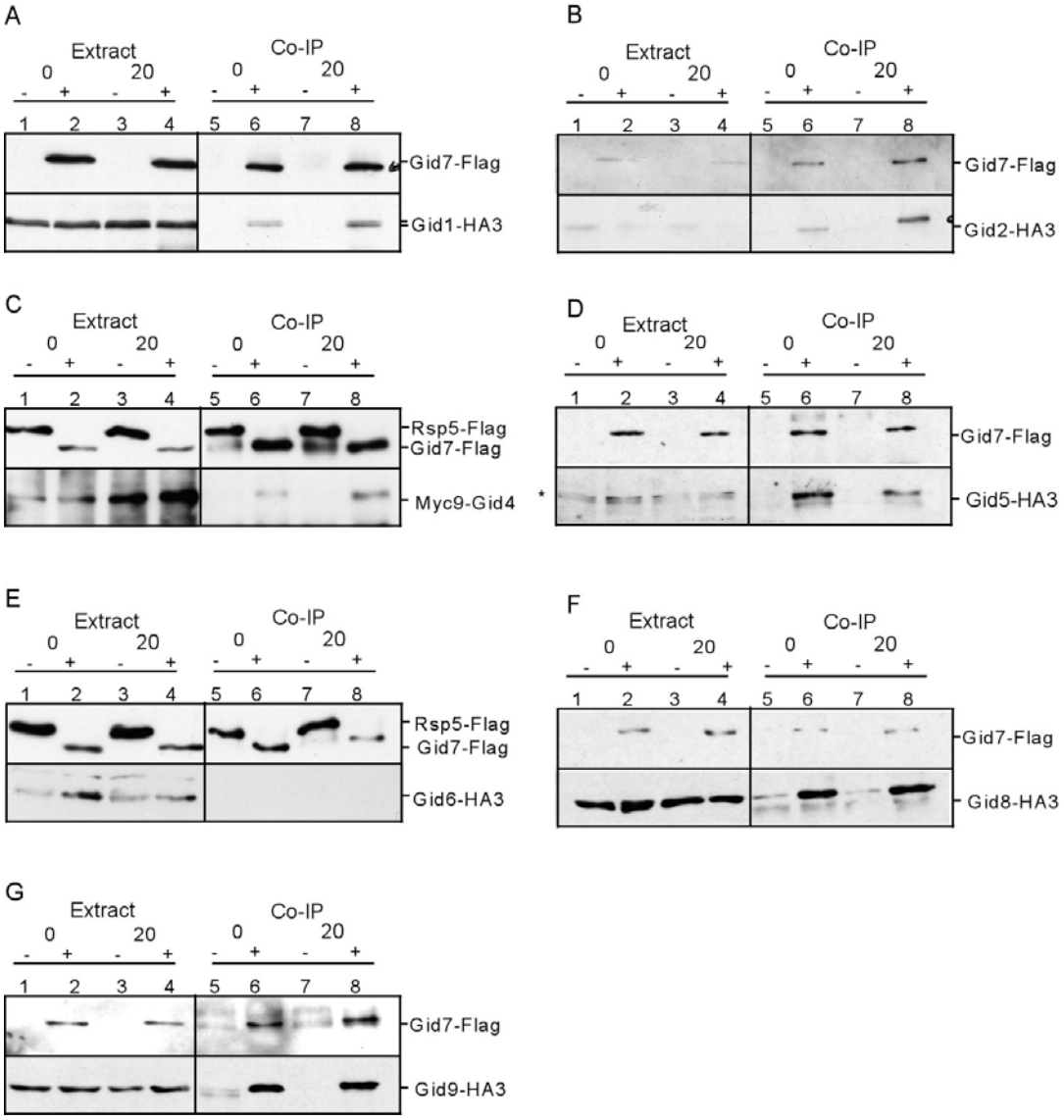

Figure 15: Interaction studies with Co-immunoprecipitation experiments. The strains expressing Gid1-HA_3 (A), Gid2-HA_3 (B), Myc_9-Gid4 (C), Gid5-HA_3 (D), Gid6-HA_3 (E), Gid8-HA_3 (F) and Gid9-HA_3 (G) containing a plasmid with a galactose inducible Gid7-FLAG were grown on media containing 2% ethanol for 14h. Gid7-FLAG and, as a control, Rsp5-FLAG was induced by adding 2% galactose. After additional 2h growth 15 OD of cells were harvested (0) or shifted to medium containing 2% glucose for 20 min (20) and harvested. 20µl of yeast extract was used as a loading control (extract). The remaining lysate was used to IP Gid7-FLAG and, as a negative control, Rsp5-FLAG with FLAG specific antibody. Immunoprecipitates were then washed solubilized in urea buffer and subjected to SDS PAGE with subsequent Western blotting. Blots were developed with FLAG specific antibodies to detect immunoprecipitated Gid7-FLAG and with antibodies against the HA or Myc epitope to detect Gid7 associated Gid proteins. As a negative control empty plasmid or a plasmid containing galactose inducible FLAG tagged Rsp5 was used (-). In lane 1-4 yeast extract shows the homogeneous expression of Gid proteins. Lane 5-8 shows immuno- and coimmunoprecipitated Gid proteins. All shown Gid proteins except Gid6 do interact with Gid7 *in vivo*. The asterisk marks a contaminating band.

In Figure 15 *in vivo* interactions of different epitope tagged Gid proteins are shown. Gid7-FLAG is only expressed in strains carrying the galactose inducible Gid7-FLAG plasmid (+) and can be seen in lanes 2 and 4 of the 'extract' panel. Successful immunoprecipitation of Gid7-FLAG can be seen in lane 6 and 8 in all experiments (A-G). Triple HA tagged Gid proteins or myc tagged Gid4 can be detected in the loading controls both in strains carrying the inducible Gid7-FLAG plasmid or the control vector without the GID7-FLAG gene. A somewhat different expression is visible in case of Gid4. Only a weak signal can be seen in the 0 min samples (lane 1 and 2) however after Co-IP a Myc signal can be detected in samples expressing Gid7-FLAG. Samples with an empty or a galactose inducible Rsp5-FLAG vector were used as a negative control and, as expected, do not show the HA or Myc specific signal. Co-immunoprecipitates of the investigated Gid proteins with Gid7-FLAG are therefore due to direct interaction and not due to unspecific binding.
Gid1 (A) and Gid2 (B) interact with Gid7 both under derepression conditions at time 0 and 20 min after onset of catabolite degradation (20). A slight increase of the signals however is observed after the onset of catabolite degradation. This can be explained by the need to recruit Gid1 and Gid2 to the Gid complex. Interestingly both the modified phosphorylated version and the non-modified Gid1 protein do interact with Gid7 (Figure 15A). Similar interaction patterns can be observed for Gid5 (D), Gid8 (F) and Gid9 (G) but the signal intensity is the same before and after onset of catabolite degradation. Gid4 (C) however is known to be upregulated after the onset of catabolite degradation. Therefore a strong Gid4 signal can only be seen in the yeast extract in the 20 min samples. This result shows that Gid4 is recruited to a present Gid complex. The protein Gid6/Ubp14 is not associated with Gid7 at all (Figure 15E). A role other than being a member of the Gid complex is suggested (Amerik et al., 1997).

3.4.2 Direct interactions of Gid proteins in a two hybrid system

The yeast two-hybrid system is a well described genetic screen to identify direct protein protein interactions. The transcriptional activator Gal4 binds to a promotor region on the chromosome with its DNA binding domain (BD). However in order to activate transcription under the control of Gal4 the second so called activation domain (AD) of Gal4 has to be in close proximity to the binding domain. The two hybrid assay uses the idea of fusing a protein of interest to the binding domain (BD-GidX) and another putative binding partner of GidX to the activation domain (AD-GidY) (Figure 16). Only when BD-GidX and AD-GidY do interact with each other the transcriptional activator Gal4 is functional. By putting some

reporter genes such as *HIS3* and *LACZ* under the control of the Gal4 promoter regions a protein protein interaction screen can be performed. Reporter genes are only expressed when both fusion proteins BD-GidX and AD-GidY physically interact with each other (Fields and Song, 1989). Successful interaction maps of proteins within multiprotein complexes have been performed for the yeast 26S proteasome (Cagney et al., 2001) and were planned for the Gid complex in the same manner.

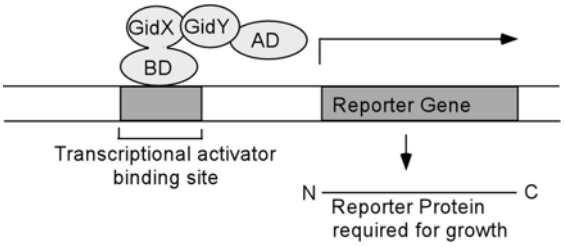

Figure 16: Model for the yeast two hybrid screen. The transcription of a reporter gene is controlled by the transcriptional activator Gal4. Two subunits, a DNA binding domain (BD) and an activation domain (AD) have to be in close proximity to each other in order to activate transcription. By fusing GidX to the DNA binding domain of Gal4 and GidY to the activation domain of Gal4 the transcription of a reporter gene is only possible when GidX binds GidY. Reporter genes are *HIS3* and *LACZ*. Positive protein protein interaction can be measured by histidine prototrophy and blue white screening on X-Gal.

To perform such a screen, fusion proteins of different Gid proteins with the activation domain and the DNA binding domain of Gal4 had to be made (5.4.9.1). These were taken to study the interaction of different Gid proteins as described in chapter 5.4.9.2.

Figure 17 shows the two hybrid assay performed to look for physical interaction of the proteins Gid4, Gid5, Gid7 and Gid9 with each other. In the first column the construct pOADGID4 was transformed into yeast Y190 together with the plasmid pOBD-2GID4, pOBD-2GID5, pOBD-2GID7 and pOBD-2GID9 respectively. Same interactions were looked at for pOADGID5, pOADGID9 and pOADGID7. To look for homogenous dilution cells were spotted on CM-Leu-Trp (lower row). The same cells were replica plated onto CM-Trp-Leu-His to screen for positive interaction partners. In all cases strains carrying the pOBD2GID7 plasmid show a very strong growth on CM-Trp-Leu-His (upper row) as well as a strong beta-D-galactosidase activity (middle row). The growth of cells carrying an empty pOAD vector together with pOBD2GID7 in the very low row (pOAD) however shows that this is not an interaction phenotype but due to so called self activation of Gid7. A weak positive direct interaction can be seen with Gid4 which is directly associated with Gid5 (left column, Y190 pOADGID4, pOBD2GID5).

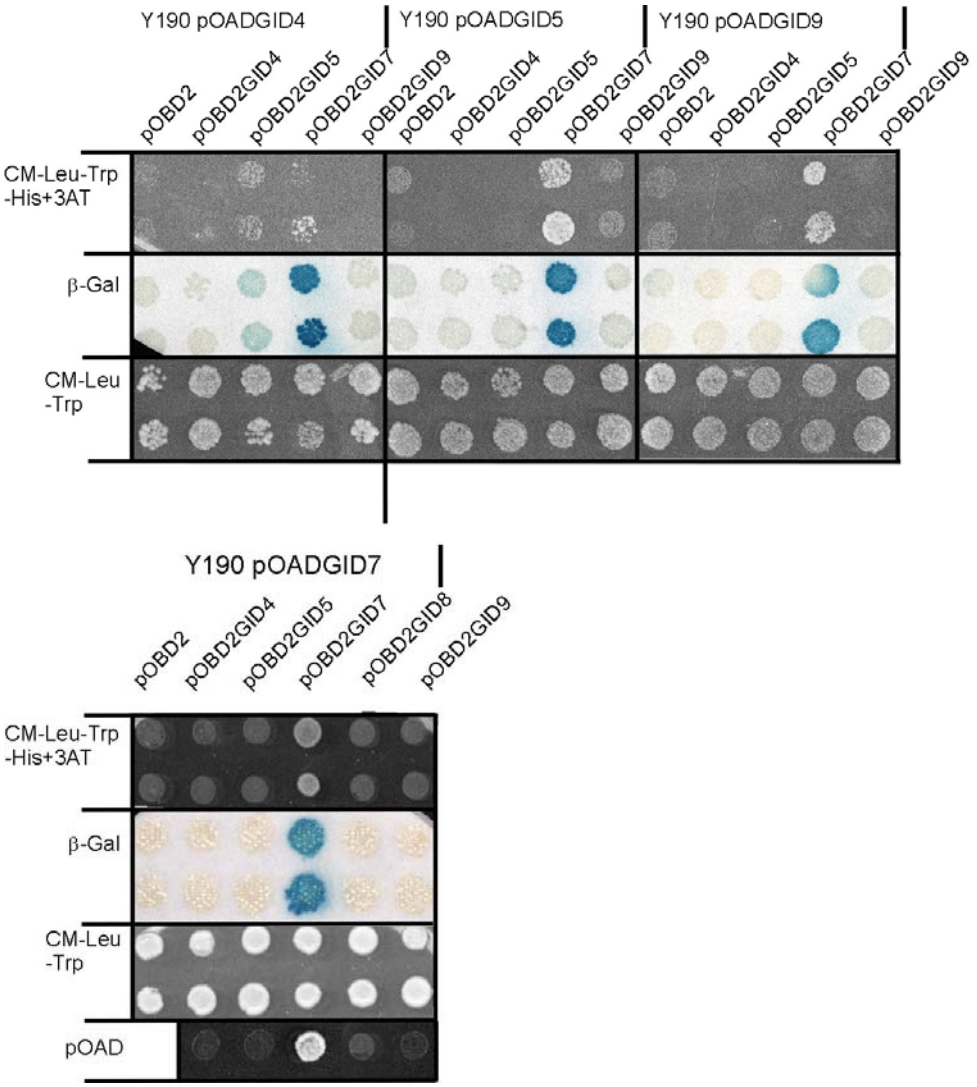

Figure 17: Two hybrid interaction assay with several Gid proteins. Yeast strain Y190 was transformed with different plasmids containing either *GID* genes fused to a GAL4 activation domain (pOAD) or to a GAL4 DNA binding domain (pOBD2). Empty plasmid was transformed as a negative control in all cases. Then 1 OD of cells was diluted in 1 ml of H_2O and 10 µl was spotted on different media. To see homologous dilution of cells samples were spotted onto CM-Leu-Trp (bottom row). To look for interaction of different Gid proteins cells were plated onto CM-Leu-Trp-His+3AT (upper row) or cells were tested for beta-D-galactosidase activity (middle row). As seen in the control experiment empty pOAD with pOBD2GID7 is positive and indicates pOBD2GID7 to be a so called self activator. Positive interactions can only be observed in case of pOADGID4 with pOBD2GID5.

3.4.3 Separation of Gid complexes by native gel electrophoresis

'Native' or 'non-denaturing' gel electrophoresis is performed in the absence of SDS. While in SDS-PAGE the electrophoretic mobility of proteins depends primarily on their molecular mass, in native PAGE the mobility depends on both the protein's intrinsic charge and its size. The intrinsic charge of a native protein is governed by its pI value and therefore changes with the pH of the buffer system. Since Gid proteins involved in the formation of the Gid complex have pI values ranging from 4.5-8.5 (www.incyte.com) a pH for the electrophoresis buffer system of 8.8 was chosen to separate the Gid complex under native conditions.

An earlier result described the recruitment of Gid4 to an otherwise stable Gid complex after onset of catabolite degradation. This raised the question of whether the recruitment of this additional protein could be visualized by native PAGE.

In Figure 18 strain W303 expressing pGid7-FLAG (+) or an empty vector (-) were grown under derepression conditions or shifted to glucose for 20 min. 15 OD of cells were taken respectively, lysed with glass beads and separated by native PAGE at a pH of 8.8. After separation the gel was soaked in blotting buffer with 0.1% SDS and proteins were transferred onto a nitrocellulose membrane by Western blotting. Afterwards the membrane was decorated with FLAG specific antibodies to visualize Gid7-FLAG (A) and with FBPase specific antibody to monitor FBPase (B).

In Figure 18A (+) Gid7-FLAG appears in three different bands. The lowest band (1) corresponds to the free non associated Gid7-FLAG protein, while band 2 and 3 can be seen in the higher molecular mass regions of the native gel both under derepression conditions (0) and 20 min after onset of catabolite degradation (20). They most likely correspond to Gid7 as a part of the earlier described Gid complex. The same distribution of Gid7 specific bands can be seen after the onset of catabolite degradation (20) with a shift upwards of band 2 and 3 (indicated by the lines). This could be caused by the recruitment of the earlier described Gid4 and other components or by the posttranslational modifications of some subunits such as the phosphorylation of Gid1. In Figure 18B the distribution of FBPase is shown in the same gel. A clear shift of the main band to the bottom of the gel can be observed for FBPase after onset of catabolite degradation (20 +/-). This could be caused by phosphorylation adding negative charge onto FBPase.

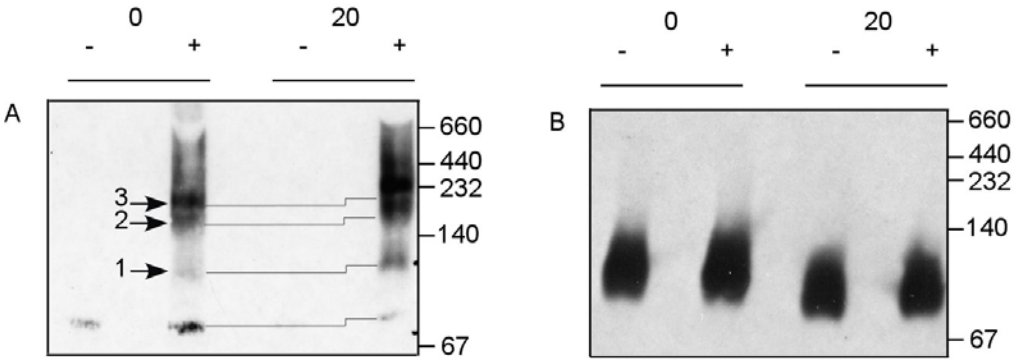

Figure 18: Separation of the Gid complex and FBPase in native PAGE. In "A" three bands of Gid7-FLAG can be seen before (0) and after glucose shift (20). The band highlighted with "1" corresponds to Gid7-FLAG not associated to a Gid complex while band 2 and 3 belong to higher molecular mass protein complexes. A shift of both bands to higher levels can be observed after glucose shift. In "B", FBPase is present in all lanes however a remarkable shift to the bottom of the gel can be seen after glucose shift (20). A protein mixture of bovine serum albumin (67 kDa), lactate dehydrogenase (140 kDa), catalase (232 kDa), ferritin (440 kDa) and thyroglobulin (669 kDa) was also subjected to native PAGE and used as marker proteins.

3.4.4 Interaction studies of Gid proteins with FBPase

To see if FBPase itself becomes part of the earlier described Gid complex, co-immunoprecipitation experiments similar to the ones described in 3.4.1 were performed.

In

Figure 19 immunoprecipitated FBPase (IP) after 16h of derepression (0) as well as after 20 and 90 min after the onset of catabolite degradation (20, 90) in the right lower corner is shown (IP). A strong FBPase signal can be observed in W303 (WT), Gid1HA_3 and Gid6HA_3 expressing cells in the 0 samples. In the 20 minutes sample the signal is much weaker and as expected almost disappears in the 90 minute sample. Therefore this sample can be taken as a negative control. The strong band above the FBPase signal is attributed to the IgGs of the antibodies used for immunoprecipitation. Gid1HA_3 and Gid6HA_3 can both be well detected in the respective yeast extracts but any Gid6HA_3 signal disappears after immunoprecipitation of FBPase. Gid6 is therefore not associated with FBPase. However Gid1HA_3 still shows up in the IP samples. Remarkably the signal is present already under derepression conditions (0 min) but is much more intense in the 20 min sample. In the 90 min sample it almost disappears. This shows that Gid1 is associated with FBPase *in vivo* and suggests the recruitment to Gid1 after the onset of catabolite degradation. The same pattern is observed for other Gid proteins like Gid2 and Gid7 Figure 19B and Figure 19C.

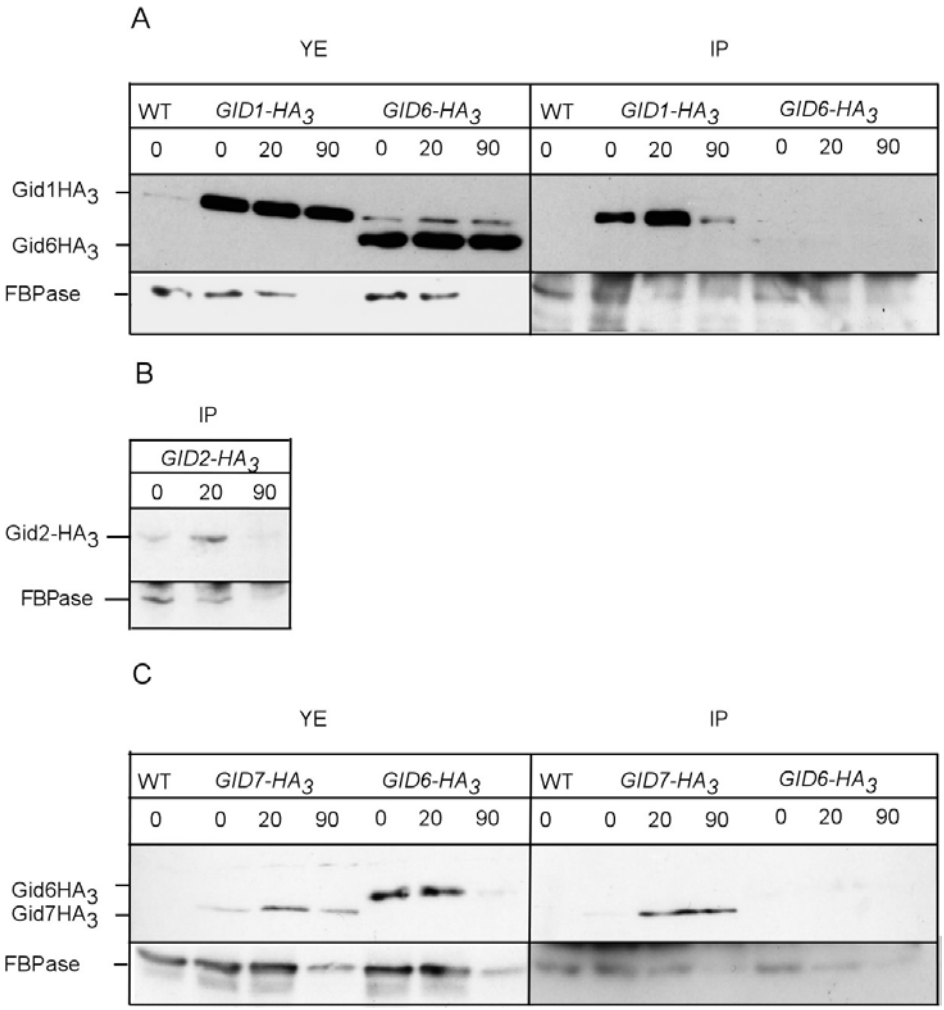

Figure 19: FBPase is associated to Gid1HA$_3$, Gid2HA$_3$ and Gid7HA$_3$ but not to Gid6HA$_3$. Strains W303 (WT), Gid1HA$_3$, Gid2HA$_3$, Gid6HA$_3$ and Gid7HA$_3$ were grown on YPEtOH for 16h and 15 OD of cells were taken (0). Same amount of cells was taken 20 and 90min after onset of catabolite degradation (20 and 90). After glass bead lysis FBPase got precipitated as described earlier (5.4.11). Precipitated proteins then got subjected to SDS PAGE and Western blotting. FBPase was visualized with FBPase specific antibody, Gid proteins with Ha monoclonal antibody. 20µl of yeast extract (YE) after lysis was used as a loading control. The 90 min sample was used as a negative control.

3.5 POSSIBLE FUNCTIONS OF GID PROTEINS AND THE GID PROTEIN COMPLEX

3.5.1 Functional domains of the Gid proteins: A bioinformatic approach

A functional domain is an element of the overall structure of a protein which folds independently and carries out a certain function. Because defined protein domains do exist in a variety of different proteins it is sometimes possible to predict the function of an unknown protein by comparing it to other proteins with similar functional domains. The possible direct involvement of Gid proteins in the ubiquitin proteasome pathway let us focus on typical

domains predominant in these processes. As it has been shown that deletion of one of the components of the Gid-complex, Gid2, leads to a defective polyubiquitination of FBPase, which might speak for E3 ligase function of the Gid-complex, a special point of interest was put on ubiquitin ligase specific domains such as the earlier described HECT or RING domains (2.1).

Table 1 shows protein domains found in Gid proteins (http://smart.embl-heidelberg.de/). A so called CRA domain could be detected in Gid1 and Gid8. This domain is described to be a protein protein interaction domain and it is uniquely found in Gid1 and Gid8 in the whole yeast proteome. Interestingly it is positioned C-terminal of the CTLH domains in Gid1 and Gid8. The CTLH domain is of unknown function and is also present in Gid2 and Gid9. The functional relationship of all Gid proteins is clearly demonstrated by the fact that all 4 CTLH domains in the yeast proteome are present only in Gid proteins as well. The name CTLH (C-terminal to LisH domain) shows the strong functional connection to the LisH domain which is present in Gid1 and Gid8. No function for this domain is known yet. Gid7 has a C-terminal stretch of 5-6 so called WD40 domains. These domains are well described and are generally believed to form a platform necessary for protein protein interactions or the assembly of multi protein complexes (Smith et al., 1999). Other domains like the 16kDa UBC domain in Gid3 are typical domains for ubiquitin conjugating enzymes (Schüle et al., 2000). The Zn finger domain in Gid6/Ubp14 is typically found in ubiquitin specific proteases (Amerik et al., 2000). Two so called UBA domains in Gid6/Ubp14 are known to bind polyubiquitin chains. All Gid proteins except Gid8 and Gid5 do have human orthologues with strong sequence conservation (right column).

		MW (kDa)	Domains	Function	H. sapiens orthologues
Gid1	Vid30	108	CRA, CTLH, LisH, SPRY	Vacuole import and degradation	RanBP10 (23%), RanBP9 (23 %), RNF123 (24%)
Gid2	Rmd5	49	CTLH	/	FLJ13910 (26%), FLJ22318 (28%)
Gid3	Ubc8	25	UBC	Ubiquitin conjugating enzyme	Ube2H (54%)
Gid4	Vid24	41	/	Vacuole import and degradation	C17ORF39 (29%)
Gid5	Vid28	105	/	Vacuole import and degradation	/
Gid6	Ubp14	89	2 UBA, ZnF-UBP	Ubiquitin specific protease	USP5 (29%), USP13 (27%), USP26 (27%)
Gid7	/	85	LisH, 5 WD40	/	WDR5 (32%), WDR26 (21%), WDR5B (31%)
Gid8	/	52	CRA, CTLH, LisH	/	/
Gid9	Fyv10	60	CTLH	Function required for yeast viability on toxin exposure	MAEA (22%), FLJ22318 (25%)

Table 1: Protein domains of Gid proteins, molecular masses and other functions apart from catabolite degradation. All Gid proteins are listed with their molecular masses (MW) in kDa. Other earlier described functions for Gid proteins were taken from Saccharomyces Genome Database. The orthologues proteins found in human cells are listed with their sequence identity in percent.

No direct hits for E3 typical domains were found in any Gid protein. However, Gid 2 contains a C-terminal stretch which could be related to a RING domain (residue 361-404). The canonical RING domain is described to be able to coordinate two zinc ions in a cross-braced arrangement. To be able to complex two zinc ions eight cysteine and histidine residues are either arranged as C3H2C3 (RING-H2) or as C3HC4 (RING-HC). To look for an evolutionary relationship of classical RING domains to the putative rudimentary RING domain found in Gid2 a sequence alignment with different classes of RING related proteins was done (Figure 20).

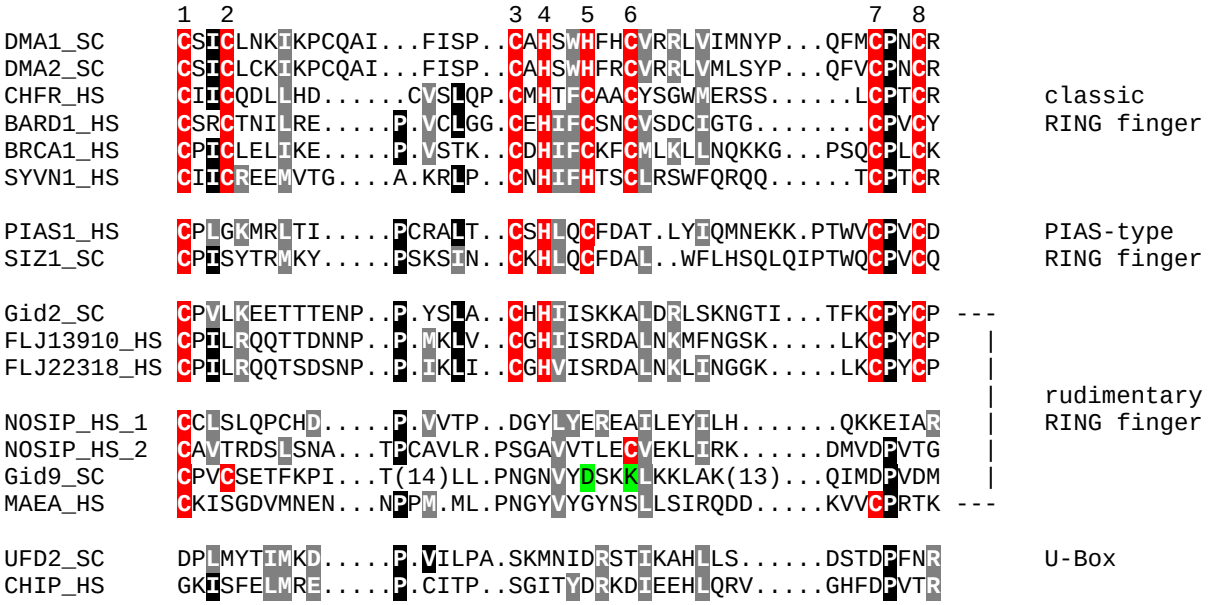

Figure 20: Alignment of representative members of each RING finger subfamily including the zinc less U-box domain. The classic RING finger proteins are shown at the top, while RING finger variants are shown below. A red background indicates zinc coordination residues or potentially zinc binding residues at positions homologous to those in the classic RING finger. Rudimentary RING domains are present in Gid2 and Gid9 in *Saccharomyces cerevisiae* (SC) and in their human orthologues FLJ13910, FLJ22318 and MAEA, respectively. (Alignments were made by MEMOREC).

Classical RING finger containing proteins such as Dma1 and Dma2 (Fraschini et al., 2004) are shown in the upper part of the alignment and show the typical distribution of eight well conserved histidine and cysteine residues (position 1-8). The coordination of one zinc ion is accomplished by residues 1, 2, 5, 6 and the other by 3, 4, 7 and 8. The yeast protein Siz1 shows a somewhat different distribution of RING typical cysteines and histidines and is

classified as PIAS-type RING finger. Siz1 is described to be a SUMO ligase which is responsible for the conjugation of the ubiquitin like modifier SUMO. It is obvious that zinc coordination residues are missing at position 2 and 6 preventing the coordination of the first zinc ion (Takahashi et al., 2001). Gid2 and Gid9 and their human orthologues were classified as 'rudimentary RING fingers' (ShRING domains). Gid2 shows a similar cysteine and histidine distribution as Siz1, however an additional cysteine residue at position 5 is additionally lacking. A more dramatic reduction of the conserved regions is detected in Gid9. Only two cysteine residues at position 1 and 2 are still present. However the strong conservation of residues present also in U-box proteins suggests the possible formation of E2 association sites independent of the coordination of 2 zinc ions for the proper function.
A sequence alignment of all known cullin proteins with the aminoacid sequences of Gid proteins showed a high degree of similarities with both Gid5 and Gid7 (see attachment). Cullin proteins are known to be subunits of multiprotein ubiquitin ligases like Cdc53 in the SCF complex (Willems et al., 2004).

3.5.2 General involvement of Gid proteins in the ubiquitin proteasome pathway

L-canavanine is an L-arginine antimetabolite which exists in plants such as legumes. The toxicity of L-canavanine is due to its close structural relationship to arginine and its incorporation into proteins instead of arginine. This incorporation leads to an increased level of functionally aberrant proteins. While low levels of this drug can still be taken by the cell in case of an intact ubiquitin proteasome system an additional defect in this degradation pathway is lethal. Growth tests on media containing low concentrations of canavanine instead of arginine can therefore be used to look for general defects in the ubiquitin proteasome pathway.

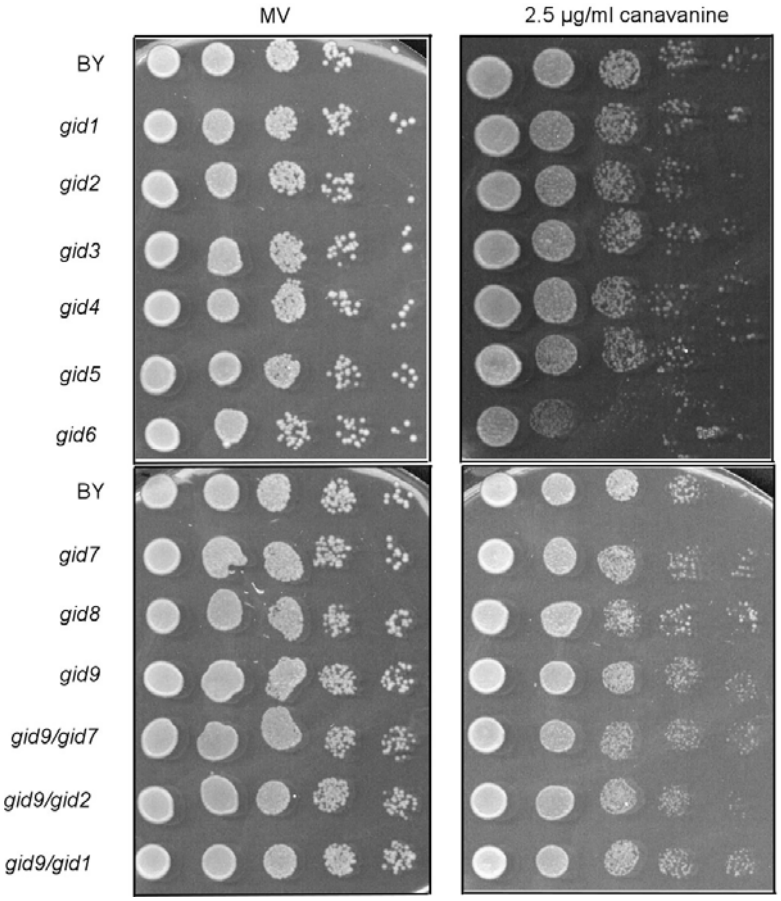

Figure 21: Growth phenotypes of *GID* deletion strains on L-canavanine. All *GID* deletion strains as well as double deletion strains *gid9/gid7*, *gid9/gid2* and *gid9/gid1* were grown on YPD over night. One OD of cells was taken and diluted in 1:10 steps respectively (left to right). Diluted cells were then plated out on MV media plus all supplements (left) and on MV media containing 2.5 µg/ml L-canavanine plus all supplements (right). BY4743 was used as a positive control.

In Figure 21 growth phenotypes of all single *GID* deletion mutants on L-canavanine can be seen. The wild type strain BY4743 was used as a positive control. Most strains with a single *GID* deletion show a growth phenotype similar to the wild type with none or a very weak growth defect. Interesting exceptions however are seen in *GID6* deleted strains which were already described to be sensitive to this drug (Amerik et al., 1997). The *gid2/9* double deletion strain shows a very slight growth defect on L-canavanine also. In addition, all strains were tested for growth on YPEtOH and under heat stress at 37°C but did not show noticable differences in growth (data not shown). Double deletion strains were constructed and analyzed together with Bernhard Braun (Braun, 2006).

3.5.3 Involvement of Gid proteins in the polyubiquitination of FBPase

In earlier experiments it was shown that Gid3/Ubc8 is necessary for the polyubiquitination of FBPase (Schüle et al., 2000). This protein is one of the major ubiquitin conjugating enzymes involved in the polyubiquitination process of FBPase. Also Gid2 was required for its polyubiquitination (Regelmann et al., 2003). To see if other Gid proteins function up- or downstream of the ubiquitination event, it was important to check the polyubiquitination level of FBPase in strains deleted in additional *GID* genes.

Figure 22 shows the polyubiquitination of FBPase during catabolite degradation in wild type cells (WT, lanes 1-4) and in strains deleted in the genes *GID1* (lane 5 and 6) and *GID7* (lane 7 and 8) respectively. Polyubiquitination of FBPase appears as a smearing protein signal which can be seen only in the wild type sample after 25 min glucose shift (lane 4). In lane 1 and 2 extracts of wild type cells transformed with an empty plasmid were run as a control. As expected, no signal can be observed. In all samples taken after 16 h of derepression no specific ubiquitination pattern of FBPase can be seen either (Figure 22, lanes 3, 5, 7). Compared to the wild type, however, both *gid1* and *gid7* deleted strains show a severe defect in polyubiquitination of FBPase. The polyubiquitination of FBPase is completly missing in both samples (Figure 22, lanes 6 and 8). This explains the importance of both proteins for the catabolite degradation of FBPase. The same phenotype could be observed for a strain deleted in *GID4/VID24* (experiment done by Olivier Santt).

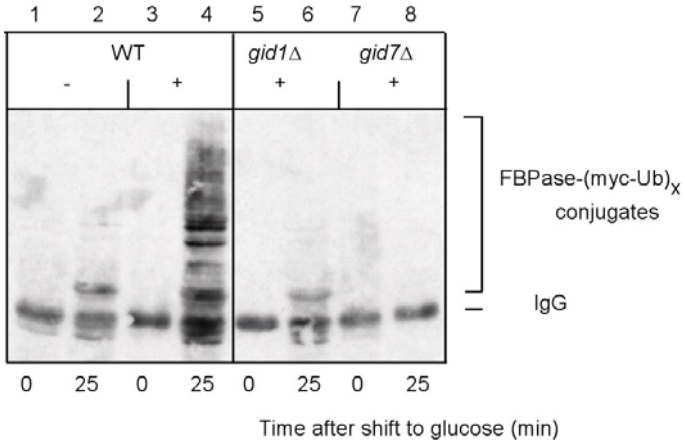

Figure 22: The polyubiquitination pattern of FBPase in *Δ*gid1 and *Δ*gid7 strains. Wild type cells (WT) were either transformed with an empty plasmid (- in lane 1 and 2) or with a copper inducible myc tagged ubiquitin plasmid (+ in lane 3 and 4). Strains deleted in *GID1* (lanes 5 and 6) or in *GID7* (lanes 7 and 8) were transformed with the same plasmid. Cells were either grown under derepression conditions for 6h (0) with 2 h copper induction or samples were taken 25 min after the addition of 2% glucose to induce catabolite degradation (25). After glass bead lysis, FBPase got pulled down with specific antibody and the precipitates were separated by SDS PAGE with subsequent Western blotting. The state of ubiquitination of FBPase was then detected with antibody directed against the myc epitope of overexpressed myc tagged ubiquitin.

3.5.4 Point mutations in the conserved cysteine residues of the Gid2 RING domain

The fact that Ubc1, Ubc4, Ubc5 and Ubc8 had been uncovered as ubiquitin conjugating enzymes and that no motif for another ubiquitin conjugating enzyme could be found in any of the additional Gid proteins, led to the hypothesis that part of the new Gid proteins might be involved in an ubiquitin protein ligase (E3) function. Therefore a respective domain search was undertaken. As shown in chapter 3.5.1 short RING domains (ShRING domains) were discovered in the proteins Gid2 and Gid9. A point mutation of the conserved cysteine residues in RING domains is known to severely disturb the function of RING E3 ubiquitin ligases (Bordallo and Wolf, 1999). Therefore the conserved cysteine residue at position 379 (cysteine379) in the aminoacid sequence of Gid2 was exchanged to a serine residue according to the protocol described in chapter 5.3.6 (Figure 23). The template plasmid for this reaction pRS316Gid2 contains the *GID2* open reading frame together with its endogenous promotor and terminator region. This plasmid was constructed together with Lise Barbin and described to be able to promote FBPase catabolite degradation in a *gid2* deletion strain (Barbin, 2005). The exchange of cysteine379 into a serine residue was verified by sequencing. Plasmids containing the described mutation were transformed into *gid2* deletion strains and tested for the ability of the mutated Gid2 protein to promote catabolite degradation of FBPase (Figure 24). As can be seen on the left hand side of Figure 24 the mutated Gid2 protein is not able to induce catabolite degradation of FBPase anymore with an almost complete stabilisation of FBPase after the onset of catabolite degradation. On the right hand side of Figure 24 the unmutated Gid2 protein expressed from the plasmid pRS316-GID2 does not seem to be fully functional as well. Therefore further FBPase inactivation experiments are underway and will be performed by my successor in the project, Bernhard Braun.

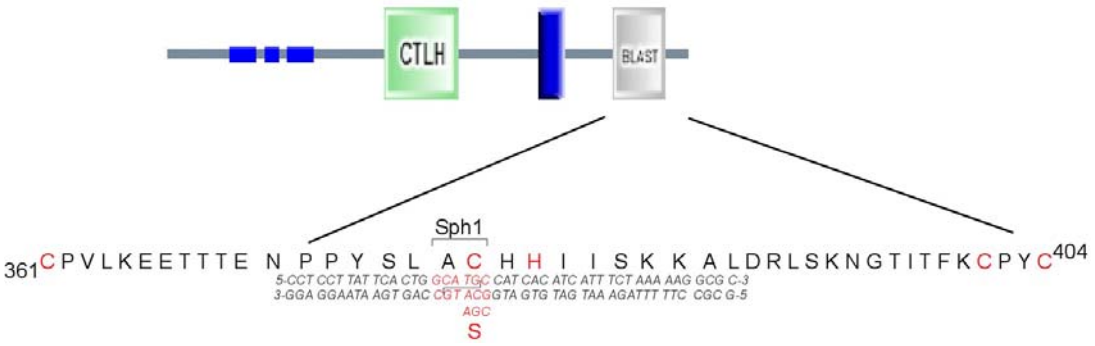

Figure 23: Mutation of the conserved cysteine residue in the ShRING domain of Gid2. A conserved cysteine residue at position 379 in the putative RING domain was changed to a serine residue according to the protocol described in 5.3.6. The template plasmid pRS316-GID2 was used to generate point mutations. A selection primer was designed to change a unique Swa1 restriction site in the backbone of pRS316 to a Pme1 restriction site (pRS Swa1-Pme1; 5.1.8). The mutation primer was designed to change the cysteine to a serine residue (P1 RING CYS1135; 5.1.8), at the same time altering the unique Sph1 restriction site in the RING domain. Conserved cysteine and histidine residues are highlighted in red.

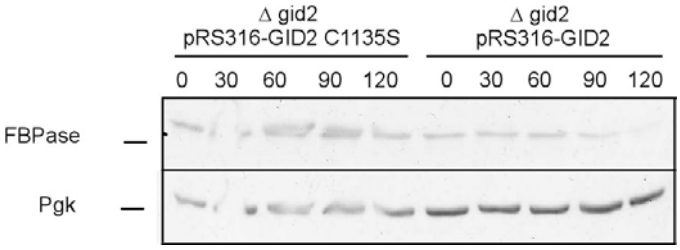

Figure 24: Influence of the conserved cysteine residue (C379) in Gid2 on the catabolite degradation of FBPase: To look if catabolite degradation of FBPase was dependent on the conserved cysteine residues within the putative RING domain of Gid2, the plasmid pRS316-GID2 (right hand side) and pRS316-GID2 C1135S (left hand side) were transformed into *gid2* deleted yeast strains. Catabolite degradation of FBPase was conducted as described in chapter 5.2.5 and samples were taken each 30 min (30-120). Cells were then lysed and total extracts were subjected to SDS-PAGE with subsequent Western blotting. The fate of FBPase was followed with FBPase specific antibodies. Homogenous protein distribution was shown with antibodies against Pgk1.

3.5.5 F-Box proteins

E3 enzymes are responsible for selection of the target substrate and provide the necessary selectivity within the ubiquitination reaction (Pickart, 2001). The Skp1/Cul1/F-box (SCF) multimeric protein complex functions as a ubiquitin ligase complex that changes its substrate specificity by alternating its F-box subunits (Willems et al., 2004). Some earlier investigations described the involvement of the F-box protein Grr1 in the process of catabolite degradation (Horak et al., 2002). The theory of the Gid complex as a novel ubiquitin ligase complex raised the question if the F-box theory could be true for the Gid complex also. The protein domain

database Smart EMBL discovers 10 yeast proteins with an F-box domain. Five of the genes coding for F-box proteins were deleted in the EUROSCARF deletion library. These strains were tested for the catabolite degradation of FBPase as described in section 5.2.5. Four of these F-box proteins were not found as subunits of the SCF complex and have unknown functions.

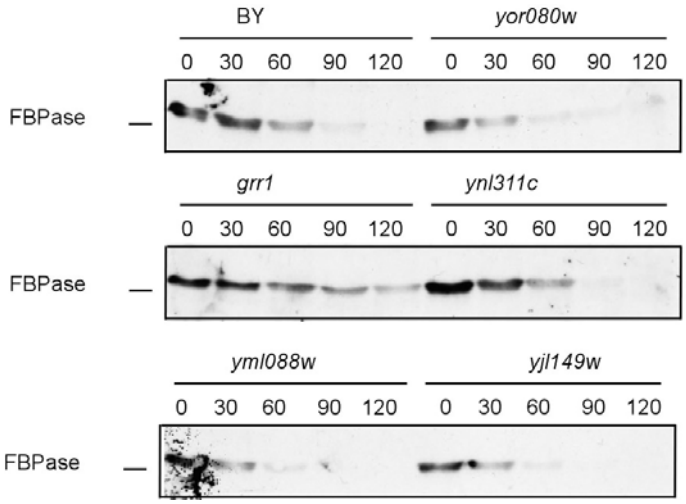

Figure 25: Involvement of F-Box proteins in the catabolite degradation of FBPase. Five F-box proteins were present in the EUROSCARF deletion collection and were tested for the catabolite degradation of FBPase as described in 5.2.5. Yor080W, Ynl311c, Yml088w and Yjl149w are hypothetical ORFs with F-box domains. In the left upper corner the catabolite degradation of FBPase can be seen in a wild type strain (BY).

As can be seen in Figure 25 the catabolite degradation of FBPase is not disturbed in *yor080W, ynl311c, yml088w* and *yjl149w* deletion strains and is comparable to the wild type pattern (BY, left upper corner). As expected the deletion of *grr1* leads to a slight defect in degradation of FBPase with an estimated two times stabilisation.

3.5.6 Construction of TAP tagged FBPase

The N-terminal proline of FBPase is essential for the polyubiquitination of FBPase and the exchange of aminoacids at the N-terminus leads to a complete stabilisation during catabolite degradation (Hämmerle et al., 1998). This unexpected result led to the question if the necessity of such a proline residue is due to the incabability of the mutated FBPase to bind its concomitant ubiquitin ligase. To test such a hypothesis the idea to purify both the mutated and the wild type FBPase seemed a good strategy to co-purify the relevant E3 ubiquitin ligase. A newly described technique to affinity purify proteins and their binding partners from low amounts of cells was chosen to do so (Puig et al., 2001). To C-terminally fuse the TAP tag to

FBPase the protocol described in chapter 5.4.10.1 was used. The correct integration of the PCR fragment was validated by PCR (data not shown) and expression tests by Western blot analysis (Figure 26).

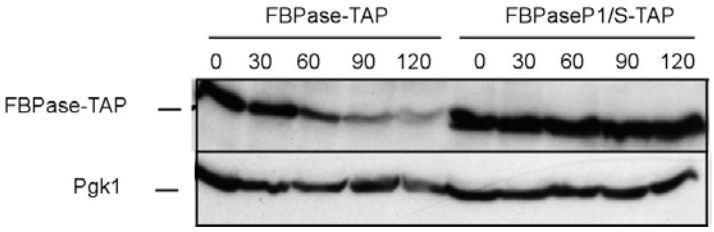

Figure 26: Expression and catabolite degradation of the C-terminally TAP tagged *FBP1* and *FBP1-P1/S* (YMH2) gene. The construction of the FBP1-TAP fusion proteins was conducted as described in 5.4.10.1. The functionality of the *FBP1* fusion product was tested by the ability to grow on a non fermentable carbon source. The expression was tested via Western blot analysis with FBPase specific antibodies.

Both fusion proteins FBPase-TAP and FBPaseP1/S-TAP are expressed at their calculated molecular mass. Wild type FBPase (37kDa) cannot be detected anymore which also shows that the PCR product had integrated at the proper gene locus. Instead a signal can be detected between 50 and 75 kDa which corresponds to the size of FBPase fused to the TAP construct (30 kDa). On the left hand side of the immunoblot in Figure 26 the catabolite degradation of FBPase-TAP can be seen. The fusion protein still undergoes the process of catabolite degradation. As expected the catabolite degradation of FBPaseP1/S-TAP does not take place. The fusion protein is stable after glucose addition (right hand side of the immunoblot Figure 26). The fact that both FBPase fusion proteins are still able to support growth of strains on a nonfermentable carbon source, with growth phenotypes similar to the wild type strain, shows that both fusion proteins are still functional in their enzymatic activity.

3.5.7 Immunoprecipitations of FBPase and detection of interacting partners

3.5.7.1 Small scale immunoprecipitation of FBPase-TAP and FBPaseP1/S-TAP

It was interesting to see if FBPase-TAP fusion proteins and possible binding partners can be immunoprecipitated together. Therefore proteins were radioactively labelled as described in 5.4.10.2 and TAP fusion proteins were pulled down with associated proteins (5.4.10.2). The second affinity purification with calmodulin beads was omitted in this experiment.

Figure 27 shows that FBPase can be purified in high amounts. Obviously, the TAP method works to purify FBPase. The letter D refers to an unknown protein that seems to interact with

FBPase only under derepression conditions but not with the P1/S mutant. A, B and E are unknown proteins which interact with FBPase during derepression conditions as well as during the process of catabolite degradation.

To make a clear statement about interaction partners of FBPase the background signals in both control lanes should be reduced by using the second purification step of the TAP method also.

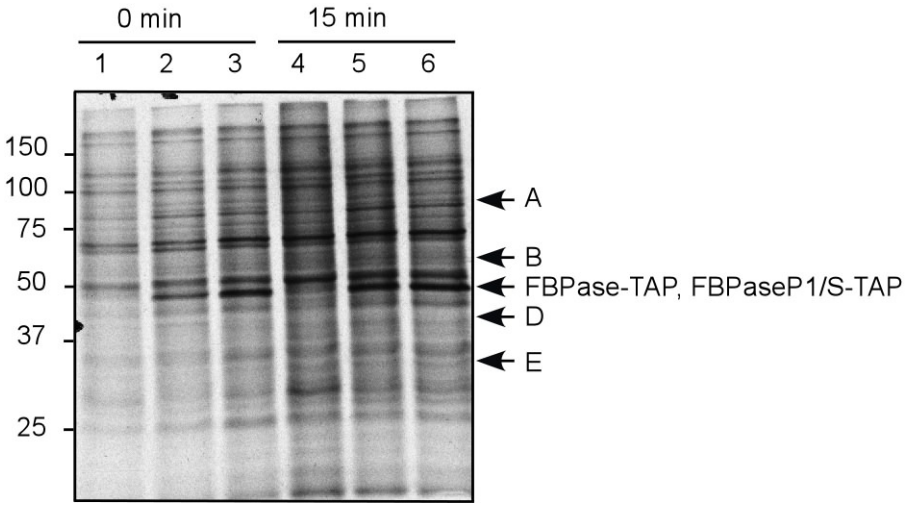

Figure 27: Immunoprecipitation of S35 labelled FBPase-TAP, FBPaseP1/S-TAP and associated proteins. FBPase-TAP and FBPaseP1/S-TAP expressing cells were grown as described in 5.4.10.2 to radioactively label all proteins. Samples were taken after 5h of derepression on a nonfermentable carbon source (0 min) and 15 min after the supplementation of 2% glucose (15 min). Cells were lysed by glass bead lysis and the supernatant was used to immunoprecipitate FBPase-TAP (lane 2 and 5), FBPaseP1/S-TAP (lane 3 and 6) and associated proteins. The wild type strain W303 was used as a negative control (lane 1 and 4). Proteins were eluted from IgG sepharose beads with 15 U of TEV protease and proteins in the eluate were precipitated with 10% (V/V) TCA. After the pellet was washed with acetone it got resuspended in urea buffer and proteins were separated by SDS-PAGE. Then the gel was dried and subjected to autoradiography. Molecular masses of proteins can be seen on the left side of the autoradiogram. C refers to precipitated FBPase in lanes 2, 3, 5 and 6. D is a protein which coprecipitates with FBPase before the onset of catabolite degradation only seen in lane 2. A, B and E are possible interaction partners of FBPase and FBPaseP1/S.

3.5.7.2 Large scale immunoprecipitation of FBPase-TAP and FBPaseP1/S-TAP

The result in chapter 3.5.7.1 showed that the newly generated TAP fusion proteins FBPase-TAP and FBPaseP1/S-TAP both can be precipitated with the TAP protocol described in 5.4.10.2. However the strong background signal in the negative control samples made it necessary to use the second purification step with calmodulin beads also. Additionally it was important to co-purify FBPase interaction partners in an amount to determine these proteins by mass spectrometry or Edman degradation. To do so, the experiment had to be scaled up as described in 5.4.10.2.

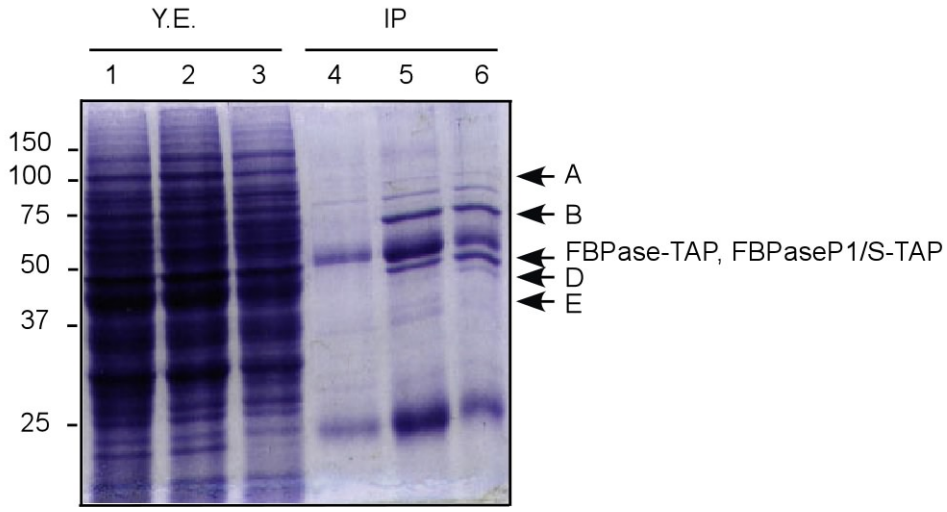

Figure 28: Large scale immunoprecipitation of FBPase-TAP and FBPaseP1/S-TAP with subsequent Coomassie staining. 1500 OD of W303, FBPase-TAP and FBPaseP1/S-TAP were grown in YPEtOH for 16 h and 1500 OD of cells were taken. After cell lysis with a French Press the lysate was clarified and used to purify FBPase protein with IgG-sepharose as described (5.4.10.2). Eluted proteins were precipitated with 10 % (V/V) TCA, washed with acetone and resuspended in urea buffer. Samples were then subjected to SDS-PAGE and proteins were stained with Coomassie. Y.E. refers to yeast extract and shows that equal amounts of protein were used for the precipitation experiments. After both affinity purification steps samples were marked with IP. The wild type strain W303 was used as a negative control in lane 1 and 4. FBPase-TAP was used in lane 2 and 5, while the strain FBPaseP1/S-TAP was used in lane 3 and 6. The molecular mass of proteins in kDa can be seen on the left side of the gel while FBPase and interacting proteins are labelled on the right side. C refers to immunoprecipitated FBPase, protein A, B, and D are unknown proteins which only coprecipitate with FBPase and FBPaseP1/S but not with the wild type FBPase. E is a protein which only coprecipitates with the FBPase-TAP protein but not with the proline exchange mutant.

Figure 28 shows a large scale immunoprecipitation experiment of FBPase-TAP and FBPaseP1/S-TAP. Several unknown proteins can be co-purified with FBPase. C refers to immunoprecipitated FBPase, protein A, B, and D are unknown proteins which only coprecipitate with FBPase and FBPaseP1/S but not with the wild type FBPase. E is a protein which only co-precipitates with the FBPase-TAP protein but not with the proline exchange mutant. The molecular mass of E is the same as protein D in Figure 27. Future determination of these unknown interacting proteins should be done by mass spectrometry.

3.6 SUBCELLULAR LOCALIZATION OF FBPASE

Localization of all investigated Gid proteins were unexpectedly found to be in the nucleus of the cell (chapter 3.2). The majority of the enzymes responsible for gluconeogenesis, including FBPase, are described to be located in the cytoplasm. In the past localisation studies of FBPase were either done by indirect immunofluorescence (Chiang and Schekman, 1991) or by cell fractionation experiments (Regelmann et al., 2003) with no focus on a nuclear

localization. Several recent publications describe FBPase to have an unknown function in the nucleus of the human cell with a possible recruitment of FBPase to the nucleus upon glucose or insulin supplementation (Yanez et al., 2003; Yanez et al., 2004; Zmojdzian et al., 2005). To analyze a possible localization or recruitment of FBPase to the nucleus, a GFP fusion of FBPase was constructed. This was done as described earlier for the Gid proteins (3.2.1). Clones were tested for the expression of GFP fusion protein (Figure 29).

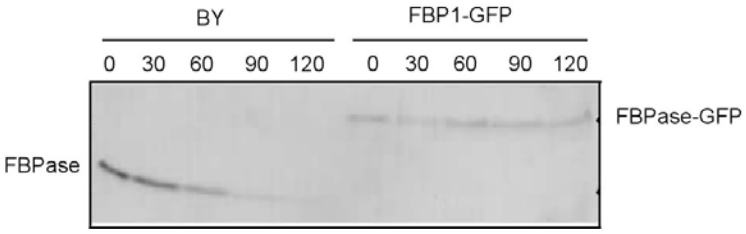

Figure 29: Expression pattern of the FBPase-GFP fusion protein. To test the expression of FBPase-GFP fusion protein, the modified strain and the respective wild type strain (BY) were grown on YPEtOH for 16 hours and 1.5 OD of cells were taken (0). Additional 1.5 OD of cells were taken every 30 minutes after these cells were shifted to YPD (30-120). Samples were lysed, subjected to SDS-PAGE with subsequent Western blot anaylsis and decoration with FBPase specific antibodies.

In Figure 29 the expression pattern and catabolite degradation of the modified FBPase-GFP protein was tested. In the wild type strain BY, the expected catabolite degradation kinetics of FBPase can be seen. A strong FBPase specific signal is observed after 16h of derepression (0) which decreases with a half life of 20 min after the cells were shifted to glucose (BY, 30-120 time points). The FBPase-GFP fusion protein is strongly expressed after 16h of derepression as well, but shows a complete stabilization of FBPase-GFP after the onset of catabolite degradation (FBP1-GFP, 30-120 min time points). The protein runs 27 kDa molecular mass higher than its corresponding wild type protein, which is the size of GFP. Positive strains were further tested for the proper integration by Southern blot analysis (Lise Barbin, diploma thesis). It is interesting to note, that in contrast to the C-terminal GFP fusion of FBPase the C-terminal TAP fusion of FBPase is degraded as the wild type protein.

In Figure 30 the distribution of GFP tagged FBPase before and after the onset of catabolite degradation can be seen. In the first column titled with ‘Nomarski’ whole yeast cells can be seen. The nuclei of the same cells are visualized in the column titled ‘Hoechst33342’, while the FBPase specific GFP signal can be seen in the very right column. Wild type cells were used as a negative control. As expected, they don’t show a GFP signal. The GFP signal of FBPase under derepression conditions (FBP1-GFP 0min) is visible in the cytosol of the cell with a somewhat stronger signal around the vacuole. No or only little signal overlaps with the nuclear staining. Very interestingly the GFP signal overlaps with the nuclear staining in cells

that were shifted to glucose for 20 min (FBP1-GFP 20min). Some signal can still be seen in the cytosol. The nuclear localisation of FBPase upon the onset of catabolite degradation suggests a glucose induced transport of FBPase into the nucleus. This result is consistent with observations made in the human cell and supports the theory of a nuclear function of FBPase (Yanez et al., 2003; Yanez et al., 2004). It is also interesting to mention that no signal at all can be seen in the vacuole of the cell, which defintely rules out a vacuolar degradation of FBPase under our growth conditions.

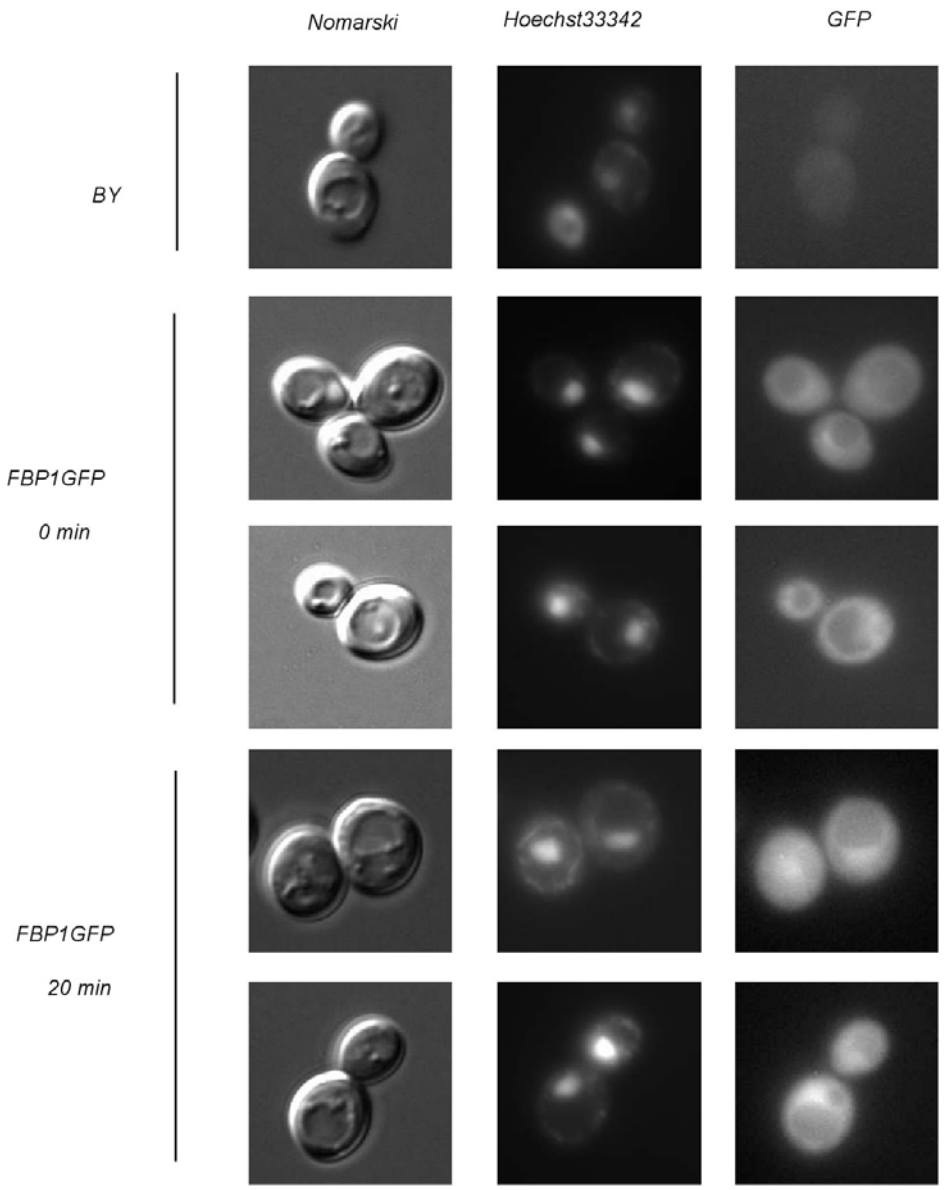

Figure 30: Localization of FBPase in the yeast cell before and after the onset of catabolite degradation. FBP1-GFP expressing cells were grown on SD-CA-EtOH medium for 16h (0 min). 20 OD of cells were harvested and resuspended in 1 ml SD-CA-EtOH medium. The same amount of cells was shifted to SD-CA-Glc medium for 5 min. To visualize the nuclei, 20 µl of Hoechst staining was added to each sample and incubated for 15 min. Cells were watched under the microscope. By using different filter units the GFP signal (right column),

the whole yeast cell (Nomarski, left column) and the nuclei (Hoechst33342, middle column) were watched. BY cells expressing non-tagged FBPase, were used as a negative control showing no GFP signal.

3.6.1 Involvement of SUMO in the catabolite degradation of FBPase

SUMO is an ubiquitin related protein modifier. The covalent modification of proteins with SUMO is comparable to the ubiquitin modification with a structurally and mechanistically related subset of enzymes (Dohmen, 2004; Dohmen et al., 1995; Saitoh et al., 1997; Stade et al., 2002). SUMOylation for instance is a necessary process for cytosol-nucleus protein shuttling (Strambio-de-Castillia and Rout, 2002). The previously shown RING domains of Gid2 strongly resemble the cysteine histidine distribution of typical SUMO ligases (Figure 20). The recruitment of FBPase into the nucleus (3.6) therefore raised the question if a nuclear localisation might be SUMO dependent and connected to its subsequent degradation. This possibility was tested with a temperature sensitive (ts) mutant of the SUMO conjugating enzyme Ubc9 (Betting and Seufert, 1996) blocking the entire SUMO pathway.

Figure 31 shows that SUMOylation has no impact on catabolite degradation of FBPase: The wild type strain has a degradation kinetics of FBPase with a half time of about 20 min (*UBC9*). A similar pattern with no or little effect on catabolite degradation of FBPase can be observed in an *ubc9-2* strain under restrictive conditions. Interestingly, the basal level of FBPase in an *ubc9-2* strain is considerably reduced. Before use the wild type strain *UBC9* and the mutant strain *ubc9-2* were tested for their ability to grow at 30°C and 37°C (not shown).

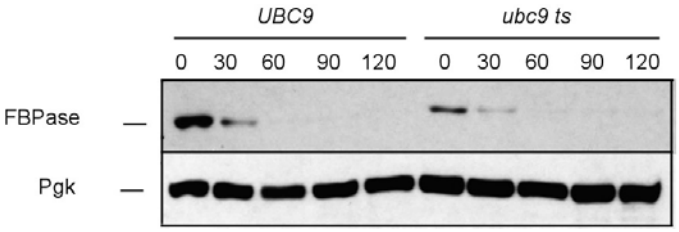

Figure 31: SUMOylation and the catabolite degradation of FBPase. For elucidation if SUMOylation is involved in catabolite degradation of FBPase, the wild type strain *UBC9* and a strain with a temperature sensitive *ubc9-2* allele were grown on YPEtOH for 16h at 30°C. Then cells were shifted to 37°C for 30 min and 1.5 OD of cells were taken (0). To activate catabolite degradation, cells were then resuspended in 37°C prewarmed YPD medium and samples were taken every 30 min up to 120 min (30-120). Cells were lysed and protein extract was subjected to SDS-PAGE with subsequent Western blotting. FBPase degradation was visualised with FBPase specific antibody. Pgk1p was used as loading control to show homogenous protein concentrations.

3.6.2 Involvement of classical nuclear import mechanisms in the catabolite degradation of FBPase

In chapter 3.6 a possible localisation of FBPase in the nucleus of the cell is proposed. To evaluate further evidence of such a result it was interesting to look for known interactions of FBPase and proteins involved in its catabolite degradation. To get an interaction network for yeast proteins of interest, a special software tool called 'Osprey' was used (http://biodata.mshri.on.ca/osprey). Osprey accesses a protein protein interaction database called 'Yeast Grid' and visualises interactions by creating an interaction network.

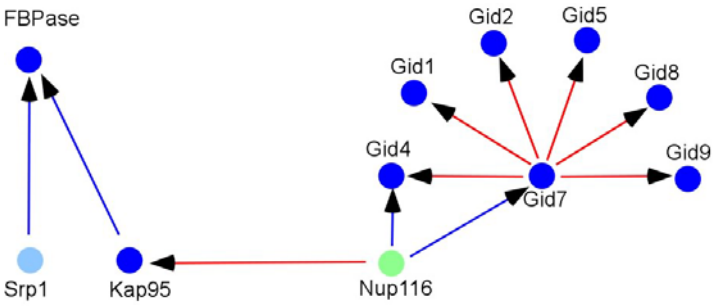

Figure 32: Simplified interaction network of FBPase and Gid proteins generated with Osprey. FBPase (*FBP1*) directly interacts with the proteins Srp1 and Kap95. Kap95 interacts with Nup116, a subunit of the nuclear pore complex (NPC). Nup116 is directly associated with Gid4 and Gid7. Bright blue nodes are proteins involved in protein transport, blue nodes indicate the involvement in carbohydrate metabolism, green stands for proteins involved in biogenesis and cell organisation. The experimental procedures used to detect interactions are represented by the colours of the arrows. Red arrows are interactions that were detected via affinity purification (Ho et al., 2002), while blue arrows are direct interactions detected by yeast two hybrid screen (Ito et al., 2001; Uetz et al., 2000).

In Figure 32 different protein protein interactions for FBPase and Gid proteins are shown. It is interesting that FBPase both interacts with Srp1 and Kap95 in a two hybrid assay. Srp1 is a so called karyopherin alpha which was described to bind classical nuclear localisation sequences of target proteins in the cytosol. After the formation of a heterotrimeric protein complex composed of the karyopherin alpha Srp1, the karyopherin beta Kap95 and the NLS containing target protein, the whole complex is translocated into the nucleus via the nuclear pore complex (NPC) (Iovine and Wente, 1997; Loeb et al., 1995). This link between cytosol and nucleus can be seen in the interaction of Kap95 with the NPC subunit Nup116 in Figure 32. Nup116 was shown to directly interact with Gid4 and Gid7 in a two hybrid screen.

This result strongly supports the nuclear translocation of FBPase via Gid proteins and proposes its import into the nucleus according to classical import mechanisms including the action of Srp1 and Kap95. Previous results (Figure 30) and some recent publications (Yanez et al., 2004) propose the regulated transport of FBPase into the nucleus of the cell upon glucose supplementation. The function of this translocation however is unclear and is therefore of our interest. The translocation of FBPase upon glucose shift raises the question of a possible catabolite degradation in the nucleus of the cell.

KAP95, *SRP1* and *NUP116* are essential genes. However some phenotypes with temperature sensitive (ts) point mutations are described (Iovine and Wente, 1997; Tabb et al., 2000; Wente and Blobel, 1993). These strains and their corresponding wild types were used to measure the catabolite degradation of FBPase.

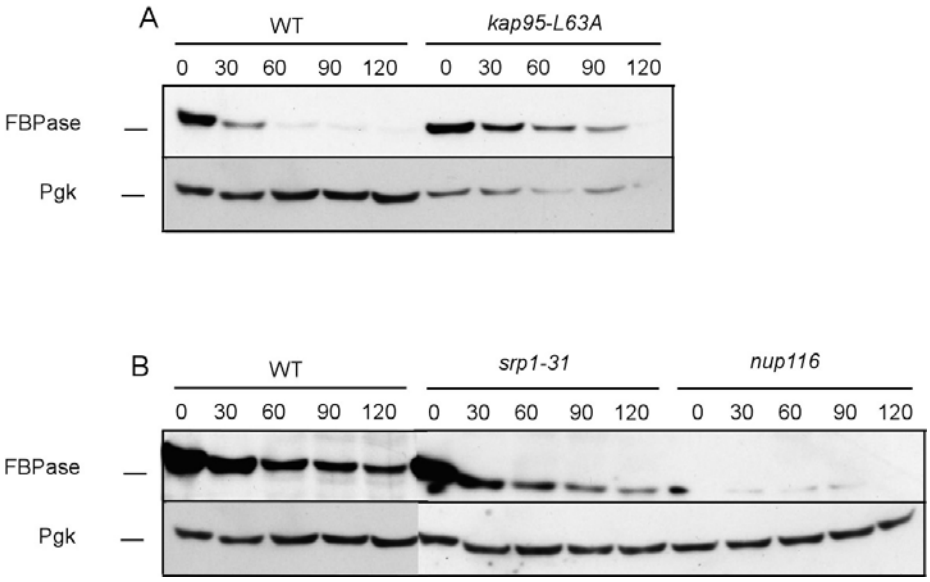

Figure 33: Impact of classical nuclear import components in the catabolite degradation of FBPase. To test if catabolite degradation of FBPase was dependent on the proteins Kap95, Srp1 and Nup116 strains were grown on YPEtOH for 16h at 23°C. Then cells were shifted to 37°C for 3h and 1.5 OD were taken (0). The rest of the cells was resuspended in prewarmed YPD to induce catabolite degradation and samples were taken every 30 min (30-120). These cells were then lysed and proteins were separated by SDS-PAGE with subsequent Western blotting. FBPase specific antibody was used to follow catabolite degradation of FBPase, while Pgk1 specific antibody was used as a loading control. Corresponding wild type strains (WT) were used as a control.

In Figure 33 the impact of Kap95, Srp1 and Nup116 on catabolite degradation of FBPase are shown. Figure 33A shows that FBPase degradation kinetics in strain *kap95-L63A* is clearly retarded compared to the degradation in the corresponding wild type strain. Figure 33B shows catabolite degradation in the strain *srp1-31*. This mutation does not seem to affect FBPase degradation at all and the degradation kinetics is comparable to the one observed in wild type cells. It is remarkable that in a *nup116* conditional deletion strain FBPase protein level is

extremely reduced. Even after extreme overexposure no or little FBPase signal can be observed while the loading control Pgk1 shows homogenous loading. The block of nuclear trafficking in such a strain seems to disturb *FBP1* gene transcription.

3.6.3 Involvement of Snl1 in the catabolite degradation of FBPase

Snl1 was found in the genome wide screen for components involved in the catabolite degradation of FBPase but was not further characterised (Regelmann et al., 2003). Previously described results suggest a probable nuclear catabolite degradation of FBPase and therefore raised the interest in this protein once again. Snl1 was first described as a high copy suppressor of a *nup116* deletion localised in the nuclear envelope and the ER membrane. (Ho et al., 1998). Newer results suggest Snl1 to be a co-chaperone of the heat shock protein Ssa1 (Sondermann et al., 2002). It is interesting that Ssa1 is involved in the catabolite degradation of FBPase (Jeannette Juretschke, unpublished results).

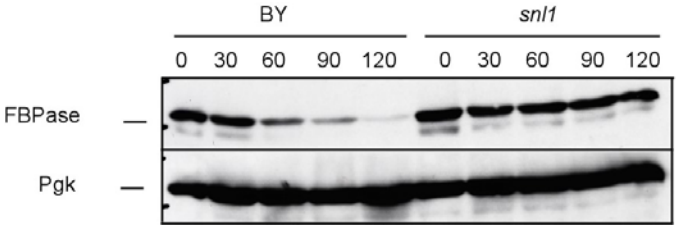

Figure 34: Western blot analysis of catabolite degradation of FBPase in a *snl1* deletion strain. To analyze for the participation of Snl1 in the catabolite degradation of FBPase a *snl1* deletion strain and the matching wild type strain were grown on YPEtOH for 16h and 1.5 OD of cells were taken (0). The remaining cells were resuspended in YPD and 1.5 OD of cells were taken every 30 min up to 120 min (30-120). Afterwards cells were lysed and total extract was subjected to SDS-PAGE with subsequent western blotting. The fate of FBPase was followed with FBPase specific antibodies.

Figure 34 shows the catabolite degradation of FBPase in a strain deleted in *snl1* with the corresponding wild type strain (BY). The degradation kinetics of FBPase with a half time of about 20 min can be seen in the left panel of the blot (BY). A different kinetics can be seen in the strain deleted in *snl1* where FBPase does not seem to be degraded anymore.

As can be seen in Figure 35 the half time of FBPase in a wild type strain (BY) is around 45 min after the onset of catabolite degradation. The *snl1* deletion strain shows a different degradation kinetic. FBPase has a half life of 70 min, and is therefore around 1.5 times stabilised compared to the wild type strain. Thus, Snl1 is involved in the catabolite degradation of FBPase.

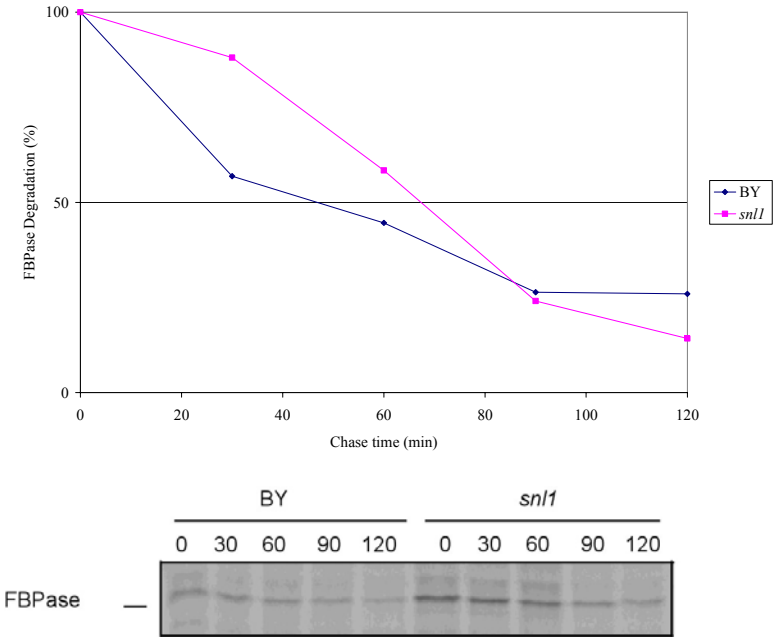

Figure 35: Pulse chase quantification of FBPase catabolite degradation in a *SNL1* deletion strain. To quantify the level of FBPase degradation in a strain deleted in *SNL1* pulse chase analysis was conducted as described in 5.4.6. After autoradiography FBPase specific bands were quantified using the software 'Image Quant'. As can be seen the wild type strain FBPase is degraded with a half life of about 45 min while in the *snl1* deletion strain the half life of FBPase is increased to 70 min.

3.7 PHOSPHORYLATION OF FBPASE AND POSSIBLE FUNCTIONS

The addition of glucose to glucose depleted cells or to cells grown on a non-fermentable carbon source causes a rapid, transient peak in intracellular cAMP concentrations. The sudden increase of cAMP triggers a cAMP dependent protein kinaseA (PKA) mediated phosphorylation cascade with several downstream substrates. One of these substrates is known to be the gluconeogenetic enzyme FBPase (Holzer and Purwin, 1986). The PKA dependent phosphorylation of this enzyme at serine11 leads to a rapid inactivation of the activity (Marcus et al., 1988). A serine11 phosphorylation dependent proteasomal catabolite degradation however does not seem to appear (Hämmerle et al., 1998; Horak et al., 2002). Several recent publications however suggest some further phosphorylation sites in FBPase rather than serine11 and raise the question if PKA dependent phosphorylation of FBPase could induce its catabolite degradation (Hung et al., 2004; Zarzycki et al., 2004).

3.7.1 Caffeine sensitivity of GID deletion strains and the catabolite degradation of FBPase

In a screen to look for phenotypes of deletion strains treated with chemical compounds that are known to disturb protein phosphorylation, a *gid7* deletion strain was described to be sensitive to caffeine (Bianchi et al., 1999). Caffeine is chemically closely related to the purine base adenine and therefore blocks the enzyme phosphodiesterase from removing the secondary messenger cAMP. This second messenger binds to the regulatory subunits of PKA and activates it. High levels of caffeine therefore disturb signal transduction via the PKA pathway by hyperactivation (Hampsey, 1997). It was interesting to test the *gid7* and all other *gid* deletion strains for such a phenotype.

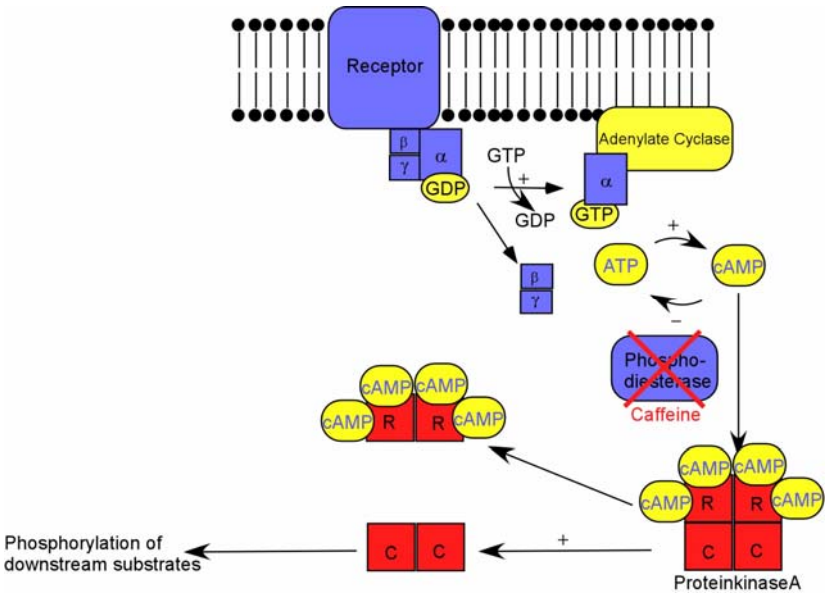

Figure 36: The biochemical function of caffeine in the protein kinase A (PKA) pathway. The enzyme phosphodiesterase converts cyclic AMP into AMP therefore reducing cAMP levels within the cell. Caffeine is known to inhibit this enzyme due to its close chemical relation to adenine. This inhibition leads to increased levels of the second messenger cAMP within the cell by hyperactivation of protein kinase A dependent phosphorylation processes.

In Figure 37 growth phenotypes of all *GID* single deletion strains on 0.3 % caffeine can be seen. The wild type strain BY4743 was used as a positive control. Most strains with a single *GID* deletion show a growth phenotype similar to the wild type with none or a very weak growth defect. Interesting exceptions however are seen in *GID5* and *GID9* deleted strains, which are both sensitive to caffeine. The earlier described sensitivity of a *GID7* deletion strain could not be verified (Bianchi et al., 1999).

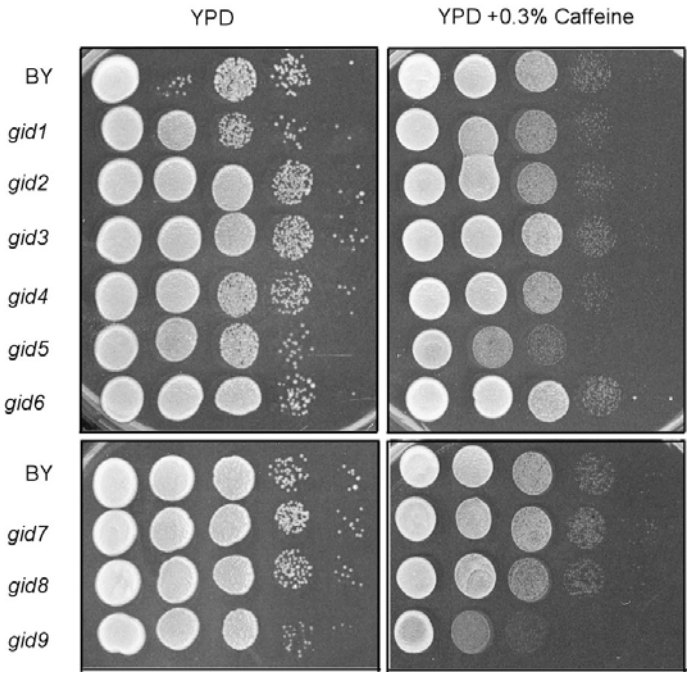

Figure 37: Growth phenotypes of *GID* deletion strains on caffeine. Caffeine disturbs PKA dependent signal transduction processes. Cells with a defect in this system show severe growth phenotypes on such media (Hampsey, 1997). A *GID7* deletion strain was published to be sensitive to caffeine (Bianchi et al., 1999). To prove such a result all *GID* deletion strains were grown on YPD over night. One OD of cells was taken and diluted in 1:10 dilution steps respectively (left to right). Diluted cells were then plated out on YPD plates (left panel) and on YPD containing 0.3 % caffeine (right panel). BY4743 was used as a positive control for growth.

The result described above and the strong connectivity of Gid proteins with the catabolite degradation of FBPase of course raised the question if caffeine could affect such degradation processes also. This was tested by the addition of 0.3% caffeine before the onset of FBPase catabolite degradation.

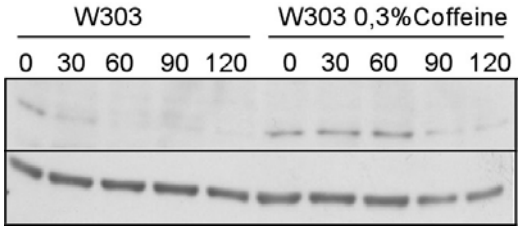

Figure 38: Influence of caffeine on the catabolite degradation of FBPase. Caffeine was shown to disturb the growth of strains deleted in *GID5* and *GID9* respectively. To look if the catabolite degradation of FBPase was dependent on processes inhibited by caffeine wild type cells were grown on YPEtOH for 16h and 1.5 OD of cells were taken (0). To induce catabolite degradation cells were then shifted to YPD and to YPD containing 0.3% of caffeine and samples were taken each 30 min (30- 120). Cells were then lysed and total extracts were subjected to SDS-PAGE with subsequent Western blotting. The fate of FBPase was followed with FBPase specific antibodies. Homogenous protein distribution was shown with antibodies against Pgk1.

In Figure 38 the influence of caffeine addition on catabolite degradation of FBPase can be seen. The wild type strain W303 without addition of caffeine was used as a positive control. The expected degradation kinetics of FBPase is visible with a half time of about 30 min. The addition of 0.3 % caffeine to the medium however changes the degradation pattern dramatically with an almost complete stabilisation of FBPase. The FBPase specific signal seems to be somewhat reduced in the samples taken 90 and 120 min after the onset of catabolite degradation. However this is probably caused by a lower protein concentration in both samples because the Pgk1 signal is reduced too.
In earlier studies the G protein Gpa2 and the G protein-coupled receptor Gpr1, which stimulate adenylate cyclase had been examined and no effect on the catabolite degradation of FBPase was observed (Horak et al., 2002). However, both proteins are acting very upstream in the pathway and other redundant components like *RAS2* are able to activate adenylate cyclase also (Wang et al., 2004). A better strategy to study the effect of PKA on the catabolite degradation of FBPase was to use a strain with disturbed PKA activity.

3.7.2 Involvement of PKA dependent phosphorylation processes in the catabolite degradation of FBPase

The yeast cAMP-dependent protein kinase A (PKA) is composed of two catalytic subunits, encoded redundantly by *TPK1*, *TPK2*, and *TPK3*, and by two regulatory subunits encoded by *BCY1* (Wang et al., 2004). Increase of cAMP upon glucose stimulation leads to dissociation of the two regulatory subunits from the kinase complex and therefore reveals the active sites of the catalytic subunits. The thereby activated PKA kinase then phosphorylates a subset of target enzymes like FBPase (Marcus et al., 1988). A serine11 phosphorylation dependent proteasomal catabolite degradation however does not seem to occur (Hämmerle et al., 1998; Horak et al., 2002). To address the possibility of other PKA dependent phosphorylation sites within FBPase being responsible to subsequently trigger catabolite degradation, it was important to work with a yeast strain disturbed in PKA dependent phosphorylation. A strain with deletions in *tpk1*, *tpk3, bcy1* and an additional temperature sensitive (ts) allele of *tpk2* (YW49) is described by Broach et al (Wang et al., 2004). Figure 39 shows the impact of protein kinase A (PKA) activity on the catabolite degradation of FBPase. FBPase is rapidly degraded in the wild type strain W303. However, in the strain YW49 FBPase is not degraded

anymore. PKA dependent phosphorylation processes seem to be a prerequisite for catabolite degradation of FBPase.

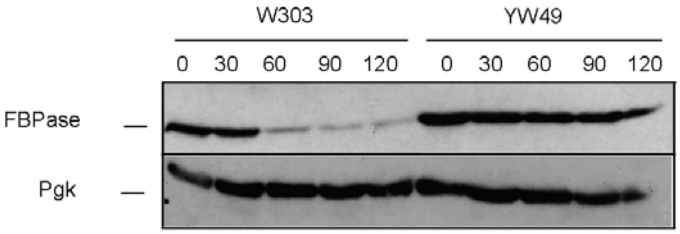

Figure 39: Impact of the cAMP dependent protein kinaseA (PKA) on the catabolite degradation of FBPase. To test if PKA catalysed phosphorylation of FBPase is necessary to trigger its catabolite degradation, a strain deleted in *tpk1*, *tpk3* and *bcy1* with an additional temperature sensitive (ts) allele of *TPK2* (YW49) was grown on YPEtOH for 14h at 23°C to induce gluconeogenesis. The corresponding wild type strain W303 was used as a positive control. Samples were then taken after additional 2 h growth on ethanol at 37°C (0) and every 30 min after the cells were shifted to YPD at 37°C (30 -120). All samples were lysed, total extracts were subjected to SDS-PAGE with subsequent Western blotting and the fate of FBPase was visualised with FBPase specific antibodies. Pgk1 specific antibodies were used to proof homogenous loading.

3.7.3 Snf1 dependent catabolite degradation of FBPase

In *S. cerevisiae* three glucose sensing systems are described. Each system detects and transmits the glucose signal differently. One mechanism works through the Snf3 and Rgt2 glucose sensors to induce the expression of glucose transporters. A second one is working via the cAMP dependent PKA pathway that is described in previous chapters (3.7.2). The pathway focused on in this chapter operates via Snf1, a protein kinase that causes the repression of many genes involved in gluconeogenesis. When glucose is limiting Snf1 becomes active and regulates transcripition by phosphorylating Mig1 and other repressors and activators (Kaniak et al., 2004).

Gid1 has been described to be involved in gene expression for nitrogen metabolism (van der Merwe et al., 2001) and it was described to be phosphorylated (Regelmann, 2005). Both facts raised the question, if Gid1 could function as a transcriptional activator for genes that are upregulated after the onset of catabolite degradation with Snf1 as a possible kinase. It was therefore interesting to look for Snf1 dependent phosphorylation of Gid1 and a possible connection to the catabolite degradation of FBPase.

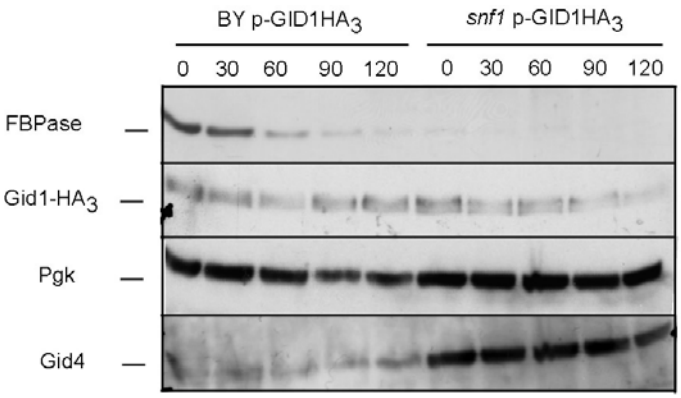

Figure 40: The Snf1p dependent catabolite degradation of FBPase. A yeast strain deleted in the gene *SNF1* (Y24311) and the corresponding wild type strain BY4743 were transformed with a plasmid containing a Ha tagged version of Gid1p (pJR15). These strains were then grown in CM–URA EtOH for 16h and 1.5 OD of cells were taken (0). The remaining cells were then shifted to the same medium containing 2% glucose instead and 1.5 OD of cells were taken every 30 min (30-120). After lysis proteins were subjected to SDS-PAGE with subsequent Western blot analysis. The fate of FBPase was followed with FBPase specific antibody, Gid1 was detected with Ha specific antibodies and Gid4 was visualised with polyclonal antiserum purified in section 3.1.3. Pgk1p was used as a loading control.

Figure 40 shows the catabolite degradation of FBPase in a strain deleted in *snf1*. As can be seen the level of FBPase is severely reduced in this strain. However, a slight signal can still be seen in the 0 min sample. At this stage it cannot be answered if this reduction of FBPase is due to a transcripitional repression caused by the *snf1* deletion or due to a turnover of FBPase already under derepression conditions. Gid1 is phosphorylated under all growth conditions. However it is interesting that the level of Gid4 seems to be strongly upregulated in a *snf1* deletion strain with Gid4 being present already under derepression conditions. This result suggests a role of Snf1 in the transcriptional regulation of Gid4 with an upregulation already under derepression conditions in case of its absence. Gid4 seems to be the trigger factor that leads to the degradation of FBPase.

3.7.4 Possible new phosphorylation sites of FBPase

As shown in chapter 3.7.2 a strain disturbed in the cAMP dependent protein kinaseA (PKA) pathway is dramatically disturbed in the catabolite degradation of FBPase. Such a result shows a clear connection between PKA dependent phosphorylation processes and FBPase catabolite degradation. This raises the question if other phosphorylation sites than serine11 could exist within the enzyme to induce such a process. A web based algorithm called 'NetPhos' (www.cbs.dtu.dk/services/NetPhos/) was used to look for the presence of such possible phosphorylation sites within the aminoacid sequence of FBPase. Five additional serine residues except serine11 were detected at position 106, 133, 281,332 and 333 which

could be possible kinase targets. In Figure 41 a sequence alignment of yeast FBPase with human liver FBPase is shown. The enourmous degree of conservation within the sequence of both enzymes with 48% identity and 69% similarity shows the significance of this enzyme in the eukaryotic metabolism. Interestingly the first 16 amino acids of yeast FBPase are missing in the human orthologue including serine11. However four of the additional phosphorylation sites which were discovered with 'NetPhos' are strongly conserved in yeast and human FBPase as well. An exception is serine333 which is not conserved. It is interesting that most of these serine residues are located in close proximity to amino acids of the active site. As can be seen in Figure 41 and Figure 42 the catalytic tetrad of FBPase is composed of two glutamates and two aspartates at position 107, 127, 130 and 292 which are coordinated around the active site cavity (highlighted in red). Recent publications propose the import of FBPase into the nucleus. Phoshorylation of serine210 was found to be the prerequisite for this translocation. A putative NLS sequence was also described at position 203-207 (KKKGK) (FEBS Congress 2004, Abstract P4. 1-45). As can be seen in Figure 41 this putative NLS sequence is not conserved in yeast.

```
Query 16   FDTDIITLPRFIIEHQKQFKNATGDFTLVLNALQFAFKFVSHTIRRAELVNLVGLAGASN 75
           FDTD+ TL RF++E  ++ +  TG+ T +LN+L  A K +S  +R+A + +L G+AG++N
Sbjct 7    FDTDVNTLTRFVMEEGRKAR-GTGELTQLLNSLCTAVKAISSAVRKAGIAHLYGIAGSTN 65

Query 76   FTGDQQKKLDVLGDEIFINAMRASGIIKVLVSEEQED-LIVFPTNTGSYAVCCDPIDGSS 134
            TGDQ KKLDVL +++ +N +++S    VLVSEE +  +IV P   G Y VC DP+DGSS
Sbjct 66   VTGDQVKKLDVLSNDLVMNMLKSSFATCVLVSEEDKHAIIVEPEKRGKYVVCFDPLDGSS 125

Query 135  NLDAGVSVGTIASIFRLLPDSSGTINDVLRCGKEMVAACYAMYGSSTHLVLTLGDGVDGF 194
           N+D  VSVGTI  I+R       +  D L+ G+ +VAA YA+YGS+T LVL +  GV+ F
Sbjct 126  NIDCLVSVGTIFGIYRKKSTDEPSEKDALQPGRNLVAAGYALYGSATMLVLAMDCGVNCF 185

Query 195  TLDTNLGEFILTHPNLRIPPQKAIYSINEGNTLYWNETIRTFIEKVKQPQADNNNKPFSA 254
            LD  +GEFIL   +++I  +  IYS+NEG    ++  +  +I++ K P   +N+ P+ A
Sbjct 186  MLDPAIGEFILVDKDVKIKKKGKIYSLNEGYARDFDPAVTEYIQRKKFP--PDNSAPYGA 243

Query 255  RYVGSMVADVHRTFLYGGLFAYPCDKKSPNGKLRLLYEAFPMAFLMEQAGGKAVNDRGER 314
           RYVGSMVADVHRT +YGG+F YP +KKSPNGKLRLLYE  PMA++ME+AGG A   + E
Sbjct 244  RYVGSMVADVHRTLVYGGIFLYPANKKSPNGKLRLLYECNPMAYVMEKAGGMATTGK-EA 302

Query 315  ILDLVPSHIHDKSSIWLGSSGEIDKFL 341
           +LD++P+ IH ++ + LGS  ++ +FL
Sbjct 303  VLDVIPTDIHQRAPVILGSPDDVLEFL 329
```

Figure 41: Blast Sequence alignment of yeast FBPase and human liver FBPase. The aminoacid sequence of yeast FBPase is shown in the upper row, while the amino acid sequence of human liver FBPase is shown in the lower row. In between the sequence lines conserved residues are shown with the one letter code for amino acids, + stands for similar aminoacids. Possible phosphorylation sites in yeast FBPase detected with the algorithm 'NetPhos' are highlighted in blue. Serine 106, 133, 281,332 and 333 are conserved also in human liver FBPase, while serine 334 is not. The catalytic tetrade of FBPase uses two aspartates (E) and two glutamates (E) at position 107, 127, 130 and 292 (highlighted in red).

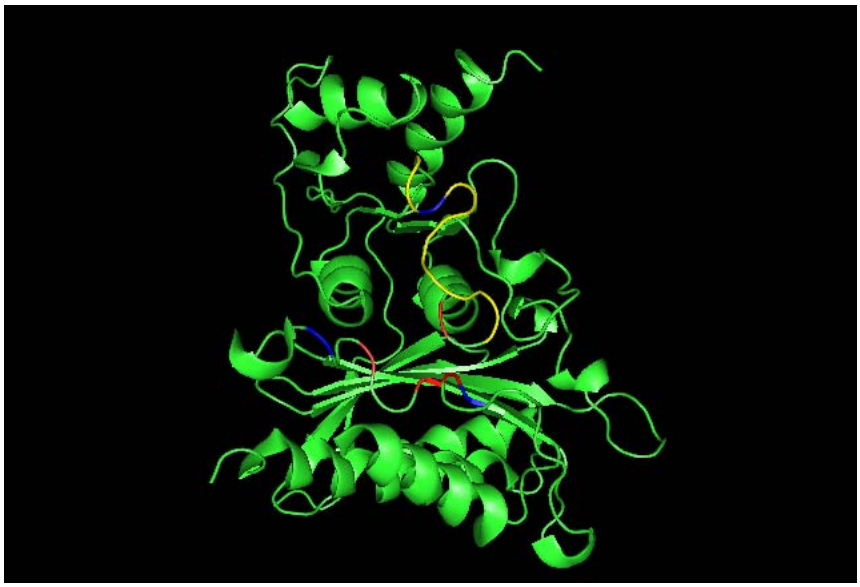

Figure 42: 3D structure of rabbit FBPase. The three dimensional structure of rabbit liver FBPase was visualised with the software PyMol. To do so the chrystallographic data from this enzyme were downloaded from www.proteome.com. The data was then visualised with PyMol and aminoacids of interest were highlighted in different colours. Aminoacids highlighted in red form the catalytic tetrad of the enzyme (Weeks et al., 1999). The earlier described highly conserved serine residues that are putative phosphorylation sites are coordinated around the active site cavity and are highlighted in blue. Another putative NLS sequence than the one described above is conserved in yeast, rabbit and *homo sapiens* is highlighted in yellow (personal communication, Cordula Enenkel).

4 DISCUSSION

For yeast cells as for many other organisms the prefered carbon and energy source is the sugar glucose. It is therefore not surprising that microorganisms have developed a highly sophisticated sensing and signalling system to permanently measure the availability of glucose in the environment ensuring a fast and efficient uptake and metabolism of this sugar.
In a pathway called glycolysis, glucose is metabolized to pyruvate under aerobic conditions or to ethanol or lactate under anaerobic conditions. The net production of ATP during glycolysis is 2 ATP compared to 36-38 ATP in case of the complete end oxidation of glucose. The physiological importance of glucose is mainly not that of an energy source but to function as a carbon source to provide precursor molecules for different essential anabolic pathways (Stryer, 2002). Because these metabolites are fundamental for life, the permanent presence of glucose is essential for every organism. Therefore, in the case of glucose depletion in the surrounding media, this molecule has to be synthesized *de novo* from non carbohydrate precursors in a process called gluconeogenesis.
In principle gluconeogenesis is the reverse process of glycolysis. However some key regulatory processes in gluconeogenesis are thermodynamically irreversible and require a set of different enzymes. One of these enzymes is fructose-1,6-bisphosphatase (FBPase) which catalyses the dephosphorylation of fructose-1,6-bisphosphate to fructose-6-phosphate. The reverse process in glycolysis is catalysed by the enzyme phosphofructokinase which catalyses the ATP dependent phosphorylation of fructose-6-phosphate. Both enzymes are antagonists and are reciprocally controlled to prevent a futile cycle of ATP hydrolysis (Purwin et al., 1982). The gluconeogenetic key enzyme FBPase is therefore only expressed when yeast cells grow under glucose depleted conditions on non fermentable carbon sources like ethanol. Under these conditions this enzyme has a half life of 90 h (Funayama et al., 1980). The addition of glucose to such starved yeast cells however leads to a quick inactivation of gluconeogenesis. This takes place on a transcriptional level by repressing the key gluconeogenetic enzymes via the transcriptional repressor Mig1 (Klein et al., 1998; Rolland et al., 2002) but also on the posttranslational level which is called catabolite inactivation. There the activity of FBPase is diminished by the PKA dependent reversible phosphorylation on a serine11 residue (Funayama et al., 1980; Holzer, 1976). Subsequently, in a process called catabolite degradation this enzyme is rapidly and specifically degraded within 20-30 min (Schork et al., 1995). Similar processes are described for other gluconeogenetic key enzymes like phosphoenolpyruvate carboxykinase (Burlini et al., 1989; Maniatis et al., 1982), the cytosolic malate dehydrogenase (Mdh2) (Minard and McAlister-Henn, 1992) but also for

several non-glucose sugar transporters like the galactose transporter Gal2 or the maltose transporter (Horak and Wolf, 2001; Riballo et al., 1995).

The location of catabolite degradation of FBPase was first described to take place in the vacuole of the cell, catalysed by vacuolar proteases (Holzer, 1976; Molano, 1974). However, with the invagination of bulk protein degradation in the vacuole is known to be relatively unspecific and slow (Thumm and Wolf, 1998). Analysis of protease mutants of the vacuole had actually excluded the involvement of this compartment in specific glucose triggered catabolite degradation of FBPase (Wolf, 1982; Wolf, 2004). Indeed, novel studies indicate selective ubiquitin-proteasome initiated proteolysis of FBPase (Schork et al., 1994a; Schork et al., 1994b; Schork et al., 1995). Nevertheless, vacuolar proteolysis of the enzyme is still under debate.

Publications from the research group H.L. Chiang (Department of Cellular and Molecular Physiology Hershey, USA) still favour the theory of a vacuolar degradation of FBPase (Chiang and Schekman, 1991). According to their findings FBPase is thought to be engulfed into so called Vid-vesicles in the cytosol. These vesicles are described to be transported to the vacuole were FBPase is finally degraded by unspecific proteases (Chiang and Schekman, 1991; Huang and Chiang, 1997). In an *in vitro* assay it could be shown that the transport of FBPase into the vacuole is dependent on ATP and cytosolic proteins (Shieh and Chiang, 1998). Several *VID* ('vacuolar import and degradation') mutants could be isolated which failed to degrade FBPase and led to an accumulation of the enzyme in the cytosol or in Vid vesicles (Brown et al., 2001; Brown et al., 2003; Brown et al., 2000; Brown et al., 2002; Hoffman and Chiang, 1996). It should be noted that the inactivation protocol of this group contains a long starvation time of 48 hours or more on the poor carbon source acetate to derepress FBPase. Such long starvation periods have been shown to induce the unspecific bulk process of autophagocytosis (Thumm, 2000). After the discovery of the 26S proteasome and its involvement in specific, ubiquitin targeted proteolysis of proteins (Heinemeyer et al., 1991), this multicatalytic and multisubunit protease was shown to be the catalyst of FBPase degradation (Schork et al., 1994a; Schork et al., 1994b; Schork et al., 1995).

In a genomic screen nine genes, *GID1* to *GID9*, had been uncovered whose expression is essential for glucose induced catabolite degradation of FBPase (Regelmann et al., 2003). Three of these *GID* gene products, Gid1, Gid2 and Gid3, had been identified previously in a mutant screen searching for defective catabolite degradation of the enzyme (Hämmerle et al., 1998). Gid3 was described to be the ubiquitin conjugating enzyme (E2) Ubc8. The lack of

this enzyme severely effects polyubiquitination of FBPase and finally degradation (Schüle et al., 2000). Among the new *GID* genes *GID6* turned out to encode the ubiquitin-deconjugating enzyme Ubp14 (Regelmann et al., 2003). Amerik *et al*. (1997) had shown that lack of of Ubp14 leads to an accumulation of uncleaved polyubiquitin chains. This result is interpreted as a competitive inhibition of free polyubiquitin chains in the *UBP14* deletion mutant with polyubiquitin substrate binding to the 26S proteasome. We analyzed the residual Gid-proteins with respect to physical behaviour and function in the FBPase degradation process. In a systematic mass spectrometry search for protein complexes with Gid7 (*YCL039W*) as bait, Gid1, Gid2, Gid4, Gid5, Gid8 and Gid9 had been found (Ho et al., 2002). After tagging these Gid-proteins, co-immunoprecipitation studies in this work could verify that Gid7 interacts with Gid1 as well as Gid2, Gid4, Gid5, Gi8 and Gid9 (Figure 15). As found for Gid2 (Regelmann et al., 2003), Gid5, Gid7, Gid8 and Gid9 do not sediment at their calculated molecular mass sizes in a glycerol gradient but in the mass range of about 600kDa instead (Figure 12). Gid1 (111 kDa), Gid3 (25 kDa) and Gid4 (41 kDa) seem to be exceptions: These proteins mainly sediment at their calculated molecular masses. However, a minor portion of Gid1, Gid3 and Gid4 molecules also appears in the higher molecular mass range (Figure 13). The deubiquitinating enzyme Ubp14/Gid6 is only present in the low molecular mass fractions together with Pgk and is not part of a high molecular mass complex. The interaction of Gid7 with Gid1, Gid2, Gid4, Gid5, Gid8 and Gid9 as well as their appearance at a higher molecular mass range of 600kDa, which roughly matches their added molecular masses (526kDa, including tags) indicates that these proteins act in a complex. The separation of this complex in a native gel showed the existence of two protein complexes in which Gid7 resides. It is not possible to conclude from this data yet, if the difference in the two complexes is due to different subunit compositions or due to different posttranslational modifications of the same subunits (Figure 18). It should also be kept in mind that such a distribution could be caused by the loss of subunits during separation. The search for direct interactions unravelled the association of Gid4 with Gid5 (Figure 17). This fact and the upregulation of Gid4 during the catabolite degradation process show that Gid4 is recruited to the Gid complex.

Analysis of the expression pattern of the Gid proteins uncovered, that Gid2 (Regelmann et al., 2003) as well as Gid1, Gid5, Gid7, Gid8 and Gid9 are present in high amount under derepressing (gluconeogenic) conditions with no or little change after glucose addition to cells (Figure 7). Thus, these five Gid proteins seem to represent a core complex, which is present already before glucose induces its signaling events. A completely different picture emerges, when the expression of Gid4 is analyzed (Figure 8): The protein is strongly upregulated after

glucose is added to the medium. Under derepressing conditions (ethanol) Gid4 seems to be rapidly degraded (Figure 8). This result could be confirmed with epitope tagged Gid4 and raises the question if Gid4 is degraded together with FBPase (Olivier Santt, unpublished data) A closer analysis of the protein pattern of Gid1-HA_3 indicated the presence of two protein bands (Figure 7A) which were resolved as a phosphorylated and a non-phosphorylated form of the protein (Pfirrmann et al., 2006; Regelmann, 2005). Interestingly both versions are associated to the Gid complex (Figure 15A) with an unclear function however.

A direct function of the Gid-complex in the catabolite degradation process of FBPase should be indicated by the direct binding of FBPase to Gid-proteins. Gid1, Gid2, Gid6 and Gid7 were therefore chosen for *in vivo* binding assays. FBPase was found to interact with these Gid proteins in the cell. Therefore it is likely that FBPase is also part of the Gid complex, most probably as a substrate for its subsequent polyubiquitnation. In this respect it is interesting that the level of precipitated FBPase is enhanced after the onset of catabolite degradation (Figure 19). This speaks for a recruitment of FBPase to the Gid complex. No interaction with Ubp14/Gid6 could be detected, which underlines the indirect effect of Ubp14/Gid6 absence on FBPase degradation: The uncleaved ubiquitin chains remaining in the *ubp14/gid6* mutant compete with the entry of ubiquitinated FBPase into the proteasome.

The protein Gid2 was first found in a functional genomic analysis for genes connected with sporulation and meiosis. It was therefore named Rmd5 (required for meiotic nuclear division) (Enyenihi and Saunders, 2003). However it was also found to be important for the polyubiquitination and subsequent degradation of FBPase (Regelmann et al., 2003). This analysis was extended to other Gid-proteins, the phosphorylatable Gid1 as well as Gid7, which was found to interact with each of the other analyzed Gid-proteins (Figure 15). Loss of either, Gid1 or Gid7 led to a block in FBPase polyubiquitination (Figure 22). The direct interaction of FBPase with subunits of the Gid complex, as well as a defective polyubiquitination of FBPase in the respective deletion strains underlines the direct function of the Gid complex in the polyubiquitination and subsequent degradation of FBPase. Rudimentary RING (ShRING) domains within Gid2 and Gid9 and the existence of both proteins in a high molecular mass complex propose a role of the Gid complex as a novel E3 ubiquitin protein ligase (Figure 20).

FBPase as most other gluconeogenetic enzymes are known to function in the cytosol of the cell. Unexpectedly, Gid1, Gid6, Gid7 and Gid8 were found in the nucleus of the cell (Figure 10). The interaction of FBPase with subunits of the Gid complex (Figure 19) raised the question if Gid proteins are to a minor extent located to the cytosol also. This could not be confirmed for Gid7. While the major amount of Gid8 is located to the nucleus a low amount could be located to the cytosol under derepression conditions (Figure 11).

In mammalian liver cells FBPase was recently described to be translocated to the nucleus upon glucose or insulin supplementation (Yanez et al., 2003; Yanez et al., 2004; Zarzycki et al., 2004). Interestingly such a process is also observed in yeast (Figure 30). However, it is unclear if this phenotype is due to the incapability of the FBPase-GFP fusion protein to be degraded during catabolite degradation (Figure 29). It is widely accepted that the major amount of yeast 26S proteasomes is localised in the nucleus (Enenkel et al., 1998; Enenkel et al., 1999; Lehmann et al., 2002; Russell et al., 1999; Wendler et al., 2004). Some reports of a nucleus-specific turnover of proteasomal substrates, like for example the transcripitional repressor Matα2 would support the theory of a FBPase specific catabolite degradation in this organelle (Lenk and Sommer, 2000).

In a two hybrid screen FBPase was found to directly interact with classical components of the nuclear import machinery (Uetz et al., 2000). The necessity of functional Kap95 for the process of catabolite degradation underlines the theory of a nuclear catabolite degradation process (Figure 33A). However, catabolite degradation of FBPase is not dependent on Srp1 (Figure 33B). In a *nup116* conditional deletion strain nuclear traffic is known to be stopped (Wente and Blobel, 1993). The basal level of FBPase in such a strain was severely reduced under restrictive growth conditions (Figure 33). Such a result is probably caused due to a disturbed transcriptional regulation of the *FBP1* gene.

In a genomic screen Snl1 was found to be involved in the catabolite degradation of FBPase (Regelmann, 2005). A possible nuclear catabolite degradation process of FBPase raised our interest in this protein again. Snl1 was first described as a high copy suppressor of a *nup116* deletion strain which is a part of the nuclear pore complex (Ho et al., 1998). Later publications describe Snl1 as a co-chaperone that interacts with all Hsp90 heat shock proteins in yeast, including the earlier described Ssa1 protein (Sondermann et al., 2002). Both proteins are described to play a role in nuclear transport as well (Shulga et al., 1999; Shulga et al., 1996). In *snl1* deletion strains a stabilisation of FBPase could be observed by Western blot analysis (Figure 34). The quantification by pulse chase analysis showed a degradation with a half time of 70 min (Figure 35) amounting to a 1.5 times stabilisation.

It was also possible to exclude the process of SUMOylation as an inducer of catabolite degradation (Figure 31). This process was described to be involved in nuclear trafficking as well (Dohmen, 2004; Pichler et al., 2002; Stade et al., 2002).

PKA dependent reversible phosphorylation of FBPase is described to take place at serine11 after the addition of glucose to starved cells . This process is known to reduce the activity of FBPase (Funayama et al., 1980). However, the degradation of FBPase was described to be independent of the serine11 phosphorylation (Hämmerle et al., 1998). Some recent publications showed the existence of different phosphorylation sites in FBPase (Hung et al., 2004; Zarzycki et al., 2004). This raised the question, if other phosphorylation sites could be used to induce the catabolite degradation of FBPase. In earlier experiments the involvement of the G protein Gpa1 and the G protein coupled receptor Gpr1 had been tested for FBPase degradation (Horak et al., 2002). These results had excluded PKA dependent FBPase catabolite degradation. However, some recent publications suggest the existence of a redundant activation of adenylate cyclase by Ras and Gpa2 (Wang et al., 2004). In a strain directly disturbed in PKA activity the catabolite degradation of FBPase is severely inhibited (Figure 39). Also the addition of caffeine to derepressed cells prevents the ongoing catabolite degradation of FBPase (Figure 38). Caffeine disturbs PKA dependent processes by inhibition of the enzyme phosphodiesterase (Hampsey, 1997). In a recent publication *gid7* mutant cells were described to be sensitive to caffeine (Bianchi et al., 1999). This could not be verified, instead, *gid5* and *gid9* mutant cells were found to be sensitive to caffeine (Figure 37). Several highly conserved phosphorylation sites in yeast and human FBPase were detected *in silico* (Figure 41). PKA dependent phosphorylation of FBPase could therefore be a prerequisite for its further catabolite degradation.

A common principle of the SCF complex is to bind phosphorylated substrates for their polyubiquitination and further destruction by the 26S proteasome (Willems et al., 2004). In the so called F-box subunits of this ubiquitin ligase complex WD40 domains bind the phosphorylated substrate. Gid7 was found to have 5 WD40 domains (Table 1). To form a ternary complex, the recruitment and binding of the concomitant ubiquitin conjugating enzyme is carried out by RING domains (Bordallo and Wolf, 1999; Borden, 2000; Freemont, 2000; Jackson et al., 2000). Rudimentary short RING (ShRING) domains were discovered in Gid2 and Gid9 (Figure 20). All Gid proteins except Gid3/Ubc8 and Gid6/Ubp14 were found in a protein complex (Figure 15) and FBPase is recruited to subunits of the Gid complex

during the onset of catabolite degradation. No polyubiquitination of FBPase occurs in several *GID* deletion strains (Figure 22 and Figure 19). Also a strong sequence similarity between Gid5 and Gid7 and all the known cullin proteins could be discovered (see attachment). Cullins are present in all species, ranging from four in budding yeast to nine in mammals. It is suggested, that all known cullin family members form bona fide ubiquitin ligases (Willems et al., 2004).

These data strongly suggest the role of the Gid complex to function as a novel ubiquitin ligase complex (Figure 43). In such a hypothesis FBPase binding to Gid7 would be induced by PKA dependent phosphorylation of FBPase at different serine residues after glucose addition to starved cells. The binding of Ubc8/Gid3 is carried out by the ShRING domain containing subunits Gid2 and Gid9. Gid4 is upregulated 5 minutes after glucose shift and functions as an activator of the ubiquitin ligase or is necessary to recruit FBPase to Gid7. The subsequent degradation of Gid4 could happen together with FBPase, Gid4 being a mediator to the 26S proteasome.

Gid6/Ubp14 plays a role independent of the Gid complex. It neither binds to FBPase nor to the Gid complex. The L-canavanine sensitivity of a *gid6* strain (Figure 21) supports a general defect in proteasomal degradation in such a strain. This is caused by competitive inhibition of the proteasome due to accumulating polyubiquitin chains (Amerik et al., 1997). A localisation of all so far tested Gid proteins in the nucleus (Figure 10, Figure 11) and the increasing FBPase signal in the nucleus after onset of catabolite degradation (Figure 30) support the theory of a degradation process in the nucleus of the cell.

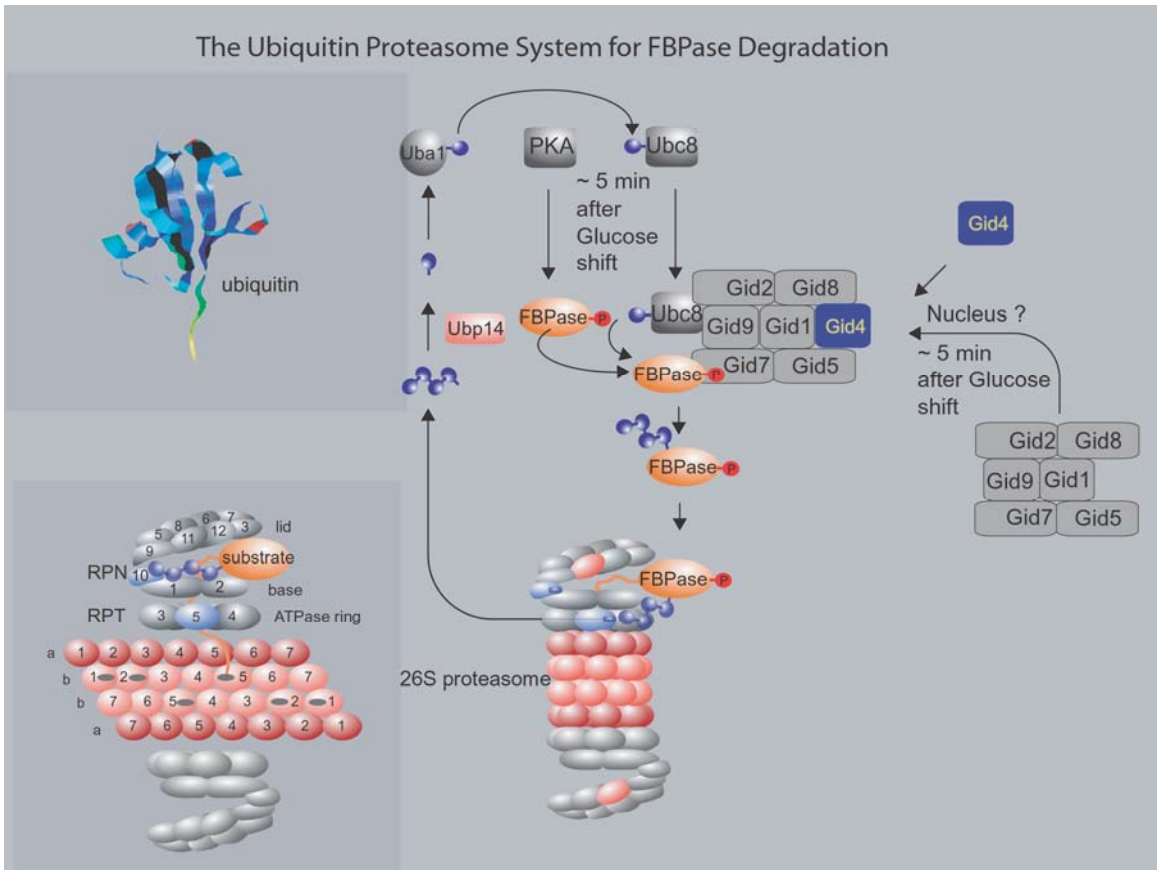

Figure 43: Proposed model for the catabolite degradation of FBPase: Most Gid proteins except Gid6 appear in a high molecular mass complex, which functions as an ubiquitin ligase complex. The RING domains in Gid2 and Gid9 bind the corresponding ubiquitin conjugating enzyme Ubc8, while the 5 WD40 domains of Gid7 bind phosphorylated FBPase as the substrate. Gid4 is upregulated roughly 5 min after the addition to glucose starved cells and recruited to the Gid complex to either activate it or to bind FBPase directly to escort it to the Gid complex. The complex polyubiquitinates FBPase and the enzyme is degraded by the 26S proteasome probably together with Gid4. Ubp14/Gid6 acts as a deubiquitinating enzyme and only plays an indirect role in the catabolite degradation of FBPase (Amerik et al., 1997). A PKA dependent phosphorylation of FBPase could induce the recruitment to Gid7. This process might occur in the nucleus.

The aminoacid sequence of human liver FBPase is to 48% identical to its yeast othologue (Figure 41). Although not much is known about catabolite degradation of FBPase in *homo sapiens*, it is more than expected that similar processes take place in that organism as well. The existence of human Gid protein orthologues with sequence identities ranging from 21% to 54% support this theory (Table 1). RanBP9, the human Gid1 orthologue, was recently found to be phosphorylated and to be part of a 670 kDa protein complex with unknown function (Denti et al., 2004; Nishitani et al., 2001).

In *homo sapiens* gluconeogenesis mainly takes place in the liver, with a low activity also in the kidneys. The human orthologue of the yeast *FBP1* gene is therefore mostly expressed in these organs (Stryer, 2002). However, a *FBP2* isoform of unknown function is also expressed in the muscle.

In humans as well as in yeast the physiological importance of gluconeogenesis is to provide cells with glucose during glucose limiting conditions to yield energy and cellular building blocks. In addition the brain and red blood cells of higher organisms depend on glucose as their sole energy source. Mutations in the *FBP1* gene and disregulations in gluconeogenesis therefore lead to severe diseases. Several mutations in the *FBP1* gene are described to lead to the autosomal recessive fructose-1,6-bisphosphatase deficiency (Kikawa et al., 1997; Kikawa et al., 1995). This disease causes episodes of hypoglycaemia and metabolic acidose with a high mortality rate. Up to 25% of the so called sudden-infant-death-syndrome is caused by FBPase deficiency (Burchell et al., 1992). It is also reported that FBPase mRNA levels are increased in patients suffering from diabetes mellitus type II (Rothschild et al., 1995). An upregulation of active FBPase leads to an increased *de novo* synthesis of glucose in the liver which increases the plasma glucose level. This process is normally controlled by insulin which inhibits gluconeogenesis in the liver and keeps the plasma glucose level on a constant level. Diabetes patients either have a lack or an increased resistence to insulin which leads to an increase of gluconeogenetic activity. The selective inhibition of fructose-1,6-bisphosphatase (FBPase) was described to lower the plasma glucose levels in a rat model of type 2 diabetes (http://www.lifescan.com/professionals/hcp/news). Such an approach could be used as an alternative to insulin injections as a possible diabetes treatment. A better understanding of the regulation of FBPase and gluconeogenesis in yeast could help to find possible drug targets for diabetes treatment in *homo sapiens*.

5 MATERIAL & METHODS

5.1 MATERIALS

5.1.1 Chemicals, materials and their suppliers

Supplier	Chemicals, materials and enzymes
Amersham	ECL™-System; Hyperfilm™ ECL; Protein A Sepharose™ CL-4B; Glutathion Sepharose™ 4B, [α-^{35}S]-L-Methionin, High molecular weight calibration kit for native electrophoresis
BIO-RAD	Protein marker (Precision Plus Protein™ standard, All Blue)
Difco, Detroit, USA	Bacto Pepton, Bacto Trypton, Bacto Yeast Extract, Yeast Nitrogen Base w/o Aminoacids
Genaxxon Bioscience, Stafflangen	Acrylamide and bisacrylamide solutions, ammonium persulfate (APS), Ampicillin
Merck, Darmstadt	Ammoniumperoxodissulfate, DMSO, β-mercaptoethanol, sodiumacetate sodiumhydroxide, PMSF, TEMED, potassiumacetate, potassiumchloride, potassiumdihydrogenphosphate
Qiagen, Hilden	QIAquick PCR Purification Kit, QIAprep Spin Miniprep Kit
Roche, Mannheim	dNTPs, DNA standard (1kb DNA-ladder), Ampicillin, Complete™ protease inhibitor tablets,
Roth, Karslruhe	Chloroform, DMF, ethanol p.a., D-glucose, L-glycine, urea, sodiumhydrogenphosphate, sodiumdihydrogenphosphate, phenol (Roti®-Phenol), Tris, Triton-X-100, methanol,
Schleicher & Schuell, Dassel	Blotting paper GB002, nitrocellulose membranes
Serva, Heidelberg	Agarose for DNA-elektrophoresis, Coomassie brilliant blue R250
Sigma-Aldrich, Steinheim	Aminoacids , Cycloheximide, EDTA,

	ethidiumbromide, HEPES, PEG 4000, SDS, Tween 20, PMSF, sodiumazide,

Chemicals used but not listed here were otherwise of the highest purity available.

5.1.2 Antibodies

Antibodies	Dilution for Western blot	Supplier
Goat-α-mouse IgG, HRPO conjugated	1:5000, 1% skim milk	Dianova, Hamburg
Goat-α-rabbit IgG, HRPO conjugated	1:5000, 1% skim milk	Medac, Hamburg
α-AP1, polyclonal, rabbit	1:5000	Klionsky et al., 1992
α-Cpy, monoclonal, mouse	1:10000	Molecular Probes, Leiden, Holland
α-Fas, polyclonal, rabbit	1:10000	Egner et al., 1993
α-Fbpase, polyclonal, rabbit	1:5000	K.D.Entian, Frankfurt
α-Flag, polyclonal, rabbit	1:10000	Sigma-Aldrich, Steinheim
α-GST, polyclonal, rabbit	1:5000 in 2% skim milk	T. Lang
α-Ha, monoclonal, mouse (clone 16B12)	1:5000 in 1% skim milk	Babco, Richmond, USA
α-Myc, monoclonal, mouse (clone 9E10)	1:10000	Calbiochem
α-Nop1, monoclonal, mouse	1:10000	Abcam, Cambridge
α-Pgk1, monoclonal, mouse	1:10000	Molecular Probes, Leiden, Holland
α-Vid24, polyclonal, rabbit (Charge 03/05/01 GP)	1:2000	(Josupeit, 2003) and this work

5.1.3 Laboratory equipment

Equipment	Supplier
Agarose gel electrophoresis apparatus	Bio-Rad, Hercules, USA

Balance *AE 163*	Mettler, Giessen, Switzerland
Balance *PM460*	Mettler,Giessen, Switzerland
Biofuges *fresco and pico*	Heraeus, Hanau
Centrifuge *5417 C and 5804R*	Eppendorf, Hamburg
Centrifuge *Centrikon T-124*	Kontron Instruments, Neufarn
Centrifuge *Sorvall RC 5B*	Kendro, Osterode
Centrifuge *Z320K*	Eppendorf, Hamburg
Electroporation apparatus *Gene Pulser*^{TM}	Bio-Rad, Hercules, USA
Film developer machine *Optimax*	Protec Medizintechnik, Oberstenfeld
Gel dryer	Fröbel Labortechnik, Lindau
Heating block *Test tube Thermostat TCR100*	Roth, Karlsruhe
Incubator *B6200*	Heraeus, Hanau
Ion exchanger *Milli-Q Academics*	Millipore, Eschborn
Multi vortexer *IKA-VIBRAX VXR*	Janke & Kunkel
Overhead rotator *REAX2*	Heidolph Instruments, Schwabach
Overhead shaker *34528*	Snijders Scientific, Tilburg, NL
Overhead shaker *REAX 2*	Heidolph, Schwabach
Overhead shaker *Roto Shake Genie*	Scientific Industries, Bohemia, USA
PCR-Machine *Robocycler® Gradient 40*	Stratagene, La Jolla, USA
pH-Meter *CG 832*	Schott, Hofheim
PhosphoImager *Storm860*	Molecular Dynamics, Sunnyvale, USA
Pipettes (2-1000µl)	Gilson
Power supply units Model *200/2,0* and *Power-Pac 300*	Bio-Rad, Hercules, USA
Protein electrophoresis apparatus *Protean II*	BioRad, Hercules, USA
Semidry blot chamber	ITF Labortechnik, Wasserburg
Shaker (different sizes)	Adolf Kuhner AG, Switzerland
Shakers, various sizes	A. Kühner, Birsfelden, Switzerland
Spektrophotometer *Jasco V-530*	Jasco, Germany
Spektrophotometer *Novaspec II*	Pharmacia Biotech, Uppsala, Sweden
Stirrer lkamag® REO	IKA®-Labortechnik, Staufen i. Br.
Supersonic Sonificator *Sonic Power*	Branson, Danbury, USA
Thermomixer *5437*	Eppendorf, Hamburg

Ultracentrifuge *Optima™ TLX*	Beckman, Palo Alto, California
Video printer for agarose gel pictures	MWG Biotech, München
Vortexer *Vibrofix VF 1* and *VF2*	IKA®-Labortechnik, Staufen i. Br.

5.1.4 Enzymes

Supplier	Enzyme
Enzogenetics, Corvallis, USA	Oxalyticase
Invitrogen, Carlsbad, USA	T4-DNA-Ligase and ligation buffer
New England BioLabs, Beverly, USA	Vent-DNA-Polymerase, alkaline phosphatase (CIP), BSA, restriction enzymes and appropriate buffer systems
Roche, Mannheim	T4-DNA-Ligase, lysozyme, Klenow enzyme, RNAseA, restriction enzymes and appropriate buffer systems
Seikagaku Kyogo, Tokio, Japan	Zymolyase 100-T
Sigma-Aldrich, Steinheim	Glusulase
Stratagene, La Jolla, USA	PfuUltra^{TM} high-fidelity DNA-polymerase

5.1.5 *E.coli* strains

E. coli strain	Genotype	Source/ Reference
DH5α	F$^-$ Φ 80d *lac* Z ΔM15 (argF-lacZYA) U169 end A1recA1 *hsd* R17(rk$^-$, mk$^+$) deo R *thi*- 1 *sup*E44 λ$^-$ gyrA96 relA1 Δ	Stratagene
BL21 (DE3)	F- *dcm ompT hsdS*(rB- mB-) *gal* λ(DE3)	Stratagene
E. coli BMH 71-18 *mut*S	*E. coli* B, *thi sup*E Δ(*lac pro*AB) [*mut*S:Tn*10*] [F‘ *pro*A+B+ *lac*I$_q$ZΔM15]	Clontech

5.1.6 S. cerevisiae strains

Name	Genotype	Reference
BY4743	*MATa/α his3Δ1/his3Δ1 leu2Δ0/leu2Δ0*	EUROSCARF

	MET15/met15Δ0 lys2Δ0/LYS2 ura3Δ0/ura3Δ0	
W303 -1B	*MATα ade2 leu2-3,112 his3 trp1 ura3*	H.L. Chiang
W303 -1BKO	*MATα ade2 leu2-3,112 his3 trp1 ura3 fbp1Δ ::LEU2*	H.L. Chiang
Y31409	*MATa/α his3Δ1/his3Δ1 leu2Δ0/leu2Δ0* MET15/met15Δ0 lys2Δ0/LYS2 ura3Δ0/ura3Δ0 *snl1Δ::KANMX4/snl11Δ::KANMX4*	EUROSCARF
Y31410	*MATa/α his3Δ1/his3Δ1 leu2Δ0/leu2Δ0* MET15/met15Δ0 lys2Δ0/LYS2 ura3Δ0/ura3Δ0 *gid5Δ::KANMX4/gid5Δ::KANMX4*	EUROSCARF
Y31488	*MATa/α his3Δ1/his3Δ1 leu2Δ0/leu2Δ0* MET15/met15Δ0 lys2Δ0/LYS2 ura3Δ0/ura3Δ0 *gid9Δ::KANMX4/gid9Δ::KANMX4*	EUROSCARF
Y33195	*MATa/α his3Δ1/his3Δ1 leu2Δ0/leu2Δ0* MET15/met15Δ0 lys2Δ0/LYS2 ura3Δ0/ura3Δ0 *gid6Δ::KANMX4/gid6Δ::KANMX4*	EUROSCARF
Y33244	*MATa/α his3Δ1/his3Δ1 leu2Δ0/leu2Δ0* MET15/met15Δ0 lys2Δ0/LYS2 ura3Δ0/ura3Δ0 *gid4Δ::KANMX4/gid4Δ::KANMX4*	EUROSCARF
Y33446	*MATa/α his3Δ1/his3Δ1 leu2Δ0/leu2Δ0* MET15/met15Δ0 lys2Δ0/LYS2 ura3Δ0/ura3Δ0 *gid7Δ::KANMX4/gid7Δ::KANMX4*	EUROSCARF
Y33614	*MATa/α his3Δ1/his3Δ1 leu2Δ0/leu2Δ0* MET15/met15Δ0 lys2Δ0/LYS2 ura3Δ0/ura3Δ0 *gid2Δ::KANMX4/gid2Δ::KANMX4*	EUROSCARF
Y34594	*MATa/α his3Δ1/his3Δ1 leu2Δ0/leu2Δ0* MET15/met15Δ0 lys2Δ0/LYS2 ura3Δ0/ura3Δ0 *gid1Δ::KANMX4/gid1Δ::KANMX4*	EUROSCARF
Y35286	*MATa/α his3Δ1/his3Δ1 leu2Δ0/leu2Δ0* MET15/met15Δ0 lys2Δ0/LYS2 ura3Δ0/ura3Δ0 *fbp1Δ::KANMX4/fbp1Δ::KANMX4*	EUROSCARF
Y36576	*MATa/α his3Δ1/his3Δ1 leu2Δ0/leu2Δ0* MET15/met15Δ0 lys2Δ0/LYS2 ura3Δ0/ura3Δ0	EUROSCARF

	gid8Δ::KANMX4/gid8Δ::KANMX4	
Y36577	*MATa/α his3Δ1/his3Δ1 leu2Δ0/leu2Δ0* MET15/met15Δ0 lys2Δ0/LYS2 ura3Δ0/ura3Δ0 *gid3Δ::KANMX4/gid3Δ::KANMX4*	EUROSCARF
Y36902	*MATa/α his3Δ1/his3Δ1 leu2Δ0/leu2Δ0* MET15/met15Δ0 ys2Δ0/LYS2 ura3Δ0/ura3Δ0 *grr1Δ::KANMX4/grr1Δ::KANMX4*	EUROSCARF
Y31856	*MATa/α his3Δ1/his3Δ1 leu2Δ0/leu2Δ0* MET15/met15Δ0 lys2Δ0/LYS2 ura3Δ0/ura3Δ0 *yor080wΔ::KANMX4/yor080wΔ::KANMX4*	EUROSCARF
Y31133	*MATa/α his3Δ1/his3Δ1 leu2Δ0/leu2Δ0* MET15/met15Δ0 lys2Δ0/LYS2 ura3Δ0/ura3Δ0 *ynl311cΔ::KANMX4/ynl311cΔ::KANMX4*	EUROSCARF
Y30482	*MATa/α his3Δ1/his3Δ1 leu2Δ0/leu2Δ0* MET15/met15Δ0 lys2Δ0/LYS2 ura3Δ0/ura3Δ0 *yml088wΔ::KANMX4/yml088wΔ::KANMX4*	EUROSCARF
Y31276	*MATa/α his3Δ1/his3Δ1 leu2Δ0/leu2Δ0* MET15/met15Δ0 lys2Δ0/LYS2 ura3Δ0/ura3Δ0 *yjl149wΔ::KANMX4/yjl149wΔ::KANMX4*	EUROSCARF
Y34311	*MATa/α his3Δ1/his3Δ1 leu2Δ0/leu2Δ0* MET15/met15Δ0 lys2Δ0/LYS2 ura3Δ0/ura3Δ0 *snf1Δ::KANMX4/snf1Δ::KANMX4*	EUROSCARF
YJR12 (W303-1B *GID1-HA$_3$*)	*MATα ade2 leu2-3,112 his3 trp1 ura3 GID1-HA$_3$::HIS5$^{S. pombe}$*	(Regelmann, 2005)
YOS1 (W3031B *myc$_9$-GID4*)	*MATα ade2 leu2-3,112 his3 trp1 ura3 Myc$_9$-GID4*	Santt, Olivier
YR312	*MATa his1*	MATα-Testerstamm
YR320	*MATα his1*	MATa-Testerstamm
YSA1 (W3031B *GID8-HA$_3$*)	*MATα ade2 leu2-3,112 his3 trp1 ura3 GID8-HA$_3$::HIS5$^{S. pombe}$*	This work with help of Alberts, Sven
YTP10 (W3031B *GID7-HA$_3$*)	*MATα ade2 leu2-3,112 his3 trp1 ura3 GID7-HA$_3$::HIS5$^{S. pombe}$*	This work
YTP11 (W3031B	*MATα ade2 leu2-3,112 his3 trp1 ura3 GID5-*	This work

GID5-HA$_3$)	*HA$_3$::HIS5*$^{S.\ pombe}$	
YTP12 (W3031B *GID9-HA$_3$*)	*MATα ade2 leu2-3,112 his3 trp1 ura3 GID9-HA$_3$::HIS5*$^{S.\ pombe}$	This work
YBB1 (W3031B *GID6-HA$_3$*)	*MATα ade2 leu2-3,112 his3 trp1 ura3 GID6-HA$_3$::HIS5*$^{S.\ pombe}$	This work with help of Braun, Bernhard
YTS3 (W303-1B *GID2-HA$_3$*)	*MATα ade2 leu2-3,112 his3 trp1 ura3 GID2-HA$_3$::HIS5*$^{S.\ pombe}$	(Regelmann et al., 2003)
YTS4 (W303-1B *GID3-HA$_3$*)	*MATα ade2 leu2-3,112 his3 trp1 ura3 GID3-HA$_3$::HIS5*$^{S.\ pombe}$	(Schüle et al., 2000)
YW97	W303-1B *tpk1::URA3tpk2wimp(V218G) tpk3::KANN bcy1::LEU2 ade2-1 can1-100 his3-11,15 leu2-3,112 trp1-1 ura3-1 GAL*	(Wang et al., 2004)
YW49	W303-1B *tpk1::HIS3 tpk2wimp(V218G) tpk3::TRP1 bcy1::LEU2 ade2-1 can1-100 his3-11,15 leu2-3, 112 trp1-1 ura3-1 GAL*	(Wang et al., 2004)
srp1-31	W303-1B *srp1-31 ade2-1 can1-100 his3-11,15 leu2-3, 112 trp1-1 ura3-1 trp1 63*	(Loeb et al., 1995)
srp1-49	W303-1B *srp1-49 ade2-1 can1-100 his3-11,15 leu2-3, 112 trp1-1 ura3-1 trp1 63*	(Loeb et al., 1995)
Kap95-L63A	W303-1B *ade2-1 can1-100 his3-11,15 leu2-3, 112 trp1-1 ura3-1 trp1 63 kap95::HIS3 p kap95-L63A*	(Iovine and Wente, 1997)
Nup116-5	W303-1B *ade2-1 can1-100 his3-11,15 leu2-3, 112 trp1-1 ura3-1 trp1 63 nup116-5::HIS3*	(Wente and Blobel, 1993)
UBC9	W303-1B *ade2-1 can1-100 his3-11,15 leu2-3, 112 trp1-1 ura3-1 ubc9-4::TRP1 pUBC9*	(Betting and Seufert, 1996)
ubc9-2	W303-1B *ade2-1 can1-100 his3-11,15 leu2-3, 112 trp1-1 ura3-1 ubc9-4::TRP1 pubc9-2*	(Betting and Seufert, 1996)
Y01488	BY4741; *Mat a; his3Δ1; leu2Δ0; met15Δ0; ura3Δ0; YIL097w::kanMX4*	Euroscarf
gid1/9	BY4741 *gid9Δ::KANMX4 gid1Δ::HIS5*	This work
gid2/9	BY4741 *gid9Δ::KANMX4 gid2Δ::HIS5*	This work
gid7/9	BY4741 *gid9Δ::KANMX4 gid7Δ::HIS5*	This work

Y00000	BY4741 MATa; *his3Δ1; leu2Δ0; met15Δ0; ura3Δ0*	Euroscarf
BY4741 GID6GFP	BY4741 MATa; *his3Δ1; leu2Δ0; met15Δ0; ura3Δ0, GID6GFP: HIS5*$^{S.Pombe}$	This work with help of Bernhard Braun
YMH2	W303-1B *Mat*α *ade2 leu2-3 112 his3 trp1 ura3 FBP1-P1S*	(Hämmerle et al., 1998)
FBPase-TAP	W303-1B *Mat*α *ade2 leu2-3 112 his3 trp1 ura3 FBP1-TAP::TRP1*$^{K.I.}$	This work
FBPase-P1/S-TAP	W303-1B *Mat*α *ade2 leu2-3 112 his3 trp1 ura3 FBP1-P1S-TAP::TRP1*$^{K.I.}$	This work

5.1.7 Plasmids

Name	Description	Reference
pFA6a-3HA-HIS3MX6	Plasmid to generate PCR integration modules for c-terminal triple HA fusion proteins. *HIS5* gene of *S. pombe*, Triple HA (Hemaglutinin) epitope from influenza virus, bla gene, multiple cloning site, pSP72 derivative.	(Longtine et al., 1998) Plasmid map see appendix
pFA6a-GFP(S65T)-HIS3MX6	Plasmid to generate PCR integration modules for c-terminal GFP fusion proteins. *HIS5* gene of *S. pombe*, green fluorescent protein gene, bla gene, multiple cloning site, pSP72 derivative.	(Longtine et al., 1998) Plasmid map see appendix
pFA6a-HIS3MX6	Plasmid to generate PCR integration modules for gene deletions. *HIS5* gene of *S. pombe*, green fluorescent protein gene, bla gene, multiple cloning site, pSP72 derivative.	(Longtine et al., 1998) plasmid map see appendix
pUb-myc	pRS425 based myc-ubiquitin	T.Sommer

	expression vector with copper inducible *CUP* promotor and *LEU2* marker gene, Amp^R	
pRS425	Yeast episomal vector pRS425 with *LEU2* marker, Amp^R	(Sikorski and Hieter, 1989) plasmid map see appendix
pJR14	YCP50 based gene bank plasmid containing a 27.3 kbp insert with the GID1 gene, *URA3* marker	(Regelmann, 2005) plasmid map see appendix
pJR15	pJR14 based vector with a C-terminal triple HA tagged GID1 gene, generated via gap repair. *HIS5*, *URA3*	(Regelmann, 2005)
pGid7-Flag	FLAG-tagged *GID7* was cloned into a galactose-inducible, C-terminal FLAG tag Gateway™ destination vector, called *pGAL1-CFLAG* with *LEU2* marker, Amp^R	(Ho et al., 2002)
pRsp5-Flag	FLAG-tagged *RSP5* was cloned into a galactose-inducible, C-terminal FLAG tag Gateway™ destination vector, called *pGAL1-CFLAG* with *LEU2* marker, Amp^R	(Ho et al., 2002)
pOAD	CEN vector to generate n-terminal fusion proteins with the *GAL4* activation domain for two hybrid assays, *ADH1* promoter, *ADH1* terminator,*LEU2* gene	(Uetz et al., 2000) plasmid map see appendix
pOBD2	CEN vector to generate n-terminal fusion proteins with the *GAL4* DNA binding domain for two hybrid assays, *ADH1* promoter, *ADH1* terminator,*TRP1* gene	(Uetz et al., 2000) plasmid map see appendix
pBS1479	Plasmid to generate PCR integration modules for c-terminal TAP fusions. *TRP1* gene, multiple cloning site,	(Puig et al., 2001) plasmid map see appendix

	TAP gene with TEV cleavage site, Amp^R	
pOAD-GID4	pOAD with *GID4* according to 5.4.9	This work plasmid map see appendix
pOAD-GID5	pOAD with *GID5* according to 5.4.9	This work plasmid map see appendix
pOAD-GID7	pOAD with *GID7* according to 5.4.9	This work plasmid map see appendix
pOAD-GID9	pOAD with *GID9* according to 5.4.9	This work plasmid map see appendix
pOBD2-GID4	pOBD2 with *GID4* according to 5.4.9	This work plasmid map see appendix
pOBD2-GID5	pOBD2 with *GID5* according to 5.4.9	This work plasmid map see appendix
pOBD2-GID7	pOBD2 with *GID7* according to 5.4.9	This work plasmid map see appendix
pOBD2-GID8	pOBD2 with *GID8* according to 5.4.9	(Uetz et al., 2000) plasmid map see appendix
pOBD2-GID9	pOBD2 with *GID9* according to 5.4.9	This work plasmid map see appendix
pOBD2-FBP1	pOBD2 with *FBP1* according to 5.4.9	(Uetz et al., 2000) plasmid map see appendix
pRS316-GID2	pRS316 based vector with a 2.754 bp DNA fragment containing GID2 and its flanking regions, *URA3*	This work together with Barbin (Barbin, 2005)
pRS316-GID9	pRS316 based vector with a 3200 bp DNA fragment containing GID9 and its flanking regions, *URA3*	This work together with Braun (Braun, 2006)

5.1.8 Oligonucleotides

Oligo	Sequence
FBP1-TAP-fwd	GTTCTTCAGGTGAAATTGACAAATTTTTAGACCATATTGGCA AGTCACAGCGGATCCCCGGGTTAATTAA

FBP1-TAP-rev	CGTACTAAAGTACAGAACAAAGAAAATAAGAAAAGAAGGC GATCATTGAAGAATTCGAGCTCGTTTAAAC
Gid4 fwd Ütz	AATTCCAGCTGACCACCATGATCAATAATCCTAAGGTAGA
Gid4 rev Ütz	GATCCCCGGGAATTGCCATGTCAAGCAAACTCAAAAGAA
Gid5 fwd Ütz	AATTCCAGCTGACCACCATGACGGTGGCTTATTCCCT
Gid5 rev Ütz	GATCCCCGGGAATTGCCATGTCATTTAACTTTCAAAAGCAGGT
Gid7 fwd Ütz	AATTCCAGCTGACCACCATGTCACACACTAATAAGATCG
Gid7 rev Ütz	GATCCCCGGGAATTGCCATGTTAATTTCTTGAAATTTTCCAGAT T
Gid9 fwd Ütz	AATTCCAGCTGACCACCATGGCAGAGAAATCAATAT
Gid9 rev Ütz	GATCCCCGGGAATTGCCATGTCAGGTTGGGTACATT
Re-2-Hybrid fwd	CTATCTATTCGATGATGAAGATACCCCACCAAACCCAAAAAAA GAGATCGAATTCCAGCTGACCACCATG
Re-2-Hybrid rev	CTTGCGGGGTTTTTCAGTATCTACGATTCATAGATCTCTGCAGG TCGACGGATCCCCGGGAATTGCCATG
Gid5-Ha fwd	AAAAGGCCAGAACGTTACTATATCACATGGACCTGCTTTTGAA AGTTAAACGGATCCCCGGGTTAATTA
Gid5-Ha rev	AAAAACTATAGCATAAATTAATTGTAGGAAATACTACGAGTTC TGTGCATGAATTCGAGCTCGTTTAAAC-
Gid6-Ha fwd	GCATTGAAGATATGAAAAAAAATGGTTATATTTATTTCTATAC AAGATGCCGGATCCCCGGGTTAATTAA
Gid6-Ha rev	ATATATATATATATGTGTGTGTGTGTGTGTGTGTGTGTAAAC GTTCTTGAATTCGAGCTCGTTTAAAC
Gid7-Ha fwd	CTTCTGGCGGTGATGACGGTAAGATAAAAATCTGGAAAATTTC AAGAAATCATCATCATCATCATCATCGGATCCCCGGGTTAATT AA
Gid7-Ha rev	TTTTTTTTGTTACATAAAACTTTGCTTACGTATATATATAAGGT GGAGTAGAATTCGAGCTCGTTTAAAC
Gid8-Ha fwd	GCGAAAATCAGCTTCATCACAACCAAATAGGGGTTCCTAGGGT CGAAAACCGGATCCCCGGGTTAATTAA
Gid8-Ha rev	ACACATGCACACGCACACACACATATATAAATATATACGTACT ATGTATGGAATTCGAGCTCGTTTAAAC
Gid9-Ha fwd	TTGACATGAAAATATTTTGCGAATCAGATTCTATCAAAATGTA CCCAACCCGGATCCCCGGGTTAATTAA

Gid9-Ha rev	AAAGTTGGACAAATCTTTATATAAAAAAATGCATATAGCTTGAAACTATTGAATTCGAGCTCGTTTAAAC
FBP1-GFP fwd	GTTCTTCAGGTGAAATTGACAAATTTTTAGACCATATTGGCAAGTCACAGCGGATCCCCGGGTTAATTAA
FBP1-GFP rev	CGTACTAAAGTACAGAACAAAGAAAATAAGAAAAGAAGGCGATCATTGAAGAATTCGAGCTCGTTTAAAC
GID2 deletion fwd	TAAGTGTGTCTTCAAGAGAGATGCAGCACTGAGTAGGGAACCAAGAAACGCGGATCCCCGGGTTAATTAA
GID2 deletion rev	TCAAAGCATAACAAAACGAACCTTTTTTGTACTGCTCATTGAAGTATTTAGAATTCGAGCTCGTTTAAAC
GID1 deletion fwd	TTAGTAGTACGTTAAAGCCAAGCGTCGAATTTCAGCATAATTAAGAGGAACGGATCCCCGGGTTAATTAA
GID1 deletion rev	TAATGACTGATATCACATGGCTTTGTTGTTTGAAGGTGCTTGTTTTATGCGAATTCGAGCTCGTTTAAAC
GID7 deletion fwd	GTCAAATATGAAAAACACTTCCAAGGGGGCGTACTACTTCAACTAATAAACGGATCCCCGGGTTAATTAA
GID7 deletion rev	TTTTTTTTGTTACATAAAACTTTGCTTACGTATATATATAAGGTGGAGTAGAATTCGAGCTCGTTTAAAC
P1 RING CYS1135	CCTCCTTATTCACTGGCAAGCCATCACATCATTTCTAAAAAGGCGC
pRS Swa1-Pme1	GCTATAAAAATAATTATAGTTTAAACTTTTTAATATAAATATATA

5.1.9 Media for yeast and *E.coli* cultivation

All media for the cultivation of *S.cerevisiae* and *E.coli* strains were prepared using double dionised water (ddH_2O) prepared with the Ion exchanger *Milli-Q Academics.* The pH was adjusted with NaOH or HCL and media got sterilised by autoclaving at 121°C for 20 min. Media used to cultivate cells for fluorescence microscopy got filter sterilised to avoid Maillard products.

To prepare agar plates 2 % of Bacto® Agar was added to the media. Synthetic media and mineral media got supplemented with supplements needed.

Name	Components

CM- medium	0,669% Yeast nitrogen base w/o amino acids 2% D-glucose 0,0117% L-alanine, L-arginine, L-asparagine, L-asparatic acid, L-cysteine , L-glutamine, L-glutamic acid, L-glycine L-isoleucine, L-methionine, L-phenylalanine, L-prolin, L-serine, L-threonine, L- tyrosine, L-valin, myo-inositol, p-amino benzoic acid pH 5.6
2 × YTAG medium	1.6 % Bacto Tryptone; 1% yeast extract; 0.5 % NaCl; 2% *D*-glucose; 100µg/ml ampicilline; pH 7.0
Labelling Medium	0.17 % Yeast Nitrogen Base w/o ammonium sulfate and w/o amino acids, 0.1 % *D*-glucose; 0.002 L-adenine, uracil, L-tryptophan, L-histidine, 0.003 % L-arginine, L-tyrosine, L-lysine, L-leucine, 0.005 % L-phenylalanine, 0.01 % L-glutamic acid, L-aspartic acid, 0.015 % L-valine, 0.02 % L-threonine, 0.04 % L-serine pH 5.6
LB Medium (Luria Broth)	0.5% Bacto® Yeast Extract 1% Bacto® Tryptone 0,5% Sodium chloride for selection of plasmid carrying *E.coli* the selective antibiotic was added : 100 µg/ml ampicilline for solid medium an addition of 2% Agar is necessary pH 7.5
SOC medium	2% Bacto® Tryptone

	0,5% yeast extract 0,4% D-glucose 10 mM NaCl 10 mM $MgCl_2$ 10 mM $MgSO_4$ 2,5 mM KCl pH 7.4
YPD- medium	1 % yeast extract 2% Bacto® Peptone 2% D-glucose pH 5.5
YPEtOH-medium	1 % yeast extract 2% Bacto® Peptone 2% Ethanol p.a. pH 5.5
Mineral medium MV	0.67% Yeast nitrogen base w/o amino acids 2% D-glucose 0.3 mM L-histidine 1.7 mM L-leucine 1 mM L-lysine 0.4 mM L-tryptophane 0.3 mM adenine 0.2 mM uracil ph 5.5
Sporulation media	1% yeast extract 2% Bacto® peptone 0.5% D-glucose 1% Potassium acetate ph 5.5
SD-CA-Medium for fluorescence microscopy	17% Yeast nitrogen base without aminoacids and ammoniumsulfate 0.5% ammoniumsulfate 0.5% casaminoacids 0.002% of each supplement

	2% glucose or ethanol p.a. pH 5.5

5.2 METHODS

5.2.1 Crossing haploid yeast strains

To cross haploid yeast strains the same amount of cell material of haploid strains with different mating types were mixed on an YPD plate and incubated for 24 h at 30°C. Diploid strains were selected by auxotrophy markers.

5.2.2 Sporulation of yeast and the dissection of tetrades

Diploid yeast strains were grown in YPD overnight. This culture was then inoculated 1:70 in fresh YPD and grown for an additional 5-6 h to an OD of 0.3- 0.5. 2 ml of this culture was taken, spun down for 4 min at 3000 rpm and washed with 1 ml of water to get rid of excess glucose. After an additional wash step with 1ml 1% KOAc the yeast was resuspended in 1ml sporulation media and inoculated at 23°C for 3-7 days until tetrades were visible under the microscope.

For the dissection of the tetrads 200 µl of the yeast culture was washed 3 times with sterile water and resuspended in 200 µl of water. To digest the ascus membrane of the tetrads 2 µl of glusulase enzyme was added and incubated at room temperature for 3 min. After the addition of 800 µl of water the spores were kept at 4°C for 4-5 h and 10 to 50 µl of the spores were carefully pipetted onto a YPD plate with cut off tips. The spores were then dissected with a micro manipulator (Wetzlar und Lawrence Instruments, Haywards, USA) and incubated at 30 °C for 2 days. To investigate the marker segregation, the haploid colonies were replica plated onto a CM plate without the auxotrophy marker and checked for growth. Afterwards the mating type was determined according to chapter 5.2.3.

5.2.3 Determination of the mating type

To determine the mating type of an unknown yeast strain it was crossed with a special mating type tester strain. Both tester strains YR312 (*MATa*) and YR320 (*MATα)* carry the rare auxotrophy marker allele *his1*. By crossing the tester strains with the unknown strain the

histidine auxotrophy was complemented in case of diploidy. Only strains that were able to mate with the tester strain grew on a CM - histidine selection plate.
After crossing the strains, cells were incubated for 2-3 days at 30 °C and the mating type of the unknown strain was determined by the ability to mate with the tester strain. Unknown diploid cells were not able to mate and therefore couldn't grow at all.

5.2.4 General growth conditions for yeast

S.*cerevisae* strains without a plasmid were grown in YPD-media at 30°C in liquid culture or on YPD agar plates. The presence of a plasmid in yeast was selected by complementation of auxotrophy. Therefore cells were grown in CM-media (minimal media) or on CM-agar plates without the marker supplement. Usually strains were not able to synthesize lysine, tryptophane, histidine, leucine and uracil. Only strains positively transformed with a plasmid containing the complementary marker were able to grow. All the other auxotrophy markers were added to the media to a concentration up to 20 µg/ml. Plates were incubated 2-3 days at 30°C and liquid cultures were incubated at 30°C in Erlenmeyerflasks at 220 rpm. Strains grown on agar plates were stored at 4°C and colonies were stroke out on new plates after 1-2 month storage. For long time storage cells were taken with a toothpick and resuspended in 1 ml of sterile glycerol (15% v/v). Vials with the corresponding yeast strain were frozen at -80°C.

5.2.5 Induction of gluconeogenesis and the catabolite degradation of FBPase

All gluconeogenetic enzymes are strongly upregulated when yeast cells are grown on a medium containing a non-fermentable carbon source such as ethanol or when cells are glucose depleted in the late stationary phase. The addition of glucose to such cells then leads to a fast repression of genes involved in gluconeogenesis and to the inactivation of gluconeogenetic enzymes. In a process called catabolite degradation the key enzyme of gluconeogenesis, FBPase, gets rapidly degraded. To study this process by western blot analysis cells were inoculated from an agar plate in 2 ml of YPD or CM medium and grown overnight. Cells were then inoculated 1:12.5 in a glucose containing main culture and grown for at least 7h. These cells were then inoculated to an OD_{600} of 0.25 (generally 1:17) in a medium containing 2% ethanol to induce gluconeogenesis. After 6-16h growth 1.5 OD_{600} (Novaspec II, Pharmacia) of cells were taken from each culture and used as a zero sample (0

min). 12 OD_{600} of the remaining cells was then transferred to a 50 ml Falcon tube and cells were spun down in a tabletop centrifuge (Centrifuge Z320K, Eppendorf*)* at 3000 rpm for 3 min. To activate catabolite degradation these cells were resuspended in 8 ml glucose containing media and incubated at 30 °C. 1 ml of these cells was generally taken every 30 min up to 2h and transferred to a 1.5 ml reaction tube. These cells got immediately spun down in a benchtop centrifuge (centrifuge 5417C or 5804R, Eppendorf) at 13000 rpm for 1 min. The supernatant was then removed and pellets were kept at -20°C. For immunoprecipitations cells were treated as described above, however 15 OD_{600} of cells were taken per time point.
As an alternative cells were grown in a glucose containing media to an OD_{600} around 1.5. To remove traces of glucose cells were washed with 5 ml ddH_2O and resuspended in 20 ml YPEtOH to obtain an OD_{600} of 1.5 per ml. After induction of gluconeogenesis for 5-6 h catabolite degradation got started by the addition of glucose to a final concentration of 2% and 1 ml of cell culture per samples was taken as described above.

5.2.6 General growth conditions for *E.coli*

E. coli strains were grown in LB-media at 37°C in liquid culture or on LB agar plates. As a selective marker Ampicillin was added to the media to a concentration of 50-100 µg/ml. Only clones containing a vector with Ampicillin resistance were able to grow. For larger culture volumes a 5ml overnight culture was used for inoculation. When necessary the cell concentration was determined measuring the optical density OD_{600} of the culture. To store a certain clone a colony was picked, stroke out on a new plate and kept at 4°C. For long time storage a single colony was grown in 3ml LB plus 50-100 µg/ml Ampicillin. After adding glycerol up to 15% the liquid culture could be stored at –80°C. Strains were transferred to a new plate after 1-2 month storage.

5.3 DNA WORK

5.3.1 Isolation of plasmid DNA from *E.coli* cultures

Solution 1	25 mM Tris/HCl pH 8,0, 50 mM D-glucose, 10 mM EDTA
Solution 2A	0,4 M NaOH
Solution 2B	2 % SDS
Solution 3	5 M KOAc pH 4,8

To isolate plasmid DNA from *E.coli* cultures a method described by Sambrook et al was used. For small scale preparation of plasmid DNA (Mini-Prep) 1.5 ml of a stationary *E.coli* culture was transferred to a 1.5 ml reaction tube and cells were pelleted by centrifugation (13000 rpm, 1 min). After removing the supernatant cells were resuspended in 100 µl solution 1. Then solution 2 was prepared freshly by mixing solution 2A and 2B (1:2). After the addition of 200 µl solution 2, the resuspended cells were incubated for 5 min on ice for alkaline lysis of *E.coli* cells. Afterwards 300 µl of solution 3 was added to each sample and left on ice for 15 min. Cell debris got then pelleted by centrifugation (13000 rpm, 10 min) and 350 µl of the supernatant was transferred to a new 1.5 ml reaction tube. In the following steps plasmid DNA was precipitated by the addition of 700 µl of ice cold ethanol p.a. (100%). After 15 min precipitation at -80°C, DNA got pelleted by centrifugation (13000 rpm, 10 min) and the pellet was washed once with 70% ethanol to remove salts. The pellets were then dried and resuspended in 40-50 µl ddH_2O. RNA was digested by the addition of 1µl RNAase (0.1 mg/ml).
Alternatively DNA was isolated according to the protocol supplied with the QIAprep Spin Miniprep Kit (Qiagen). Columns were recycled by storing them in 70 % ethanol. Before use columns were washed with 700µl of 0.1M NaCL.

5.3.2 Isolation of chromosomal DNA from *S.cerevisiae*

To isolate chromosomal DNA a yeast culture was grown in 2 ml YPD overnight. Cells were transferred to a 2 ml SafeLock® Eppendorf reaction tube and spun down (13000 rpm, 1 min). After washing the cells with 1 ml of ddH_2O the pellet was resuspended in 200 µl breaking buffer (2% Triton X-100, 1% SDS, 100 mM NaCl, 10 mM Tris/HCl pH8, 1 mM EDTA). Then 200 µl of a 1:1 mixture phenol: chloroform was added to the cells together with 200 µl of acid washed glass beads. Cells were then vigorously lysed on a Vortexer for 4 min. After the addition of 200µl water all samples were spun in a benchtop centrifuge (13000 rpm, 5 min) and 300µl of the upper phase was taken and transferred to a new 1.5 ml reaction tube. DNA was then precipitated by adding 1 ml of ice cold ethanol (100%) and incubation at -80°C for 10 min. After a centrifugation step (13000 rpm, 10 min) the remaining pellet got resuspended in 400 µl ddH_2O containing 30 µg RNAse A. RNA was then digested for 5 min at 37°C. To precipitate DNA once more 1 ml of ice cold ethanol (100%) and 10 µl of 3 M NaOAc (pH5) was added, mixed and incubated at -80°C for 10 min. In a final centrifugation

step (13000 rpm, 10 min) DNA got pelleted and supernatant was carefully removed. The remaining DNA pellet was dried and resuspended in 22µl H_2O.

5.3.3 Isolation of plasmid DNA from yeast (plasmid rescue)

In a method similar to the one described in section 5.3.2 very low amounts of plasmid DNA can be isolated from yeast to afterwards transform it into *E.coli* for amplification.
To do so cells from a 2 ml overnight culture were spun down and resuspended in breaking buffer (2% Triton X-100, 1% SDS, 100 mM NaCl, 10 mM Tris/HCl pH8, 1 mM EDTA). After the addition of 200 µl phenol/chloroform (1:1 mixture) and 200 µl of glass beads cells were lysed by vortexing for 4 min. The mixture was then centrifuged for 5 min at 13000 rpm and 50 µl of the aqueous upper phase were mixed with 5µl 3M NaOAc (pH5) and 140µl of ice cold ethanol (100%). The DNA was then precipitated for 25 min at -80°C and then centrifuged for 10 min at 13000 rpm. The pellet was washed once with 70 % ethanol, dried and resuspended in 30 µl of ddH_2O.
For the transformation of *E.coli* 1µl of the DNA was used.

5.3.4 Transformation Methods

5.3.4.1 Preparation of competent *E. coli* cells for electrotransformation

E.coli DH5α or BL21 from a single cell colony was grown in 4ml LB-medium at 37°C over night to inoculate a 1000 ml Erlenmeyerflask with 200ml LB-Medium. These cells were grown to an OD_{600} of ~0.2 and put on ice for 30 minutes. After that cells were spun down in a refrigerated centrifuge (Centrikon H-401, Kontron instruments) at 6000 rpm (4°C) for ten minutes. For the centrifugation 200 ml GSA centrifugation vials were used. Then the medium was completely removed by decanting and the pellet was sequentially washed with 500 ml, 250 ml and 20 ml ice cold glycerol (10%). After resuspension of the pellet in 5 ml glycerol (10%) cells were aliquoted into sterile Eppendorf tubes, frozen in liquid nitrogen and stored at –80°C.

5.3.4.2 Standard Transformation Method for E. coli

Competent cells prepared in section 5.3.4.1 were taken out of –80° and thawed on ice. 50 µl of the cell suspension were then mixed with up to 1 µl of plasmid DNA and incubated for 1 minute on ice. This mixture was transferred to a cold electroporation cuvette (0.2 mm) and transformation was done using a Gene Pulser (BioRad). The settings were put to 25 µF, 400W and 2.3 V. After the pulse, cells were immediately resuspended in 1 ml of SOC media, transferred to a 1.5 ml reaction tube and kept at 37 °C for 1h to recover. These cells were then spun down for 1 min at 13000 rpm, resuspended in 50 µl ddH_2O and plated out on an LB_{Amp} plate. Plates were then incubated at 37°C over night.

For a so called 'Blue-White' screen 100 µl of X-Gal (20 mg X-Gal / ml DMF) and 40µl of a 100 mM IPTG stock were stroke out on an LB_{Amp} plate and kept open on the sterile bench for 30 min. Plasmids containing a multiple cloning site in the LACZ gene (e.g. pRS series) were then plated out on LB_{Amp} plates. Clones carrying a plasmid with an intact LACZ gene were able to metabolize X-Gal and turned blue. However clones carrying an insert in the multi cloning site (MCS) were not able to metabolize X-Gal and stayed white.

With this method clones carrying a DNA fragment in the MCS can be distinguished from clones without.

To be able to increase the amount of plasmid DNA for electroporation to up to 10 µl, DNA was desalted by dialysis before transformation. Therefore a small nitrocellulose membrane filter (Millipore) was put in a petridish with ddH_2O. Plasmid DNA was then pipetted onto the floating membrane and kept there for 30 min.

5.3.4.3 Standard transformation method for *S. cerevisae*

10x TE	100 mM Tris/HCl pH 7,5, 10 mM EDTA
10x LiOAc	1 M LiOAc
40 % PEG	240 µl 50 % PEG-4000, 30 µl 10x TE, 30 µl 10x LiOAc
Li-Sorb	1x TE, 1x LiOAc, 1 M Sorbitol

To prepare competent yeast cells, a colony from the selected yeast strain was picked and grown in 5ml YPD-medium by shaking at 30°C. The OD of the overnight culture was measured and diluted in 10 ml of YPD to get an OD_{600} of 0.2. After approximately 3 h shaking at 30°C, cells had an OD_{600} of ~ 0.8. These cells were transferred into 15 ml tubes

and spun down for 3 min in a *Sorvall RC 5B* benchtop centrifuge with a speed of 3000 rpm. The pelleted cells were then washed twice with Li-Sorb buffer and got finally resuspended in 500µl Li-Sorb. The amount of cells was suitable for 10 transformations. 50 µl per transformation were aliquoted in sterile 1.5 ml reaction tubes and incubated at 30°C for 30 min. To each aliquot 5 µl of herring sperm DNA, 5- 20 µl of the DNA to transform and 300 µl of 40% PEG solution were added and cells were incubated an additional 30 min at 30 °C. Prior to use, herring sperm DNA was denatured for 5 min at 95 °C and kept on ice for 5 min afterwards. The heat shock transformation was then done by keeping the aliquots for 20 min at 42 °C. Then cells were pelleted by centrifugation for 3 min at 3000 rpm. The supernatant was decanted and the remaining cells were resuspended in 50 µl of sterile water. These cells were plated out on selective media and positive clones grew after 2-4 days incubation at 30 °C.

5.3.5 Southern blot analysis

(Southern, 1975)

The Southern blot is a method to identify a specific DNA fragment of a complex mixture of genomic DNA fragments (Maniatis et al., 1982; Southern, 1975). To do so genomic DNA first has to get digested with a restriction enzyme to get a complete digestion of the genomic DNA.

After that the DNA fragments is separated via agarose gel electrophoresis and fragments are transferred to a nylon membrane. A DNA sonde which is complementary to the genomic fragment to be studied is then hybridised with the genomic fragment which can then be visualised by autoradiography.

5.3.5.1 DNA digestion and transfer onto a nylon membrane

20 x SSC-buffer	0.3 M sodium citrate, pH 7 ; 3 M NaCl
Denaturing buffer	0.5 M NaOH, 1.5 M NaCl
Neutralising buffer	0.5 M Tris/HCl, pH 7; 3 M NaCl
Primary wash buffer	2 M urea; 3.46 mM SDS; 50 mM sodiumphosphatebuffer, pH 7.0; 149 mM NaCl; 1 mM magnesium chloride; 2% blocking reagent (provided with the kit)
Secondary wash buffer	50 mM Tris/HCl, pH 10; 500 mM NaCl ; 2 mM $MgCl_2$

Genomic DNA of the yeast strain of interest was extracted according to the protocol described in subsection 5.3.2. The DNA sequence of the gene to be investigated plus additional 5000 bp up- and downstream was downloaded from www.yeastgenome.org. Then a suitable restriction enzyme was chosen with the programme 'Clone Manager 5' to yield a fragment of 2000-6000 bp size. First of all 3-5 µl of the chromosomal DNA was digested in a total volume of 20 µl according to the protocol of the manufacturer (New England Biolabs or Boeringer Mannheim) in 2 µl of the proposed 10 × restriction buffer and 1µl of the specific enzyme (see also 5.3.9). Usually the digestion was kept at 37°C over night. To assure a complete digestion an additional 0.5µl of enzyme was added the next morning and kept for an additional 4-5 h at 37°C. 2µl of 10 × DNA sample buffer was then added to each sample and the digested DNA was subjected to DNA electrophoresis in a 1% agarose gel with 20 slots (5.3.8). After 60- 90 min separation of the DNA fragments a picture was taken with a ruler next to the DNA length standard.

In the following steps the separated DNA was transferred to a nylon membrane (Hybond®, Amersham). All steps were done according to the manual of the manufacturer (AlkPhosDirect®, Amersham). The membrane was cut to be as big as the agarose gel with approximately 0.25 cm overlap on each side. After equilibration in 2 × SSC-buffer the membrane got transferred to the wet surface of a blotting chamber. The surface of the blotting chamber was then covered with a plastic foil with the membrane uncovered. Afterwards the agarose gel with the separated DNA was put right on top of the membrane and the vacuum pump was started (Pharmacia, VacuGene Pump; 40 mbar). Then the gel got covered with 25 ml of 'Denaturing buffer' for 10 min and the buffer was removed and replaced by 25 ml of 'Neutralising buffer' for an additional 10 min. The DNA got finally transferred by replacing the 'Neutralising buffer' with 20 × SSC buffer for 1 h. After that the transferred DNA was covalently linked to the membrane by exposing it to UV light for 5 min and the membrane was put into a hybridisation tube.

5.3.5.2 Generation of a sequence specific DNA sonde

The Gene Images® AlkPhos Direct® labelling and detection system from Amersham Biosciences is based on a dioxetane chemiluminescence system. It involves directly labelling probe DNA with a specially developed thermostable alkalinephosphatase. This is achieved by completely denaturing the probe so that it is in single-stranded form. The addition of the cross-linker then covalently couples the enzyme to the nucleic acid

A DNA fragment homologous to the region to be detected (5.3.5.1) was made by PCR (5.3.7). The quantity of the DNA was determined with a spectrophotometer. All following steps were done according to the manufacturer and buffers used and not described were part of the kit (Amersham). To produce the DNA sonde, 10 µl of a 10 ng/µl DNA solution was taken, boiled for 5 min at 95°C and cooled down on ice immediately afterwards for 5 min. Then 10 µl of reaction buffer 2 µl of labelling reagent and 10 µl of crosslinker solution was added to the DNA and kept at 37°C for 30 min. The sonde was then ready for hybridisation with the membrane.

5.3.5.3 Hybridisation and detection of the DNA sonde

The hybridisation buffer AlkPhos Direct was prepared according to the manufacturer and preheated to 55°C. For prehybridisation 30 ml of this buffer was added to the membrane in a hybridisation tube and incubated for 30 min at 55°C in a hybridisation oven. Then 32 µl of the DNA sonde were added to the membrane and kept over night at 55°C for hybridisation. The next day the blot was washed twice for 15 min with 50 ml of prewarmed (55°C) Primary wash buffer. Then the membrane was removed from the hybridisation tube and washed twice with 250 ml of Secondary wash buffer for 5 min. The blot was carefully transferred into a film cassette, and covered with 3 ml CDP Star®detection reagent (Amersham). A signal was observed after 30 min- 24 h of exposure to an ECL film.

5.3.6 Site directed mutagenesis

Site directed mutagenesis was performed as described by Clontech (Tranformer® Site-directed mutagenesis kit). Therefore two oligonucleotides were designed: one oligonucleotide was designed to carry the mutation in the gene of interest (mutagenic primer), the other was chosen to be homologous to a region in the backbone of the vector carrying the gene of interest. The second primer carried a mutation to change a unique restriction site (selection site) in the wild type plasmid to another selection restriction site (selection primer). Primers were also designed to carry the mutations in the middle of the primers with about 15 bps overlap on each side and similar annealing temperatures.

First of all, oligonucleotide primers had to be phosphorylated. Therefore 1µl of primer was transferred into a 1.5 ml reaction tube. After the addition of 2µl 10 mM ATP (Roche), 1 µl of T4 polynucleotide kinase (NEB), 14µl of water and 2 µl of kinase buffer (500 mM Tris-HCl, pH7.5, 100 mM $MgCl_2$, 50 mM DTT, 10 mM ATP) the preparation got incubated at 37°C for 60 min. Afterwards the phosphorylated primers were kept at -20°C.

Then 300 ng of template plasmid DNA, 2 µl 10 × annealing buffer (200 mM Tris pH 7.5, 100 mM $MgCl_2$, 500 mM NaCl), 4 µl of both phosphorylated selection primer and mutagenic primer were add up to 20 µl with water and boiled in a water bath for 5, 6.5, 8 and 9 min. All samples were immediately cooled down on ice for 5 min for the proper annealing of the primers to the plasmid template. Afterwards single stranded plasmid DNA with the annealed primers was refilled. For this reaction 3µl of 10 × synthesis buffer (100 mM Tris pH 7.5, 5 mM dNTPs, 10 mM ATP, 20 mM DTT), 1 µl of T4 DNA polymerase (NEB), 1 µl of T4 DNA ligase (Invitrogen), 1 µl of ATP (100mM), 3 µl BSA (1 mg/ml) and 1 µl of water were added to each annealing reaction and kept at 37°C for 1-3 hours. Then the reaction was stopped by putting the samples for 5 min at 70 °C.

To eliminate the wild type template plasmid not carrying the mutation, all samples were digested with the restriction enzyme which site is not existing in the mutated gene. Therefore 1 µl of the restriction enzyme, 4 µl of the corresponding buffer system, 4 µl of BSA (1mg/ml) and 1 µl of water was added to each sample and incubated at 37°C for 1-2 hours. Then 7 µl of each sample was transformed into *E.coli* (strain BMH 71-18 *mutS*) according to the manufacturer and cells were grown in a 15 ml Falcon tube overnight. The plasmid DNA was then isolated according to section 5.3.1 and the recovered plasmid DNA was digested again. Therefore 10 µl of the miniprep DNA was mixed with 0.5 µl selection enzyme, 2 µl restriction buffer, 2 µl BSA (1mg/ml) and 5 µl water. After incubation at 37°C for 1-2 hours, 1-2 µl of the sample was transformed into *DH5α* and plated out on LB-Amp plates. After overnight incubation positive clones were picked and plasmids were tested for the mutations by restriction enzyme digestions and sequencing.

5.3.7 The Polymerase Chain Reaction (PCR)

(Mullis, 1990)

The polymerase chain reaction is a state of the art method to amplify defined DNA segments from either plasmid DNA or genomic DNA *in vitro*. In a first step template DNA gets denatured at 95°C. Two short synthetic oligonucleotides, called primers determine the beginning and end of the region to be amplified. They anneal to the denatured template DNA at the calculated annealing temperature (T_m). At a third temperature the 3 prime ends of the primers are filled up catalysed by a heat stable DNA polymerase. By repeating these steps DNA gets amplified.

The *in vitro* amplification of specific regions was conducted using a RoboCycler Gradient 40 PCR machine (Stratagene, La Jolla) with a reaction specific temperature programm. Therefore a 50µl reaction mix was prepared in 200µl thin wall Eppendorf tubes. This reaction mix consisted of a dNTP mix, each oligonucleotide primer (5.1.8), template DNA and the DNA polymerase with the appropriate reaction buffer. The whole mix was filled up to 50µl volume with sterile ddH_2O. Volumes and concentrations for a conventional PCR reaction are listed in Table 2. A 5:1 (v/v) mixture of Taq polymerase (Roche) and Vent polymerase gave the best results.

Table 2: Reagents and their volumes used for conventional PCR reactions

Reagent	Volume [µl]	concentration/activity
DNA Polymerase	1	0.1-1.0 U
Reaction buffer	5	10 ×
dNTP's	1	25 mM
Template DNA	1	0.2-0.4 µg/µl
Oligonucleotide 1	1	0.1µg/µl
Oligonucleotide 2	1	0.1µg/µl
H_2O	Add to 50µl	

The annealing temperature of the primers (T_m) was calculated with the following formula:
$T_m = [(4°C \times (dGTP's + dCTP's)) + (2°C \times (dATP's + dTTP's)) – 4°C]$. For very long primers (≥ 30 bp) the annealing temperature was calculated with the online algorithm www.stratagene.com/QPCR/tmCalc.aspx.
Denaturing of template DNA was conducted for 5 min in a single beginning step and then for 45 s every cycle. The amplification step took place at 72°C. One minute extension time was calculated for each 1000 bp to be amplified. For a complete extension the temperature was kept at 72°C for 5 minutes in a final step. 30 rounds of amplification were sufficient for a suitable yield of DNA. For optimisation of PCR reaction an optional 1 µl of magnesium sulfate was added to the reaction mix.
To look for PCR product 3 µl of the reaction mix was run on a 1% agarose gel after amplification. Purification of PCR products was carried out with the *QIAquick PCR Purification* kit according to the manual instructions.

5.3.8 Agarose Gel Electrophoresis

TAE-buffer	40 mM Tris/ acetic acid, pH 7.5; 1mM EDTA
Agarose gel (1 %)	1.5 g agarose; TAE buffer ad 150 ml
DNA Loading buffer (5×)	50 % (v/v) glycerol in 10 × TAE; 2 mg/ ml bromophenol blue

DNA fragments were separated in a 1% agarose gel by electrophoresis. Gels were prepared by melting the agarose gel in a microwave oven and by pouring the gel in an appropriate chamber. 0.5 µl/ml of ethidium bromide was added to the agarose and mixed. The hard gel was then transferred to an electrophoresis chamber (Pharmacia), covered with TAE-buffer and loaded with the DNA samples. Conventionally fragments were separated at 120 V for 30 min and afterwards visualised on a UV screen. For analytical use UV was set on 100 % and photographed afterwards, for preparative purposes UV was set on 70% and bands were cut out of the gel. Pictures were taken with the photosystem from MWG Biotech. As a length standard the 1 kb ladder from Boehringer Mannheim or Invitrogen was used (50 µl in 450 µl DNA loading buffer)

5.3.9 DNA Digestion with Restriction Endonucleases

A restriction endonuclease type II cuts the DNA at an enzyme specific site which is always a palindrome. Digestion of DNA with such enzymes is a necessary tool for cloning DNA fragments. A huge variety of such enzymes with highly specific restriction sites are commercially available from NEB and Boehringer Mannheim and are provided with the corresponding buffer system (www.neb-online.de).

The digestion of DNA was generally carried out in a volume of 10µl. Therefore 10 U (often 1 µl) of enzyme (Boehringer Mannheim or NEB), 1 µg of purified DNA (2-3 µl) and 1µl of the appropriate buffer system was filled up with sterile water to 10µl and incubated for 1-2 hours at 37°C. Restriction enzymes working at different temperatures were highlighted by the manufacturer. Double digests of DNA were executed in a buffer system suitable for both enzymes or digestions were carried out subsequently.

To use digested DNA for cloning, subsequent gel electrophoresis was necessary to get rid of small complementary DNA fragments (5.3.8). DNA was then cut out of the gel and purified with the Gel Purification kit (Quiagen) according to the manufacturer manuals.

5.3.10 5' Dephosphorylation of linearised plasmid DNA

Digested plasmid DNA was dephosphorylated on the 5'end using Calf Intestinal Alkaline Phosphatase (CIP, New England Biolabs) to prevent self ligation. Therefore 1-5µg DNA, 1-2U of the enzyme and 4µl of the appropriate buffer (10×) were filled up to 40µl with sterile water.
The mix was incubated at 37°C for 30 minutes and purified using the Gel Purification Kit (Quiagen).

5.3.11 Nucleic acid ligations

The enzyme T4-ligase (Invitrogen) was used to insert DNA fragments in linearised and dephosphorylated plasmid DNA. T4 ligase catalyses a phosphodiester bond between the vector and the insert. This reaction was carried out using an insert/plasmid molar ratio of 3/1 to 6/1 in a volume of 30µl. The crude concentration ratio was determined by running 3µl of each sample on a 1% agarose gel. DNA was mixed with 1µl of T4 ligase (Invitrogen), 6µl of the appendant buffer system (5 × ligation buffer) and was filled up to 30 µl with water. All samples were kept at 16°C over night for proper ligation and were afterwards transformed into *E. coli* (5.3.4.2).

5.3.12 Sequencing of plasmid DNA

To sequence certain DNA regions on a plasmid the plasmid DNA was isolated according to chapter 5.3.1. Conventionally the concentration of plasmid DNA from two *QIAprep Miniprep* reactions was eluted with 50 µl of ddH_2O and pooled in a 1.5 ml reaction tube. The amount of DNA should then be between 1-2 µg. Then the complete DNA got precipitated by adding 250 µl of ethanol (100%) and 35 µl of 3 M NaOAc (pH5) to the eluted 100 µl DNA. Samples were kept at room temperature for 30 min and the coagulated DNA got then spun down for 30 min at 13000 rpm. After carefully removing the supernatant the pellet was dried for 30 -60 min and samples were send for sequencing.
Sequencing was conducted at MWG-Biotech, Ebersberg and primers for sequencing were either ordered or 10 µl were sent at a concentration of 10 pmol/µl.

5.4 PROTEIN WORK

5.4.1 SDS-PAGE (SDS Gel Electrophoresis)

(Laemmli, 1970)

Table 3: Components and volumes used for SDS- gels

Components	7.5%	10%	12%	Stacking Gel
ddH_2O	4.85 ml	4.02 ml	3.35	6.1 ml
1.5 M Tris pH 8.8	2.5	2.5 ml	2.5	
0.5 M Tris pH 6.8				2.5 ml
10% SDS (w/v)	100 µl	100 µl	100 µl	100 µl
Acrylamide solution (30%)	2.5 ml	3.33 ml	4.0 ml	1.3 ml
10% APS (w/v)	100 µl	100µl	100 µl	100µl
TEMED	10 µl	10µl	10 µl	10µl

SDS-PAGE was used for the separation of proteins by their molecular mass and performed as described earlier (Laemmli, 1970). Sodium dodecyl sulfate (SDS) is an anionic detergent which denatures secondary and non–disulfide–linked tertiary structures of proteins and applies a negative charge in proportion to the proteins mass. Separation of proteins can therefore be conducted in an electrical field in a polyacrylamide gel. The narrow pores of this gel allow small proteins to migrate faster than bigger proteins.

Conventionally polyacrylamide gels were 1mm thick and consisted of a 4 % stacking gel with the loading pockets for protein samples on top and a 10 % resolving gel. Resolving gel and stacking gel were prepared freshly and filled between the glass plates of a gel pouring system after the addition of ammonium persulfate and TEMED. Around 5 ml of resolving gel was poured first and covered with isobutanol till the polymerisation was finished. As soon as the resolving gel was set the isobutanol was rinsed off and the stacking gel was poured. Before setting of the stacking gel a 10 slot comb was put in the gel and removed after setting.

For electrophoresis the Bio-Rad Mini Protean II electrophoresis chamber was filled with 800 ml SDS-buffer (25 mM Tris, 200 mM Glycin, 0,1 % SDS) and the gel was transferred into the chamber. After loading the gel with 10 -20 µl of protein sample and 8 µl of protein molecular mass standard (Precision Plus Protein^{TM} standard, BioRad) proteins were separated at a voltage of 150 V for 60- 90 min.

Prior to loading 20µl of protein sample was mixed with urea buffer (200mMTris/Hce pH6.8, 8M urea, 5% SDS, 0.1 mMEDTA, 1% 2-mercaptoethanol, 0.05% bromphenol blue) and the protein was denatured by heating it for 5 minutes at 95°C. After electrophoresis proteins were

either stained with Coomassie blue (5.4.3), silver stained or transferred onto a membrane by Western Blot (5.4.5).

5.4.2 Native gel electrophoresis

(Betts and Speed, 1999)

Native gel electrophoresis is a method similar to the SDS-PAGE. By omitting the SDS for the preparation of the polyacrylamide gel it is possible to keep proteins in their native state. Separation of native proteins by electrophoresis is dependent on the netto charge, the size and the shape of the proteins separated. The pH of the gel determines the netto charge on the protein. Below its isoelectric point (pI) a protein has a net positive charge, whereas above its pI it will have a net negative charge.

To find a suitable pH for the acrylamide gel and the buffer system to separate the Gid complex the pI values of all Gid proteins were checked at www.yeastgenome.org.

Table 4: Isoelectric points (pI) of Gid proteins involved in the formation of the Gid complex.

Gid1	4.54
Gid2	8.54
Gid4	6.51
Gid5	5.76
Gid7	5.97
Gid8	7.11
Gid9	6.92

5.4.2.1 Sample preparation

BY4743 yeast strains carrying a galactose inducible GID7-FLAG plasmid or an empty plasmid were cultivated as described in section 5.2.5 in 100 ml CM-Leu (2% ethanol). After 14 hours of growth the OD_{600} was between 2-3. The induction of Gid7-Flag protein was started by the addition of 2% galactose. After 2h additional incubation 15 OD of cells were harvested and kept on ice. Another 15 OD of cells was resuspended in 10 ml CM-Leu (2% glucose) and kept for 30 min. Cells were then spun down at 3000 rpm for 3 min in a benchtop centrifuge and the pellet got resuspended in 400 µl PBS buffer pH 7.4 (137 mM NaCl, 1.25 g/l Na_2HPO_4, 0.35 g/l NaH_2PO_4) containing protease inhibitors (Complete™, Roche

Diagnostics; 1.1 mM PMSF; 1 µg/ml each of antipain, pepstatin A, chymostatin, leupeptin, pefabloc). Cells were afterwards lysed at 4°C with 100µl glass beads for 20 min on a multivortexer. The lysate got clarified by centrifugation at 13000 rpm for 10 min and 300 µl of each lysate was transferred to a new 1.5 ml reaction tube. Then the protein concentration of each sample was determined by Bradford (5.4.14) and equal amount of total protein was used from each sample and lysis buffer was added up to 300 µl. After the addition of 30 µl of 20 × sample buffer (1.25 M Tris/ HCl, pH 8.8; 20% (v/v) glycerol; 0.1 mg/ ml bromphenol blue) probes got frozen at -20°C or were subjected to native gel electrophoresis.

5.4.2.2 Separation of the Gid complex by native gel electrophoresis

For the preparation of native gels all buffers were prepared as described in 5.4.1 by omitting the SDS. To avoid SDS contamination electrophoresis equipment was washed with water for several hours and kept separately. Continuous non denaturing gels were chosen to have a final acrylamide concentration of 7.5 % and a pH of 8.8. The gels were also prepared as described earlier but without SDS. Samples prepared in subsection 5.4.2.1 were then separated at 15 mA in the cold room for 1-2 hours.

As molecular mass markers the 'High Molecular Weight Calibration kit' from Amersham Bioscience was used. Each vial contained thyroglobulin (669 kDa), ferritin (440 kDa), catalase (232 kDa), lactate dehydrogenase (140 kDa) and bovine serum albumin (67 kDa, 8mg/ml). The contents were resuspended in 100 µl of PBS buffer without SDS and 10 µl were used for each gel.

After separation of proteins the gel was soaked in blotting buffer (0.1% SDS) for 10 min and then subjected to western blot analysis (5.4.5). Gid complexes were then visualised by the use of Flag specific antibodies. FBPase was detected with FBPase specific antibodies.

5.4.3 Coomassie staining of SDS-gels

Staining Solution (Coomassie)

Coomassie brilliant blue	0.1 % (w/v)
Methanol	50 % (v/v)
Acetic acid	10 % (v/v)
ddH_2O	39.9 % (v/v)

Destaining Solution

Methanol	40 % (v/v)
Acetic acid	10 % (v/v)
ddH_2O	50 % (v/v)

After electrophoresis the gel was put in Coomassie blue staining solution. The gel in the solution was heated for 30 seconds in the microwave oven and thereafter rocked for at least one hour. After that the gel was put in destaining solution and heated for 30 seconds again. Pieces of sponge were added to the solution to absorb the dye. The gel was rocked until the background colour disappeared. Thereafter the gel was put on a Whatman Paper and vacuum dried for one hour at 80°C.
Alternatively proteins were visualised with the GelCode® Blue reagent according to the users manual from Pierce.

5.4.4 Silver staining of SDS gels

(Heukeshoven and Dernick, 1988)
Silver staining of proteins is a highly sensitive visualisation method which allows the detection of proteins in a nanogram range. The following protocol is based on an in gel silver protein stain described by (Heukeshoven and Dernick, 1988)).

Fixing solution (30 % ethanol)	Ethanol 75 ml
	Glacial acetic acid 25 ml
	Water to 250 ml
Sensitizing solution	Ethanol 75 ml
	Sodium thiosulphate (5% w/v) 10 ml
	Sodium acetate (17 g)
	Water to 250 ml
Silver solution	Silver nitrate solution (2.5% w/v) 25 ml
	Water to 250 ml
Developing solution	Sodium carbonate (6.25 g)
	Water to 250 ml
Stop solution	EDTA (3.65 g)
	Water to 250 ml
Washing solution	Water

Preserving solution	Ethanol 75 ml
	Glycerol (87% w/w) 11.5 ml
	Water to 250 ml

All working steps were performed with gloves and only fresh solution and clean equipment was used to prevent protein contamination.
After the protein samples were separated by SDS gel electrophoresis the gel was transferred into a glass tray. The following steps were all performed with gentle agitation of the staining tray. For protein fixation the gel was soaked in fixing solution for 60 min. Then the solution was discarded and the sensitizing solution was added and left for an additional 60 min. Before use of the sensitising solution 1.25 ml of glutardialdehyde (25% w/v) was added. Then the gel was washed four times with 50 ml of ddH_2O. Right before the use of the silver solution 0.1 ml formaldehyde (37% w/v) was supplemented and put into the gel tray for another 60 min. The silver solution got removed and the gel was washed four times for 1 min with ddH_2O. To activate the developer solution 0.2 ml of formaldehyde (37% w/v) was added and poured into the gel tray. After 4-6 min protein bands started appearing. To stop protein staining the developing solution was exchanged by the stop solution when the protein bands reached their desired intensity. After 60 min the gel was then put into preserving solution and kept shaking for another 60 min. Gels were then dried in a vacuum gel drier system for 60 min at 80 °C.

5.4.5 Western Blot

(Towbin et al., 1979)

5 × blotting buffer	6,5 g/l Tris; 72 g/l glycine
TBS-T	20 mM Tris/HCl, pH 7,6; 137 mM sodiumchlorid; 0,1 % Tween-20

In a western blot proteins that were separated by SDS-PAGE (5.4.1) are transferred out of the gel onto a nitrocellulose membrane were proteins are probed with protein specific antibodies for their visualisation.
This method was conducted as described by Towbin et al. using a semidry blotting apparatus. A ‘sandwich’ consisting of three layers Whatman paper (GB002), the SDS-gel from 5.4.1, a cellulose membrane and an additional layer of three Whatman paper was put on the cathode of the blotting apparatus. Before use the Whatman papers and the nitrocellulose membrane

were soaked in blotting buffer (25 ml 5x blotting buffer, 20 ml methanol, 80 ml water). After removing excess buffer and bubbles between the gel and the membrane the anode lid was set onto the sandwich. Proteins got then transferred onto the membrane for 90 min at 70 mA per gel.

All following steps were done at room temperature with agitation on a shaker.

After blotting the membrane was blocked in 10 % skim milk dissolved in TBS-T for one hour at room temperature or overnight at 4°C followed by a 5 min washing step in TBS-T. Then the membrane was incubated in the first antibody solution for one hour (5.1.2). After washing away the first antibody with TBS-T (2× for 5 min) the second antibody solution was applied to the membrane and rocked for an additional 60 minutes. The membrane was washed again three times for 5 min with TBS-T and then transferred to a glass plate. Then 600 µl of ECL western blot detection reagent (Amersham) was spread onto each membrane and membranes were immediately transferred into a film cassette. ECL films were exposed to the membrane for 30 s to 45 min and films were developed.

Stripping of the membranes was done with 10% acetic acid for 10 min and excessive washing with TBS-T afterwards. All antibodies and their dilution are listed in section 5.1.2.

5.4.6 Pulse chase analysis

The pulse chase analysis is a method to measure the half life of certain proteins with the possibility to quantify them.

5.4.6.1 Growth conditions and radioactive labelling of the samples

To analyse the catabolite degradation of FBPase in pulse chase experiments, a stationary preculture grown in CM-media was inoculated in CM media without methionine to an OD_{600} of 0.01. These cells were incubated overnight to an OD_{600} of 4-5. For each strain 20 OD_{600} of cells were taken, spun down and washed with 4 ml of water. These cells were then resuspended in 5 ml labelling media containing 2% ethanol and kept in a 50 ml tube. To induce gluconeogenesis these cells were incubated in a water bath (30 °C) for 2.5 h. Afterwards 25 µl of ^{35}S-methionine was added to the cells to radioactive label newly synthesized proteins. After an additional 3-3.5 h incubation at 30°C cells were spun down for 5 min at 2000 rpm in a benchtop centrifuge and cells got resuspended in 5.5 ml chase medium (10 mM methionine, 2% glc) to induce catabolite degradation. Then a 1 ml sample was taken straight away and every half an hour after the onset of catabolite degradation. After the

addition of 100 µl 110% TCA samples were kept at -80°C. All samples were kept in 1.5 ml SafeLock® Eppendorf tubes.

5.4.6.2 Cell lysis and immunoprecipitation

BB1-buffer	6M urea; 1% SDS; 1 mM EDTA, 50 mM Tris/HCl pH 7.5
IP-buffer	50 mM Tris/HCl pH 7.5; 190 mM NaCl, 1.25 % (w/v) Triton X-100 ; 6 mM EDTA; 1 mM PMSF; Complete® protease inhibitor cocktail (25×)
Urea buffer	200mMTris/Hcl pH6.8; 8M urea; 5% SDS; 0.1 mM EDTA; 1% 2-mercaptoethanol; 0.05% bromphenol blue)

The samples were thawed and cells were spun down for 15 min at 13000 rpm. After removing the supernatant the pellet was washed with 100 µl acetone and dried. Then the cell pellet was resuspended in 100 µl BB1-buffer with the help of a toothpick. The amount of 50-100 µl of glass beads was then added and the cells were lysed by 3 × vortexing on a multivortexer for 5 min and incubation at 95°C for 1 min in between. Afterwards the samples were cooled down on ice for 2 min and 900 µl of IP buffer was added. The buffers were mixed and the cell debris together with the glass beads were spun down for 10 min at 13000 rpm. 850 µl of the supernatant from each sample was transferred into a new 1.5 ml reaction tube and 3µl of FBPase specific antibody was added. Binding of the antibody to the antigene was performed for 2 h on an overhead shaker (RT). Then 50 µl of 5% (w/v) Protein A Sepharose™ CL-4B (Amersham) was added to each sample with cut off yellow tips and rotated for an additional 1.5 h at room temperature (RT). Finally the beads were spun down at 3000 rpm for 2 min and the supernatant was carefully removed. After 3 washes of the pellet with IP buffer it was resuspended in 50µl urea buffer and samples were boiled for 10 min at 95°C. A short spin (13000 rpm; 1 min) was performed to pull down all the contents of the 1.5 ml reaction tube and all samples were subjected to SDS-PAGE as described in subsection 5.4.1. Then the gel was vacuum dried for 1.5 h at 60 °C and fixated with sticky tape in a film cassette. To visualise the radioactive signal of the precipitated FBPase a PhosphoImager screen was put on top of the gel and exposed for 2-3 d. Signals were scanned with a PhosphoImager (Storm 860) and quantified using the software ImageQuant 5.2 (Molecular Dynamics).

5.4.7 Expression and purification of GST fusion proteins in *E.coli*

For the expression of GST fusion proteins the protease deficient *E.coli* strain BL21 was used. The plasmid pGEX-4T1 VID24 (Josupeit, 2003) was transformed into BL21 according to the previous chapter (5.3.4.2) and positive clones were inoculated in 4 ml LB_{Amp} media. 2 ml of such an overnight culture was used to inoculate 200 ml of prewarmed 2 × YTAG. The expression of GST-Vid24 was then induced by the addition of 500 µl IPTG (100 mM) to the remaining culture. After 2.5 h of induction the cells were harvested by centrifugation for 10 min at 8500 × g in a 250 ml GSA bottle and the pellet was resuspended in 10 ml icecold PBS buffer (140 mM NaCl; 2.7 mM KCl; 10 mM Na_2HPO_4; 1.8 mM KH_2PO_4; pH 7.3). The resuspended cells were transferred to two 15 ml Falcon tubes and lysed by supersonification (Supersonic Sonificator *Sonic Power)* five times for 10 s with 1 min on ice in between. The degree of lysis was checked by scrutinizing the cells under the microscope. The lysates were pooled and 500 µl of 20 % Triton X-100 (w/v) was added and rotated at room temperature for 30 – 45 min. Then the cells were spun down for 10 min at 10000 rpm at 4°C and the supernatant was kept for affinity purification of the GST fusion protein.

To purify GST-fusion proteins 200 µl of 50% Glutathion Sepharose 4B (Amersham) were transferred to the *E.coli* lysate containing the GST fusion proteins. After 30 min overhead shaking the beads were spun down at 500 × g for 5 min and washed with cold PBS buffer three times. The elution of the GST fusion proteins was performed by adding 100 µl of urea sample buffer and boiling for 5 min at 95°C. After centrifugation at 13000 rpm for 1 min the sample was frozen at -20°C.

5.4.8 Purification of crude antiserum with purified GST-antigene

Antibodies were purified from crude rabbit serum by affinity purification. Therefore the particular antigen protein was purified (5.4.7) and fractionated on a 10% SDS-Gel (5.4.1). A small slot for the molecular weight marker and a large slot for the target antigen solution was used. The sample with the purified antigene GST fusion prepared in 5.4.7 (650 -1000µg protein) was loaded on a SDS gel and run at 150V. Afterwards the proteins were blotted on a nitrocellulose membrane (5.4.5) and stained with PonceauS.

The protein band with the size of the target protein was then cut out with a scalpel and blocked in 10% skim milk powder in TBS-T for 60 minutes. After blocking the membrane

was cut into small pieces and the slices were transferred into a 1.5 ml reaction tube. Then 800µl of TBS together with 200µl antiserum and the membrane slices were incubated for 3h at room temperature on a wheel. The supernatant was removed and the membrane pieces were rinsed three times with 1ml TBS-T first and then three times washed with 1ml TBS-T for 30 minutes on the wheel. To elute the antibodies from the membrane pieces the stripes were finally incubated in 200µl 200mM glycine (pH2.5) solution containing 1mM EGTA for 30 minutes. The supernatant with the antibodies was then transferred into a fresh Eppendorf tube and the solution was neutralized with 30µl Tris (1M). This step was repeated 2 times with 50µl glycine solution and 10 minutes incubation. The pH was tested with pH paper and was set around seven. Then the antibody solution was stored at –20°C in 5mM sodiumazide and tested for the reactivity in a western blot.

5.4.9 The Two Hybrid Screen

(Fields and Song, 1989)

The two hybrid screen is a genetical screen to search for protein protein interactions by taking advantage of the properties of the yeast transcriptional activator GAL4. This protein is required for the expression of genes encoding enzymes for galactose utilisation. The fact that this protein consists of two separable domains, the n-terminal GAL4 DNA binding domain (BD) and the c-terminal GAL4 activating region (AD), makes it a useful tool to study protein interactions. Two different proteins fused to either BD or AD reconstitute a functional GAL4 activator only when both proteins interact with each other and AD and BD are in close proximity to each other. The use of specially constructed *S.cerevisiae* strains with reporter genes under the control of the GAL4 activator allow to screen for protein protein interaction by selection of histidine auxotrophy or β-Gal activity (Fields and Song, 1989).

5.4.9.1 Preparation of Two Hybrid Constructs

The construction of fusion proteins to either the DNA binding domain (BD) or the transcriptional activating domain (AD) was conducted as described earlier (Cagney and Uetz, 2001). In a two step PCR the open reading frame of interest was first amplified using primers specifying the 5' and 3' terminal ends of the open reading frame with 20 nucleotides tails homologous to sequences in the multi cloning sites of the two hybrid vectors (1st round fwd primer GIDX, 1st round rev primer GIDX; 5.1.8). In the second round PCR a universal set of primers (2nd round fwd primer; 2nd round rev primer; 5.1.8) was used to enlarge the homologous region in the two hybrid vectors to 50 bps on each side. The protocol for both PCR reactions is described in section 5.3.7. For the construction of two hybrid vectors

chromosomal DNA from BY strain was isolated according to 5.3.2. 2µl of chromosomal DNA was used as a template with 5U Taq polymerase and 0.02U Pfu polymerase (Stratagene) for the first round PCR. The second round PCR was conducted using 2.5 pmol of each primer, 0.6 U Taq polymerase together with 0.003U Pfu polymerase and 5 ng of 1st round PCR product. The correct length of the PCR products was then analysed by running an agarose gel (5.3.8). The two hybrid vectors pOAD and pOBD2 containing either the transcriptional activating domain or the DNA binding domain under the control of an ADH promoter with a following multi cloning site and an ADH terminator were digested with NcoI and PvuII (5.3.9) to linearize them. After separation on an agarose gel, the linearized plasmid was cut out and purified (5.3.9). The linearized plasmid and the PCR product was then transformed into the yeast strain Y190 (5.3.4.3). After 2-3 days of growth positive homologous recombinants were selected by tryptophane prototrophy for pOBD2 and by leucine prototrophy for pOAD, respectively. Clones were then selected and plasmids got recovered (5.3.3) and transformed in *E.coli.* After overnight inoculation at 37°C plasmids were isolated and the correct integration of the PCR fragment into the linearized plasmid was analyzed by digestion with chosen restriction enzymes (5.3.9). Finally the insert was sequenced by MWG Biotech to screen for PCR dependent mutations in the inserts.

5.4.9.2 Screening for two hybrid interactions

Z-buffer 16.1 g/l (m/v) $Na_2HPO_4 \times 7H_2O$, 5.5 g/l (m/v) $NaH_2PO_4 \times H_2O$, 0.75 g/l KCl, 0.25 g/l $MgSO_4 \times 7H_2O$

To screen for protein protein interactions among the Gid proteins individual constructs were transformed into the yeast strain Y190 and plated on CM –His, -Leu, -Trp. To look for self activation of constructs empty pOAD and the POBD2 plasmid containing the chosen open reading frame were transformed and plated on CM –His, -Leu, -Trp as well. After 3 days of growth at 30°C colonies should appear. After that a toothpick was used to pick cells from each colony and cells were resuspended in 100µl sterile water in a 96 well plates. From each transformation 4-8 positive clones were picked. A 48 well rocker was then used to plate all cell dilutions onto a CM-His,-Leu,-Trp plate containing an additional 35-50 mM 3-aminotriazol (3AT). After 3 days incubating these cells at 30°C positive protein protein interaction was shown by the ability of the strains to grow on CM plates without histidine.
An additional reporter gene under the control of the GAL4 promotor is the *lacZ* gene. To test the two hybrid clones for β-galactosidase activity, clones grown on CM-His,-Leu,-Trp plates

were replica plated onto a fresh CM-His,-Leu,-Trp plate with a sterile round filter (Ø82mm, GB002, Schleicher & Schuell) on top. After another day of incubation at 30°C the filter membrane containing the cell colonies was deep frozen in liquid nitrogen.
Another membrane was soaked in freshly prepared β-Gal buffer (2.5 ml Z-buffer, 6.75µl β-mercaptoethanol, 25 µl X-Gal (10mg/ 100µl DMF)), transferred into a petry dish and the membrane containing the cells was layered on top. After 2-3 h of incubation at 30°C positive protein protein interactions appeared blue. False positive interactions were sorted out by the ability to grow on CM–histidine plates plus 3-AT with an empty pOAD plasmid also.

5.4.10 The tandem affinity purification (TAP)

(Puig et al., 2001)
The tandem affinity purification method has been developed as a tool that allows the fast purification of protein complexes under native conditions at endogenous protein levels. The TAP tag is either N- or C-terminally fused to a protein of interest via homologous recombination. The TAP tag carries an n-terminal calmodulin binding peptide with a c-terminal proteinA and a TEV cleavage site in between. This allows two affinity purification steps, first via IgG-Sepharose with a following TEV elution, second the affinity purification via calmodulin beads with EGTA elution.

5.4.10.1 Construction of TAP fusion proteins

The construction of c-terminal TAP fusion proteins was conducted as described earlier based on the homologous recombination of a PCR product at a specific gene locus on the chromosome (Puig et al., 2001). With the use of the template plasmid pBS1479 and two primers designed to contain 40-50 mers upstream the stop codon (upstream primer) and 40-50 mers downstream the stop codon (downstream primer) of the ORF, a PCR fragment was generated via PCR. The PCR was done according to the protocol described in 5.3.7 with an additional 2.5 µl DMSO and 1µl of $MgSO_4$. The annealing temperature was chosen as described at www.emblheidelberg.de/ExternalInfo/Seraphin/TAP.html with 48°C. The quality and the size of the PCR products were checked on an agarose gel and transformed in yeast as described before (5.3.4.3). Positive clones were collected by tryptophane prototrophy. After 2-3 days of growth on CM-Trp positive clones were picked and plated out again. The expression of the newly generated fusion proteins was checked by western blot analysis with the use of FBPase specific antibodies (5.4.5) (ProteinA reacts with all IgG antibodies) and afterwards the correct integration was proved via PCR.

5.4.10.2 Purification of TAP fusion proteins

The purification of TAP tagged proteins was conducted according to the protocol described earlier (Puig et al., 2001). Briefly cells were grown as described in chapter 5.2.5 upgraded to collect 1400 OD of cells. These cells were washed once with water and pelleted again in a 50 ml Falcon tube. The pellet volume was determined and got resuspended in the same volume bufferA (10 mM K-Hepes pH 7.9, 10 mM KCl, 1.5 mM $MgCl_2$, 0.5 mM DTT, 0.5 mM PMSF, 2mM benzamidine, 1 µM leupeptine, 2 µM pepstatinA, 4 µM chymostatin, 2.6 µM aprotinin). These cells were then lysed by passing them through a french press 5 times (1200 psi) with intermittent cooling on ice. After that the lysate was cleared by centrifugation at 25,000g for 30 min and the supernatant was transferred to a new Beckman centrifuge tube (Polycarbonate Thick Wall, 3.2 ml) and centrifuged in a TLA110 rotor (Beckman) for 1 h at 100,000g. The supernatant was then carefully transferred into a 0.8 × 4 cm chromatography column (Bio-Rad) and 200 µl of 50% slurry IgG-sepharose (Pharmacia) was added. Sepharose beads were washed in 10 ml IPP150 buffer (10 mM Tris-Cl, pH 8.0, 150 mM NaCl, 0.1% NP40) before use. The lysate was then rotated at 4°C for 2-3 h and the pellet was washed 3 × with 10 ml IPP150 buffer. Then the pellet was washed once more with TEV cleavage buffer (IPP150 adjusted to 0.5 mM EDTA and 1 mM DTT). and got finally resupended in 1ml of TEV cleavage buffer. The elution was performed by the addition of 100 U of TEV protease (Invitrogen) and subsequent rotation at 16°C for 2 h. The supernatant was then recovered and transferred to a new chromatography column. The second affinity purification was then performed by the addition of 200 µl of 50% slurry calmodulin beads (Stratagene) which were washed with 10 ml IPP150 calmodulin binding buffer (10 mM Tris-Cl, pH 8.0, 10 mM 2-mercaptoethanol, 150 mM NaCl, 1 mM magnesium acetate, 1 mM imidazole, 2 mM $CaCl_2$, 0.1 % NP-40) before. Additionally 3 µl of 1 M $CaCl_2$ and 3 ml of IPP150 calmodulin binding buffer were added to the eluate and the affinity purification was conducted for 1 h on a rotating wheel at 4°C. The pellet was then washed 3 times with 10 ml calmodulin binding buffer and bound protein were eluted 5 × with 200µl calmodulin elution buffer (10 mM Tris-Cl, pH 8.0, 10 mM 2-mercaptoethanol, 150 mM NaCl, 1 mM magnesium acetate, 1 mM imidazole, 0.1 % NP-40, 2 mM EGTA). All eluates were collected and proteins got precipitated with 10% final concentration of TCA. After washing the protein pellet with acetone it was resuspended in 50µl urea buffer and subjected to SDS-Page (5.4.1) with subsequent Coomassie staining (5.4.3) or silver staining (5.4.4).

Alternatively proteins were radioactive labelled to look for interaction partners in a small scale experiment. Therefore cells were grown as described for pulse chase analysis (5.4.6) and

lysed with glass beads. A cell density of 2.5 OD was taken for each sample and elution was performed with 15U TEV protease.

5.4.11 Co-Immunoprecipitation

For immunoprecipitations cells were cultivated as described above for FBPase turnover assays (5.2.5) and samples were withdrawn at the indicated time points. 30 OD_{600} cells were harvested washed with water resuspended in 500 µl PBS buffer pH 7.4 (137 mM NaCl, 1.25 g/l Na_2HPO_4, 0.35 g/l NaH_2PO_4) containing protease inhibitors (Complete™, Roche Diagnostics; 1.1 mM PMSF; 1 µg/ml each of antipain, pepstatin A, chymostatin, leupeptin, pefabloc) and lysed at 4 °C with 100µl glass beads (Ø 0.4-0.6 mm, Sartorius) for 20 min on a multivortexer. After centrifugation the supernatant was transferred to a new tube. FBPase- or Flag-antibody, respectively, was added and the samples were gently agitated for 2 h at room temperature. Immunoprecipitates were collected by adding 50 µl of 5 % Protein A Sepharose™ CL-4B (Amersham Biosciences, Sweden) and further incubation for 1-1.5 h. For co-immunoprecipitations the Sepharose beads were centrifuged and washed three times with PBS buffer. For co-immunoprecipitation of tagged Gid proteins 0.2% Triton-X100 was added to the PBS buffer. Proteins were released from the Sepharose by boiling in 50 µl of urea buffer (5.4.5) and separated by SDS-PAGE.

5.4.12 Glycerol density gradient fractionation

Cells were grown for 16 hours in YPEthanol and shifted to YPD medium for 20 min. 50 OD_{600} cells were harvested, resuspended in 600 µl of 0.1 M KH_2PO_4, pH 7.0 in the presence of Complete™ (Protease inhibitor cocktail tablets; Roche Diagnostics), 1.1 mM PMSF and protease inhibitors (1 µg/ml each of antipain, pepstatin A, chymostatin, leupeptin, pefabloc), lysed with glass beads (20 min., 4°C), and centrifuged at 10,000 x g for 15 min. 200 µl aliquots of the resulting cell extracts were layered on top of a glycerol step gradient (450 µl each of 50 %, 40 %, 30 % and 20 % of glycerol in 20 mM Pipes buffer pH 6.8) and centrifuged for 4 hours at 55,000 rpm and 15°C in a TLS-55 rotor (Beckman Instruments). Thereafter 240 µl fractions were collected, precipitated with trichloroacetic acid (10%), solubilized in urea buffer and subjected to SDS PAGE with subsequent immunoblotting.

5.4.13 Polyubiquitination of FBPase

For polyubiquitination experiments a pRS425 (2µ, Leu2, Myc-ubiquitin) based *S. cerevisiae/E. coli* shuttle vector containing a myc tagged Ubiquitin under control of a copper inducible *COP1* promotor (5.1.7) was transformed into WT (BY4743), *Δgid1 (Y34594)* and *Δgid7* (Y33446) strains. As a control empty pRS425 was transformed into BY4743. To test the polyubiquitination of FBPase in WT, *Δgid1* and *Δgid7* strains respectively, cells containing the Ub-myc encoding plasmid were grown on CM- Leu medium containing 2% glucose to an OD of 3-4. A control strain of BY4743 contained an empty plasmid pRS425. After harvesting (5 min. at 500 x g), cells were resuspended in CM –Leu medium containing 2% Ethanol. To induce myc tagged ubiquitin 100 µM $CuSO_4$ was added and cells were incubated for 6h to derepress FBPase. 50 OD cells were taken before and 25 min after addition of glucose (final concentration 2%). Cells were harvested and resuspended in 1ml water containing 20 mM NEM, 20 mM NaN_3, 1 mM PMSF) and stored at -80°C. After thawing cells were pelleted at 500g for 4 min at 4°C and resuspended in 600 µl PBS buffer containing protease inhibitors (Complete™, Roche Diagnostics; 1.1 mM PMSF; 1 µg/ml each of antipain, pepstatin A, chymostatin, leupeptin, pefabloc, 20mM NEM) and lysed at 4 °C with glass beads for 20 min on a multivortexer. Immunoprecipitation of FBPase was performed as described before (5.4.11) and the pellet was washed 5 times with PBS buffer containing 0.2% Triton X-100. Beads were resuspended in 50 µl urea buffer, boiled for 5 min at 95 °C and used for immunoblotting with Myc antibody from Calbiochem (clone 9E10, monoclonal, mouse).

5.4.14 Determination of protein concentrations

The Bradford Reagent can be used to determine the concentration of proteins in solution. The procedure is based on the formation of a complex between the dye, Brilliant Blue G, and the proteins in solution. The protein-dye complex absorbs at a wavelength of 595 nm and can therefore be quantified.

To prepare a stock solution, 100 mg of Coomassie Blue G were dissolved in 50 ml of methanol. This solution was then added to 100 ml of 85% H_3PO_4, and diluted to 200 ml with water and kept at 4°C.

To prepare a calibration curve a BSA stock with a concentration of 1mg/ml was prepared and diluted 1:10. This solution was further diluted according to the following dilution scheme.

Table 5: Dilutions for a BSA calibration curve

BSA stock (1:10) [µl]	0	10	20	40	60	80	100
Water [µl]	100	90	80	60	40	20	0

To each dilution 1ml of Bradford reagent was added and mixed. After 10 min the OD_{595} of each sample was measured and put against the protein concentration in a graph. The gradient of the line was used to determine protein concentrations of unknown samples.

6 LITERATURE

Achstetter, T., Ehmann, C., Osaki, A. and Wolf, D.H. (1984) Proteolysis in eukaryotic cells. Proteinase yscE, a new yeast peptidase. *J Biol Chem*, **259**, 13344-13348.

Alberts, S. (2005) Studien zur Funktion von Gid8p in der Katabolitdegradation der Fructose-1,6-bisphosphatase. *Diploma thesis*.

Amerik, A., Swaminathan, S., Krantz, B.A., Wilkinson, K.D. and Hochstrasser, M. (1997) In vivo disassembly of free polyubiquitin chains by yeast Ubp14 modulates rates of protein degradation by the proteasome. *Embo J*, **16**, 4826-4838.

Amerik, A.Y. and Hochstrasser, M. (2004) Mechanism and function of deubiquitinating enzymes. *Biochim Biophys Acta*, **1695**, 189-207.

Amerik, A.Y., Li, S.J. and Hochstrasser, M. (2000) Analysis of the deubiquitinating enzymes of the yeast Saccharomyces cerevisiae. *Biol Chem*, **381**, 981-992.

Ausubel, F.M., Kingston, R.E., Seidman, F.G., Struhl, K., Moore, D.D., Brent, R. and Smith, F.A. (1992) Current protocols in molecular biology. *New-York, John Wiley and Sons*.

Bajorek, M. and Glickman, M.H. (2004) Keepers at the final gates: regulatory complexes and gating of the proteasome channel. *Cell Mol Life Sci*, **61**, 1579-1588.

Barbin, L. (2005) Studies on the mechanisms of catabolite degradation of Fructose-1,6-bisphophatasein the yeast Saccharomyces cerevisiae. *Diploma thesis*.

Baumeister, W., Walz, J., Zuhl, F. and Seemuller, E. (1998) The proteasome: paradigm of a self-compartmentalizing protease. *Cell*, **92**, 367-380.

Betting, J. and Seufert, W. (1996) A yeast Ubc9 mutant protein with temperature-sensitive in vivo function is subject to conditional proteolysis by a ubiquitin- and proteasome-dependent pathway. *J Biol Chem*, **271**, 25790-25796.

Betts, S. and Speed, M. (1999) Detection of early aggregation intermediates by native gel electrophoresis and native western blotting. *Methods Enzymology*, **309**, 333-350.

Bianchi, M.M., Sartori, G., Vandenbol, M., Kaniak, A., Uccelletti, D., Mazzoni, C., Di Rago, J.P., Carignani, G., Slonimski, P.P. and Frontali, L. (1999) How to bring orphan genes into functional families. *Yeast*, **15**, 513-526.

Bordallo, J. and Wolf, D.H. (1999) A RING-H2 finger motif is essential for the function of Der3/Hrd1 in endoplasmic reticulum associated protein degradation in the yeast Saccharomyces cerevisiae. *FEBS Lett*, **448**, 244-248.

Borden, K.L. (2000) RING domains: master builders of molecular scaffolds? *J Mol Biol*, **295**, 1103-1112.

Braun, B. (2006) Studien zur Funktion von Gid-Proteinen bei der Katabolitdegradation der Fructose-1,6.bisphosphatase der Hefe. *Diploma thesis*.

Braun, B.C., Glickman, M., Kraft, R., Dahlmann, B., Kloetzel, P.M., Finley, D. and Schmidt, M. (1999) The base of the proteasome regulatory particle exhibits chaperone-like activity. *Nat Cell Biol*, **1**, 221-226.

Breitschopf, K., Bengal, E., Ziv, T., Admon, A. and Ciechanover, A. (1998) A novel site for ubiquitination: the N-terminal residue, and not internal lysines of MyoD, is essential for conjugation and degradation of the protein. *Embo J*, **17**, 5964-5973.

Brown, C.R., Cui, D.Y., Hung, G.G. and Chiang, H.L. (2001) Cyclophilin A mediates Vid22p function in the import of fructose-1,6-bisphosphatase into Vid vesicles. *J Biol Chem*, **276**, 48017-48026.

Brown, C.R., Liu, J., Hung, G.C., Carter, D., Cui, D. and Chiang, H.L. (2003) The Vid vesicle to vacuole trafficking event requires components of the SNARE membrane fusion machinery. *J Biol Chem*, **278**, 25688-25699.

Brown, C.R., McCann, J.A. and Chiang, H.L. (2000) The heat shock protein Ssa2p is required for import of fructose-1, 6-bisphosphatase into Vid vesicles. *J Cell Biol*, **150**, 65-76.

Brown, C.R., McCann, J.A., Hung, G.G., Elco, C.P. and Chiang, H.L. (2002) Vid22p, a novel plasma membrane protein, is required for the fructose-1,6-bisphosphatase degradation pathway. *J Cell Sci*, **115**, 655-666.

Burchell, A., Lyall, H., Busuttil, A., Bell, E. and Hume, R. (1992) Glucose metabolism and hypoglycaemia in SIDS. *J Clin Pathol*, **45**, 39-45.

Burlini, N., Morandi, S., Pellegrini, R., Tortora, P. and Guerritore, A. (1989) Studies on the degradative mechanism of phosphoenolpyruvate carboxykinase from yeast Saccharomyces cerevisiae. *Biochim Biophys Acta*, **1014**, 153-161.

Cagney, G. and Uetz, P. (2001) High throughput screening for protein protein interactions using yeast two hybrid arrays. *Current protocols in protein science*, 19.16.11- 19.16.12.

Cagney, G., Uetz, P. and Fields, S. (2001) Two-hybrid analysis of the Saccharomyces cerevisiae 26S proteasome. *Physiol Genomics*, **7**, 27-34.

Chen, P., Johnson, P., Sommer, T., Jentsch, S. and Hochstrasser, M. (1993) Multiple ubiquitin-conjugating enzymes participate in the in vivo degradation of the yeast MAT alpha 2 repressor. *Cell*, **74**, 357-369.

Chiang, H.L. and Schekman, R. (1991) Regulated import and degradation of a cytosolic protein in the yeast vacuole. *Nature*, **350**, 313-318.

Chiang, M.C. and Chiang, H.L. (1998) Vid24p, a novel protein localized to the fructose-1, 6-bisphosphatase-containing vesicles, regulates targeting of fructose-1,6-bisphosphatase from the vesicles to the vacuole for degradation. *J Cell Biol*, **140**, 1347-1356.

Ciechanover, A., Elias, S., Heller, H. and Hershko, A. (1982) "Covalent affinity" purification of ubiquitin-activating enzyme. *J Biol Chem*, **257**, 2537-2542.

Ciechanover, A., Finley, D. and Varshavsky, A. (1984) The ubiquitin-mediated proteolytic pathway and mechanisms of energy-dependent intracellular protein degradation. *J Cell Biochem*, **24**, 27-53.

Dahlmann, B., Kopp, F., Kuehn, L., Niedel, B., Pfeifer, G., Hegerl, R. and Baumeister, W. (1989) The multicatalytic proteinase (prosome) is ubiquitous from eukaryotes to archaebacteria. *FEBS Lett*, **251**, 125-131.

Denti, S., Sirri, A., Cheli, A., Rogge, L., Innamorati, G., Putignano, S., Fabbri, M., Pardi, R. and Bianchi, E. (2004) RanBPM is a phosphoprotein that associates with the plasma membrane and interacts with the integrin LFA-1. *J Biol Chem*, **279**, 13027-13034.

DeRisi, J.L., Iyer, V.R. and Brown, P.O. (1997) Exploring the metabolic and genetic control of gene expression on a genomic scale. *Science*, **278**, 680-686.

Dohmen, R.J. (2004) SUMO protein modification. *Biochim Biophys Acta*, **1695**, 113-131.

Dohmen, R.J., Stappen, R., McGrath, J.P., Forrova, H., Kolarov, J., Goffeau, A. and Varshavsky, A. (1995) An essential yeast gene encoding a homolog of ubiquitin-activating enzyme. *J Biol Chem*, **270**, 18099-18109.

Dubiel, W. and Gordon, C. (1999) Ubiquitin pathway: another link in the polyubiquitin chain? *Curr Biol*, **9**, R554-557.

Dupre, S., Urban-Grimal, D. and Haguenauer-Tsapis, R. (2004) Ubiquitin and endocytic internalization in yeast and animal cells. *Biochim Biophys Acta*, **1695**, 89-111.

Egner, R., Thumm, M., Straub, M., Simeon, A., Schuller, H.J. and Wolf, D.H. (1993) Tracing intracellular proteolytic pathways. Proteolysis of fatty acid synthase and other cytoplasmic proteins in the yeast Saccharomyces cerevisiae. *J Biol Chem*, **268**, 27269-27276.

Ehring, B., Meyer, T.H., Eckerskorn, C., Lottspeich, F. and Tampe, R. (1996) Effects of major-histocompatibility-complex-encoded subunits on the peptidase and proteolytic activities of human 20S proteasomes. Cleavage of proteins and antigenic peptides. *Eur J Biochem*, **235**, 404-415.

Elsasser, S. and Finley, D. (2005) Delivery of ubiquitinated substrates to protein-unfolding machines. *Nat Cell Biol*, **7**, 742-749.

Enenkel, C., Lehmann, A. and Kloetzel, P.M. (1998) Subcellular distribution of proteasomes implicates a major location of protein degradation in the nuclear envelope-ER network in yeast. *Embo J*, **17**, 6144-6154.

Enenkel, C., Lehmann, A. and Kloetzel, P.M. (1999) GFP-labelling of 26S proteasomes in living yeast: insight into proteasomal functions at the nuclear envelope/rough ER. *Mol Biol Rep*, **26**, 131-135.

Enyenihi, A.H. and Saunders, W.S. (2003) Large-scale functional genomic analysis of sporulation and meiosis in Saccharomyces cerevisiae. *Genetics*, **163**, 47-54.

Fenteany, G., Standaert, R.F., Lane, W.S., Choi, S., Corey, E.J. and Schreiber, S.L. (1995) Inhibition of proteasome activities and subunit-specific amino-terminal threonine modification by lactacystin. *Science*, **268**, 726-731.

Ferrell, K., Wilkinson, C.R., Dubiel, W. and Gordon, C. (2000) Regulatory subunit interactions of the 26S proteasome, a complex problem. *Trends Biochem Sci*, **25**, 83-88.

Fields, S. and Song, O. (1989) A novel genetic system to detect protein-protein interactions. *Nature*, **340**, 245-246.

Finley, D. and Chau, V. (1991) Ubiquitination. *Annu Rev Cell Biol*, **7**, 25-69.

Fraschini, R., Bilotta, D., Lucchini, G. and Piatti, S. (2004) Functional characterization of Dma1 and Dma2, the budding yeast homologues of Schizosaccharomyces pombe Dma1 and human Chfr. *Mol Biol Cell*, **15**, 3796-3810.

Freemont, P.S. (2000) RING for destruction? *Curr Biol*, **10**, R84-87.

Fu, H., Sadis, S., Rubin, D.M., Glickman, M., van Nocker, S., Finley, D. and Vierstra, R.D. (1998) Multiubiquitin chain binding and protein degradation are mediated by distinct domains within the 26 S proteasome subunit Mcb1. *J Biol Chem*, **273**, 1970-1981.

Funayama, S., Gancedo, J.M. and Gancedo, C. (1980) Turnover of yeast fructose-bisphosphatase in different metabolic conditions. *Eur J Biochem*, **109**, 61-66.

Glickman, M.H., Rubin, D.M., Coux, O., Wefes, I., Pfeifer, G., Cjeka, Z., Baumeister, W., Fried, V.A. and Finley, D. (1998a) A subcomplex of the proteasome regulatory particle required for ubiquitin-conjugate degradation and related to the COP9-signalosome and eIF3. *Cell*, **94**, 615-623.

Glickman, M.H., Rubin, D.M., Fried, V.A. and Finley, D. (1998b) The regulatory particle of the Saccharomyces cerevisiae proteasome. *Mol Cell Biol*, **18**, 3149-3162.

Goldknopf, I.L. and Busch, H. (1977) Isopeptide linkage between nonhistone and histone 2A polypeptides of chromosomal conjugate-protein A24. *Proc Natl Acad Sci U S A*, **74**, 864-868.

Goldstein, G., Scheid, M., Hammerling, U., Schlesinger, D., Niall, H. and Boyse, E. (1975) Isolation of a polypeptide that has lymphocyte-differentiating properties and is probably represented universally in living cells. *Proc Natl Acad Sci U S A*.

Hämmerle, M., Bauer, J., Rose, M., Szallies, A., Thumm, M., Dusterhus, S., Mecke, D., Entian, K.D. and Wolf, D.H. (1998) Proteins of newly isolated mutants and the amino-terminal proline are essential for ubiquitin-proteasome-catalyzed catabolite degradation of fructose-1,6-bisphosphatase of Saccharomyces cerevisiae. *J Biol Chem*, **273**, 25000-25005.

Hampsey, M. (1997) A review of phenotypes in Saccharomyces cerevisiae. *Yeast*, **13**, 1099-1133.

Hatakeyama, S. and Nakayama, K.I. (2003) U-box proteins as a new family of ubiquitin ligases. *Biochem Biophys Res Commun*, **302**, 635-645.

Heinemeyer, W., Kleinschmidt, J.A., Saidowsky, J., Escher, C. and Wolf, D.H. (1991) Proteinase yscE, the yeast proteasome/multicatalytic-multifunctional proteinase: mutants unravel its function in stress induced proteolysis and uncover its necessity for cell survival. *Embo J*, **10**, 555-562.

Heinemeyer, W., Ramos, P.C. and Dohmen, R.J. (2004) The ultimate nanoscale mincer: assembly, structure and active sites of the 20S proteasome core. *Cell Mol Life Sci*, **61**, 1562-1578.

Hershko, A. (2005) The ubiquitin system for protein degradation and some of its roles in the control of the cell division cycle. *Cell Death Differ*, **12**, 1191-1197.

Hershko, A. and Ciechanover, A. (1992) The ubiquitin system for protein degradation. *Annu Rev Biochem*, **61**, 761-807.

Hershko, A. and Ciechanover, A. (1998) The ubiquitin system. *Annu Rev Biochem*, **67**, 425-479.

Heukeshoven, J. and Dernick, R. (1988) Improved silver staining procedure for fast staining in PhastSystem Development Unit. I. Staining of sodium dodecyl sulfate gels. *Electrophoresis*, **9**, 28-32.

Hicke, L. and Dunn, R. (2003) Regulation of membrane protein transport by ubiquitin and ubiquitin-binding proteins. *Annu Rev Cell Dev Biol*, **19**, 141-172.

Hicke, L. and Riezman, H. (1996) Ubiquitination of a yeast plasma membrane receptor signals its ligand-stimulated endocytosis. *Cell*, **84**, 277-287.

Hilt, W. and Wolf, D.H. (1995) Proteasomes of the yeast S. cerevisiae: genes, structure and functions. *Mol Biol Rep*, **21**, 3-10.

Ho, A.K., Raczniak, G.A., Ives, E.B. and Wente, S.R. (1998) The integral membrane protein Snl1p is genetically linked to yeast nuclear pore complex function. *Mol Biol Cell*, **9**, 355-373.

Ho, Y., Gruhler, A., Heilbut, A., Bader, G.D., Moore, L., Adams, S.L., Millar, A., Taylor, P., Bennett, K., Boutilier, K., Yang, L., Wolting, C., Donaldson, I., Schandorff, S., Shewnarane, J., Vo, M., Taggart, J., Goudreault, M., Muskat, B., Alfarano, C., Dewar, D., Lin, Z., Michalickova, K., Willems, A.R., Sassi, H., Nielsen, P.A., Rasmussen, K.J., Andersen, J.R., Johansen, L.E., Hansen, L.H., Jespersen, H., Podtelejnikov, A., Nielsen, E., Crawford, J., Poulsen, V., Sorensen, B.D., Matthiesen, J., Hendrickson, R.C., Gleeson, F., Pawson, T., Moran, M.F., Durocher, D., Mann, M., Hogue, C.W., Figeys, D. and Tyers, M. (2002) Systematic identification of protein complexes in Saccharomyces cerevisiae by mass spectrometry. *Nature*, **415**, 180-183.

Hoffman, M. and Chiang, H.L. (1996) Isolation of degradation-deficient mutants defective in the targeting of fructose-1,6-bisphosphatase into the vacuole for degradation in Saccharomyces cerevisiae. *Genetics*, **143**, 1555-1566.

Holzer, H. (1976) Catabolite inactivation in yeast. *Trends Biochem Sci*, **1**, 178-181.

Holzer, H. and Purwin, C. (1986) How does glucose initiate proteolysis of yeast fructose-1,6-bisphosphatase? *Biomed Biochim Acta*, **45**, 1657-1663.

Horak, J., Regelmann, J. and Wolf, D.H. (2002) Two distinct proteolytic systems responsible for glucose-induced degradation of fructose-1,6-bisphosphatase and the Gal2p transporter in the yeast Saccharomyces cerevisiae share the same protein components of the glucose signaling pathway. *J Biol Chem*, **277**, 8248-8254.

Horak, J. and Wolf, D.H. (2001) Glucose-induced monoubiquitination of the Saccharomyces cerevisiae galactose transporter is sufficient to signal its internalization. *J Bacteriol*, **183**, 3083-3088.

Hoyt, M.A. and Coffino, P. (2004) Ubiquitin-free routes into the proteasome. *Cell Mol Life Sci*, **61**, 1596-1600.

Huang, P.H. and Chiang, H.L. (1997) Identification of novel vesicles in the cytosol to vacuole protein degradation pathway. *J Cell Biol*, **136**, 803-810.

Huh, W., Falvo, J., Gerke, L., Carroll, A., Howson, R., Weissman, J. and O'Shea, E. (2003) Global analysis of protein localization in budding yeast. *Nature*, **425**, 686-691.

Hung, G.C., Brown, C.R., Wolfe, A.B., Liu, J. and Chiang, H.L. (2004) Degradation of the gluconeogenic enzymes fructose-1,6-bisphosphatase and malate dehydrogenase is mediated by distinct proteolytic pathways and signaling events. *J Biol Chem*, **279**, 49138-49150.

Iovine, M.K. and Wente, S.R. (1997) A nuclear export signal in Kap95p is required for both recycling the import factor and interaction with the nucleoporin GLFG repeat regions of Nup116p and Nup100p. *J Cell Biol*, **137**, 797-811.

Ito, T., Chiba, T., Ozawa, R., Yoshida, M., Hattori, M. and Sakaki, Y. (2001) A comprehensive two-hybrid analysis to explore the yeast protein interactome. *Proc Natl Acad Sci U S A*, **98**, 4569-4574.

Jackson, P.K., Eldridge, A.G., Freed, E., Furstenthal, L., Hsu, J.Y., Kaiser, B.K. and Reimann, J.D. (2000) The lore of the RINGs: substrate recognition and catalysis by ubiquitin ligases. *Trends Cell Biol*, **10**, 429-439.

Jelinsky, S.A., Estep, P., Church, G.M. and Samson, L.D. (2000) Regulatory networks revealed by transcriptional profiling of damaged Saccharomyces cerevisiae cells: Rpn4 links base excision repair with proteasomes. *Mol Cell Biol*, **20**, 8157-8167.

Johnson, E.S., Schwienhorst, I., Dohmen, R.J. and Blobel, G. (1997) The ubiquitin-like protein Smt3p is activated for conjugation to other proteins by an Aos1p/Uba2p heterodimer. *Embo J*, **16**, 5509-5519.

Josupeit, F.S. (2003) Die Glucose-induzierte Katabolitinaktivierung der Fructose-1,6-bisphosphatase der Hefe Saccharomyces cerevisiae: Neue Komponenten ihres Ubiquitin-Proteasom-katalysierten Abbaus. *PhD Thesis*.

Kaiser, P., Seufert, W., Hofferer, L., Kofler, B., Sachsenmaier, C., Herzog, H., Jentsch, S., Schweiger, M. and Schneider, R. (1994) A human ubiquitin-conjugating enzyme homologous to yeast UBC8. *J Biol Chem*, **269**, 8797-8802.

Kaniak, A., Xue, Z., Macool, D., Kim, J.H. and Johnston, M. (2004) Regulatory network connecting two glucose signal transduction pathways in Saccharomyces cerevisiae. *Eukaryot Cell*, **3**, 221-231.

Kikawa, Y., Inuzuka, M., Jin, B.Y., Kaji, S., Koga, J., Yamamoto, Y., Fujisawa, K., Hata, I., Nakai, A., Shigematsu, Y., Mizunuma, H., Taketo, A., Mayumi, M. and Sudo, M. (1997) Identification of genetic mutations in Japanese patients with fructose-1,6-bisphosphatase deficiency. *Am J Hum Genet*, **61**, 852-861.

Kikawa, Y., Inuzuka, M., Jin, B.Y., Kaji, S., Yamamoto, Y., Shigematsu, Y., Nakai, A., Taketo, A., Ohura, T., Mikami, H. and et al. (1995) Identification of a genetic mutation in a family with fructose-1,6-bisphosphatase deficiency. *Biochem Biophys Res Commun*, **210**, 797-804.

Kisselev, A.F., Akopian, T.N. and Goldberg, A.L. (1998) Range of sizes of peptide products generated during degradation of different proteins by archaeal proteasomes. *J Biol Chem*, **273**, 1982-1989.

Klein, C.J., Olsson, L. and Nielsen, J. (1998) Glucose control in Saccharomyces cerevisiae: the role of Mig1 in metabolic functions. *Microbiology*, **144 (Pt 1)**, 13-24.

Kleinschmidt, J.A., Escher, C. and Wolf, D.H. (1988) Proteinase yscE of yeast shows homology with the 20 S cylinder particles of Xenopus laevis. *FEBS Lett*, **239**, 35-40.

Kloetzel, P.M. (2004) The proteasome and MHC class I antigen processing. *Biochim Biophys Acta*, **1695**, 225-233.

Knop, M., Schiffer, H.H., Rupp, S. and Wolf, D.H. (1993) Vacuolar/lysosomal proteolysis: proteases, substrates, mechanisms. *Curr Opin Cell Biol*, **5**, 990-996.

Kohler, A., Bajorek, M., Groll, M., Moroder, L., Rubin, D.M., Huber, R., Glickman, M.H. and Finley, D. (2001) The substrate translocation channel of the proteasome. *Biochimie*, **83**, 325-332.

Kolling, R. and Hollenberg, C.P. (1994) The ABC-transporter Ste6 accumulates in the plasma membrane in a ubiquitinated form in endocytosis mutants. *Embo J*, **13**, 3261-3271.

Kostova, Z. and Wolf, D.H. (2003) For whom the bell tolls: protein quality control of the endoplasmic reticulum and the ubiquitin-proteasome connection. *Embo J*, **22**, 2309-2317.

Kumar, S., Kao, W.H. and Howley, P.M. (1997) Physical interaction between specific E2 and Hect E3 enzymes determines functional cooperativity. *J Biol Chem*, **272**, 13548-13554.

Laemmli, U. (1970) Cleavage of structural proteins during the assembly of the head of bacteriophage T4. *Nature*, **227**, 680-685.

Lam, Y.A., Lawson, T.G., Velayutham, M., Zweier, J.L. and Pickart, C.M. (2002) A proteasomal ATPase subunit recognizes the polyubiquitin degradation signal. *Nature*, **416**, 763-767.

Lehmann, A., Janek, K., Braun, B., Kloetzel, P.M. and Enenkel, C. (2002) 20 S proteasomes are imported as precursor complexes into the nucleus of yeast. *J Mol Biol*, **317**, 401-413.

Lenk, U. and Sommer, T. (2000) Ubiquitin-mediated proteolysis of a short-lived regulatory protein depends on its cellular localization. *J Biol Chem*, **275**, 39403-39410.

Liakopoulos, D., Doenges, G., Matuschewski, K. and Jentsch, S. (1998) A novel protein modification pathway related to the ubiquitin system. *Embo J*, **17**, 2208-2214.

Loeb, J.D., Schlenstedt, G., Pellman, D., Kornitzer, D., Silver, P.A. and Fink, G.R. (1995) The yeast nuclear import receptor is required for mitosis. *Proc Natl Acad Sci U S A*, **92**, 7647-7651.

London, M.K., Keck, B.I., Ramos, P.C. and Dohmen, R.J. (2004) Regulatory mechanisms controlling biogenesis of ubiquitin and the proteasome. *FEBS Lett*, **567**, 259-264.

Longtine, M.S., McKenzie, A., 3rd, Demarini, D.J., Shah, N.G., Wach, A., Brachat, A., Philippsen, P. and Pringle, J.R. (1998) Additional modules for versatile and economical PCR-based gene deletion and modification in Saccharomyces cerevisiae. *Yeast*, **14**, 953-961.

Lowe, J., Stock, D., Jap, B., Zwickl, P., Baumeister, W. and Huber, R. (1995) Crystal structure of the 20S proteasome from the archaeon T. acidophilum at 3.4 A resolution. *Science*, **268**, 533-539.

Maniatis, T., Fritsch, E.F. and Sambrook, J. (1982) Molecular cloning: a laboratory manual. *Cold Spring Harbour*.

Marcus, F., Rittenhouse, J., Moberly, L., Edelstein, I., Hiller, E. and Rogers, D.T. (1988) Yeast (Saccharomyces cerevisiae) fructose-1,6-bisphosphatase. Properties of phospho and dephospho forms and of two mutants in which serine 11 has been changed by site-directed mutagenesis. *J Biol Chem*, **263**, 6058-6062.

McGrath, J.P., Jentsch, S. and Varshavsky, A. (1991) UBA 1: an essential yeast gene encoding ubiquitin-activating enzyme. *Embo J*, **10**, 227-236.

Medicherla, B., Kostova, Z., Schaefer, A. and Wolf, D.H. (2004) A genomic screen identifies Dsk2p and Rad23p as essential components of ER-associated degradation. *EMBO Rep*, **5**, 692-697.

Minard, K.I. and McAlister-Henn, L. (1992) Glucose-induced degradation of the MDH2 isozyme of malate dehydrogenase in yeast. *J Biol Chem*, **267**, 17458-17464.

Molano, G. (1974) Specific inactivation of fructose-1,6-bisphosphatase from Saccharomyces cerevisiae by a yeast protease. *Eur J Biochem*, **44**, 213-217.

Mullis, K.B. (1990) The unusual origin of the polymerase chain reaction. *Sci Am*, **262**, 56-61, 64-55.

Nishitani, H., Hirose, E., Uchimura, Y., Nakamura, M., Umeda, M., Nishii, K., Mori, N. and Nishimoto, T. (2001) Full-sized RanBPM cDNA encodes a protein possessing a long stretch of proline and glutamine within the N-terminal region, comprising a large protein complex. *Gene*, **272**, 25-33.

Nussbaum, A.K., Dick, T.P., Keilholz, W., Schirle, M., Stevanovic, S., Dietz, K., Heinemeyer, W., Groll, M., Wolf, D.H., Huber, R., Rammensee, H.G. and Schild, H. (1998) Cleavage motifs of the yeast 20S proteasome beta subunits deduced from digests of enolase 1. *Proc Natl Acad Sci U S A*, **95**, 12504-12509.

Ohi, M.D., Vander Kooi, C.W., Rosenberg, J.A., Chazin, W.J. and Gould, K.L. (2003) Structural insights into the U-box, a domain associated with multi-ubiquitination. *Nat Struct Biol*, **10**, 250-255.

Ozkaynak, E., Finley, D., Solomon, M.J. and Varshavsky, A. (1987) The yeast ubiquitin genes: a family of natural gene fusions. *Embo J*, **6**, 1429-1439.

Pfirrmann, T., Regelmann, J., Santt, O., Alberts, S., Braun, B., Thumm, M. and Wolf, D.H. (2006) Function of Gid Proteins in Ubiquitin-Proteasome Dependent Catabolite Degradation of Fructose-1,6-bisphosphatase in Yeast. *Journal of Biological Chemistry submitted*.

Pichler, A., Gast, A., Seeler, J.S., Dejean, A. and Melchior, F. (2002) The nucleoporin RanBP2 has SUMO1 E3 ligase activity. *Cell*, **108**, 109-120.

Pickart, C.M. (1997) Targeting of substrates to the 26S proteasome. *Faseb J*, **11**, 1055-1066.

Pickart, C.M. (2001) Mechanisms underlying ubiquitination. *Annu Rev Biochem*, **70**, 503-533.

Pickart, C.M. and Eddins, M.J. (2004) Ubiquitin: structures, functions, mechanisms. *Biochim Biophys Acta*, **1695**, 55-72.

Puig, O., Caspary, F., Rigaut, G., Rutz, B., Bouveret, E., Bragado-Nilsson, E., Wilm, M. and Seraphin, B. (2001) The tandem affinity purification (TAP) method: a general procedure of protein complex purification. *Methods*, **24**, 218-229.

Purwin, C., Leidig, F. and Holzer, H. (1982) Cyclic AMP-dependent phosphorylation of fructose-1,6-bisphosphatase in yeast. *Biochem Biophys Res Commun*, **107**, 1482-1489.

Regelmann, J. (2005) Katabolitinaktivierung der Fructose-1,6-bisphosphatase: Identifizierung und Charakterisierung neuer, für ihren Ubiquitin-Proteasom katalysierten, Abbau benötigter Proteine. *PhD Thesis*.

Regelmann, J., Schule, T., Josupeit, F.S., Horak, J., Rose, M., Entian, K.D., Thumm, M. and Wolf, D.H. (2003) Catabolite degradation of fructose-1,6-bisphosphatase in the yeast Saccharomyces cerevisiae: a genome-wide screen identifies eight novel GID genes and indicates the existence of two degradation pathways. *Mol Biol Cell*, **14**, 1652-1663.

Riballo, E., Herweijer, M., Wolf, D.H. and Lagunas, R. (1995) Catabolite inactivation of the yeast maltose transporter occurs in the vacuole after internalization by endocytosis. *J Bacteriol*, **177**, 5622-5627.

Rock, K.L., Gramm, C., Rothstein, L., Clark, K., Stein, R., Dick, L., Hwang, D. and Goldberg, A.L. (1994) Inhibitors of the proteasome block the degradation of most cell proteins and the generation of peptides presented on MHC class I molecules. *Cell*, **78**, 761-771.

Rolland, F., Winderickx, J. and Thevelein, J.M. (2002) Glucose-sensing and -signalling mechanisms in yeast. *FEMS Yeast Res*, **2**, 183-201.

Rothschild, C.B., Freedman, B.I., Hodge, R., Rao, P.N., Pettenati, M.J., Anderson, R.A., Akots, G., Qadri, A., Roh, B., Fajans, S.S. and et al. (1995) Fructose-1,6-bisphosphatase: genetic and physical mapping to

human chromosome 9q22.3 and evaluation in non-insulin-dependent diabetes mellitus. *Genomics*, **29**, 187-194.

Rubin, D.M. and Finley, D. (1995) Proteolysis. The proteasome: a protein-degrading organelle? *Curr Biol*, **5**, 854-858.

Rubin, D.M., Glickman, M.H., Larsen, C.N., Dhruvakumar, S. and Finley, D. (1998) Active site mutants in the six regulatory particle ATPases reveal multiple roles for ATP in the proteasome. *Embo J*, **17**, 4909-4919.

Russell, S.J., Steger, K.A. and Johnston, S.A. (1999) Subcellular localization, stoichiometry, and protein levels of 26 S proteasome subunits in yeast. *J Biol Chem*, **274**, 21943-21952.

Saitoh, H., Pu, R., Cavenagh, M. and Dasso, M. (1997) RanBP2 associates with Ubc9p and a modified form of RanGAP1. *Proc Natl Acad Sci U S A*, **94**, 3736-3741.

Saville, M.K., Sparks, A., Xirodimas, D.P., Wardrop, J., Stevenson, L.F., Bourdon, J.C., Woods, Y.L. and Lane, D.P. (2004) Regulation of p53 by the ubiquitin-conjugating enzymes UbcH5B/C in vivo. *J Biol Chem*, **279**, 42169-42181.

Schork, S.M. (1995) Die Katabolitinaktivierung der Fruktose-1,6-bisphosphatase in der Hefe Saccharomyces cerevisiae: Aufklärung ihres Ubiquitin - Proteasom vermittelten Abbaus. *PhD Thesis*.

Schork, S.M., Bee, G., Thumm, M. and Wolf, D.H. (1994a) Catabolite inactivation of fructose-1,6-bisphosphatase in yeast is mediated by the proteasome. *FEBS Lett*, **349**, 270-274.

Schork, S.M., Bee, G., Thumm, M. and Wolf, D.H. (1994b) Site of catabolite inactivation. *Nature*, **369**, 283-284.

Schork, S.M., Thumm, M. and Wolf, D.H. (1995) Catabolite inactivation of fructose-1,6-bisphosphatase of Saccharomyces cerevisiae. Degradation occurs via the ubiquitin pathway. *J Biol Chem*, **270**, 26446-26450.

Schüle, T., Rose, M., Entian, K.D., Thumm, M. and Wolf, D.H. (2000) Ubc8p functions in catabolite degradation of fructose-1, 6-bisphosphatase in yeast. *Embo J*, **19**, 2161-2167.

Shieh, H.L. and Chiang, H.L. (1998) In vitro reconstitution of glucose-induced targeting of fructose-1, 6-bisphosphatase into the vacuole in semi-intact yeast cells. *J Biol Chem*, **273**, 3381-3387.

Shulga, N., James, P., Craig, E.A. and Goldfarb, D.S. (1999) A nuclear export signal prevents Saccharomyces cerevisiae Hsp70 Ssb1p from stimulating nuclear localization signal-directed nuclear transport. *J Biol Chem*, **274**, 16501-16507.

Shulga, N., Roberts, P., Gu, Z., Spitz, L., Tabb, M.M., Nomura, M. and Goldfarb, D.S. (1996) In vivo nuclear transport kinetics in Saccharomyces cerevisiae: a role for heat shock protein 70 during targeting and translocation. *J Cell Biol*, **135**, 329-339.

Sikorski, R.S. and Hieter, P. (1989) A system of shuttle vectors and yeast host strains designed for efficient manipulation of DNA in Saccharomyces cerevisiae. *Genetics*, **122**, 19-27.

Smith, T.F., Gaitatzes, C., Saxena, K. and Neer, E.J. (1999) The WD repeat: a common architecture for diverse functions. *Trends Biochem Sci*, **24**, 181-185.

Sondermann, H., Ho, A.K., Listenberger, L.L., Siegers, K., Moarefi, I., Wente, S.R., Hartl, F.U. and Young, J.C. (2002) Prediction of novel Bag-1 homologs based on structure/function analysis identifies Snl1p as an Hsp70 co-chaperone in Saccharomyces cerevisiae. *J Biol Chem*, **277**, 33220-33227.

Southern. (1975) Detection of specific sequences among DNA fragments separated by gel electrophoresis. *J Mol Biol*, **98**, 503-517.

Stade, K., Vogel, F., Schwienhorst, I., Meusser, B., Volkwein, C., Nentwig, B., Dohmen, R.J. and Sommer, T. (2002) A lack of SUMO conjugation affects cNLS-dependent nuclear protein import in yeast. *J Biol Chem*, **277**, 49554-49561.

Strambio-de-Castillia, C. and Rout, M.P. (2002) The structure and composition of the yeast NPC. *Results Probl Cell Differ*, **35**, 1-23.

Stryer. (2002) *Biochemistry*.

Tabb, M.M., Tongaonkar, P., Vu, L. and Nomura, M. (2000) Evidence for separable functions of Srp1p, the yeast homolog of importin alpha (Karyopherin alpha): role for Srp1p and Sts1p in protein degradation. *Mol Cell Biol*, **20**, 6062-6073.

Takahashi, Y., Kahyo, T., Toh, E.A., Yasuda, H. and Kikuchi, Y. (2001) Yeast Ull1/Siz1 is a novel SUMO1/Smt3 ligase for septin components and functions as an adaptor between conjugating enzyme and substrates. *J Biol Chem*, **276**, 48973-48977.

Thrower, J.S., Hoffman, L., Rechsteiner, M. and Pickart, C.M. (2000) Recognition of the polyubiquitin proteolytic signal. *Embo J*, **19**, 94-102.

Thumm, M. (2000) Structure and function of the yeast vacuole and its role in autophagy. *Microsc Res Tech*, **51**, 563-572.

Thumm, M. and Wolf, D.H. (1998) From proteasome to lysosome: Studies on yeast demonstrates the principles of protein degradation in the eucaryotic cell. *Mol. Cell Biol*, 41-67.

Towbin, H., Staehelin, T. and Gordon, J. (1979) Electrophoretic transfer of proteins from polyacrylamide gels to nitrocellulose sheets: procedure and some applications. *Proc Natl Acad Sci U S A*, **76**, 4350-4354.

Uetz, P., Giot, L., Cagney, G., Mansfield, T.A., Judson, R.S., Knight, J.R., Lockshon, D., Narayan, V., Srinivasan, M., Pochart, P., Qureshi-Emili, A., Li, Y., Godwin, B., Conover, D., Kalbfleisch, T., Vijayadamodar, G., Yang, M., Johnston, M., Fields, S. and Rothberg, J.M. (2000) A comprehensive analysis of protein-protein interactions in Saccharomyces cerevisiae. *Nature*, **403**, 623-627.

van der Merwe, G.K., Cooper, T.G. and van Vuuren, H.J. (2001) Ammonia regulates VID30 expression and Vid30p function shifts nitrogen metabolism toward glutamate formation especially when Saccharomyces cerevisiae is grown in low concentrations of ammonia. *J Biol Chem*, **276**, 28659-28666.

van Nocker, S., Deveraux, Q., Rechsteiner, M. and Vierstra, R.D. (1996) Arabidopsis MBP1 gene encodes a conserved ubiquitin recognition component of the 26S proteasome. *Proc Natl Acad Sci U S A*, **93**, 856-860.

Verma, R., Aravind, L., Oania, R., McDonald, W.H., Yates, J.R., 3rd, Koonin, E.V. and Deshaies, R.J. (2002) Role of Rpn11 metalloprotease in deubiquitination and degradation by the 26S proteasome. *Science*, **298**, 611-615.

Wach, A., Brachat, A., Alberti-Segui, C., Rebischung, C. and Philippsen, P. (1997) Heterologous HIS3 marker and GFP reporter modules for PCR-targeting in Saccharomyces cerevisiae. *Yeast*, **13**, 1065-1075.

Walters, K.J., Goh, A.M., Wang, Q., Wagner, G. and Howley, P.M. (2004) Ubiquitin family proteins and their relationship to the proteasome: a structural perspective. *Biochim Biophys Acta*, **1695**, 73-87.

Wang, G., Yang, J. and Huibregtse, J.M. (1999) Functional domains of the Rsp5 ubiquitin-protein ligase. *Mol Cell Biol*, **19**, 342-352.

Wang, Y., Pierce, M., Schneper, L., Guldal, C.G., Zhang, X., Tavazoie, S. and Broach, J.R. (2004) Ras and Gpa2 mediate one branch of a redundant glucose signaling pathway in yeast. *PLoS Biol*, **2**, E128.

Weeks, C.M., Roszak, A.W., Erman, M., Kaiser, R., Jornvall, H. and Ghosh, D. (1999) Structure of rabbit liver fructose 1,6-bisphosphatase at 2.3 A resolution. *Acta Crystallogr.*, 93-102.

Wendler, P., Lehmann, A., Janek, K., Baumgart, S. and Enenkel, C. (2004) The bipartite nuclear localization sequence of Rpn2 is required for nuclear import of proteasomal base complexes via karyopherin alphabeta and proteasome functions. *J Biol Chem*, **279**, 37751-37762.

Wente, S.R. and Blobel, G. (1993) A temperature-sensitive NUP116 null mutant forms a nuclear envelope seal over the yeast nuclear pore complex thereby blocking nucleocytoplasmic traffic. *J Cell Biol*, **123**, 275-284.

Wilkinson, K.D. (2004) Ubiquitin: a Nobel protein. *Cell*, **119**, 741-745.

Willems, A.R., Goh, T., Taylor, L., Chernushevich, I., Shevchenko, A. and Tyers, M. (1999) SCF ubiquitin protein ligases and phosphorylation-dependent proteolysis. *Philos Trans R Soc Lond B Biol Sci*, **354**, 1533-1550.

Willems, A.R., Schwab, M. and Tyers, M. (2004) A hitchhiker's guide to the cullin ubiquitin ligases: SCF and its kin. *Biochim Biophys Acta*, **1695**, 133-170.

Wolf, D.H. (1982) Proteinase action in vitro versus protein function in vivo: mutants shed light on intracellular proteolysis in yeast. *Trends Biochem Sci*, 35-37.

Wolf, D.H. (2004) From lysosome to proteasome: the power of yeast in the dissection of proteinase function in cellular regulation and waste disposal. *Cell Mol Life Sci.*, **61**, 1601-1614.

Wolf, D.H. and Hilt, W. (2004) The proteasome: a proteolytic nanomachine of cell regulation and waste disposal. *Biochim Biophys Acta*, **1695**, 19-31.

Xie, Y. and Varshavsky, A. (2001) RPN4 is a ligand, substrate, and transcriptional regulator of the 26S proteasome: a negative feedback circuit. *Proc Natl Acad Sci U S A*, **98**, 3056-3061.

Yanez, A.J., Bertinat, R., Concha, II and Slebe, J.C. (2003) Nuclear localization of liver FBPase isoenzyme in kidney and liver. *FEBS Lett*, **550**, 35-40.

Yanez, A.J., Garcia-Rocha, M., Bertinat, R., Droppelmann, C., Concha, II, Guinovart, J.J. and Slebe, J.C. (2004) Subcellular localization of liver FBPase is modulated by metabolic conditions. *FEBS Lett*, **577**, 154-158.

Yao, T. and Cohen, R.E. (2002) A cryptic protease couples deubiquitination and degradation by the proteasome. *Nature*, **419**, 403-407.

Young, P., Deveraux, Q., Beal, R.E., Pickart, C.M. and Rechsteiner, M. (1998) Characterization of two polyubiquitin binding sites in the 26 S protease subunit 5a. *J Biol Chem*, **273**, 5461-5467.

Zarzycki, M., Eschrich, K., Rakus, D. and Dzugaj, A. (2004) Phosphorylation of mammalian muscle fructose-1,6-bisphosphatase in vitro and in vivo. *Abstract number: P4.1-45*.

Zmojdzian, M., Dziewulska-Szwajkowska, D. and Dzugaj, A. (2005) Localization of chicken muscle FBPase in cardiomyocyte nuclei. *Comp Biochem Physiol B Biochem Mol Biol*, **140**, 37-43.